University of Alberta

Yield Stresses of Mixtures with Bimodal Size Distributions

by

Md. Hafizur Rahman

A thesis submitted to the Faculty of Graduate Studies and Research
in partial fulfillment of the requirements for the degree of

Master of Science

in

Chemical Engineering

Department of Chemical and Materials Engineering

Spring 2011
Edmonton, Alberta

Abstract

The addition of coarse particles to a flocculating fine particle slurry increases the Bingham yield stress of the resulting mixture, which can drastically alter the laminar-to-turbulent transition velocity. The objective of this study is to quantify the effect of coarse particle size and volume concentration on mixture rheology. Fine particle (kaolin) mixtures of 10% to 22% (by volume) were prepared, to which sand particles were added to provide a coarse solid concentration of 5% to 20% (by volume). Sand particles of two different sizes – 90 and 190 microns – were added and these kaolin-sand-water mixtures tested with a concentric cylinder viscometer. At higher total solids concentrations, the Bingham yield stress of the bimodal mixture can increase by as much as 80% over that of a kaolin-only slurry. Coarse particle diameter had little effect. This study demonstrates that the use of existing correlations should be eschewed. System-specific high-quality measurements are necessary.

Acknowledgements

I would like to thank my parents and younger sisters for their unconditional love and support. They always believed in me and it has given me strength in my mind at difficult times. They contributed a great deal to shape my life into what I am now and what I want to be in future. I also wish to thank Towhidul Bashar, ASM Junaid, Syed Zakaria, Susanjib Sarkar, Sayeed Rushd, Mahshad Pazouki, Farid Vaezi and Reza Hashemi for their friendship, support and words of encouragement.

I wish to express my deepest gratitude to Dr. Sean Sanders for his support and guidance throughout the research program, and most importantly, for helping me to learn how to conduct meaningful research. He helped me a lot, from introducing me to the field of fluid- particle systems to the final preparation of this thesis.

I would like to thank NSERC Industrial Research Chair in Pipeline Transport Processes for arranging necessary financial support. I feel grateful to staff of the Saskatchewan Research Council's Pipe Flow Technology Centre, as they shared their expertise on many occasions and provided technical information from their database which saved a considerable amount of time. I wish to thank Barry Bara, Samson Ng and the analytical services staff at Syncrude Research Centre, Edmonton for their technical support in the form of laboratory services.

Table of Contents

List of Tables

List of Figures

List of Symbols

Symbols	Description	Units
A, B	Correlation parameters	-
C	Solids volume concentration	-
D	Diameter	m
d_p	Diameter of particles	μm
H	Height	m
L	Length	m
n	Index	-
P_1, P_2	Pressure at pipe inlet and outlet	Pa
Q	Volumetric flow rate	m^3/s
R_1, R_2	Radii of spindle and cup	mm
T	Torque	N.m
V	Velocity	m/s
$\overline{V}$	Volume of a component	cm^3
$\dot{\gamma}$	Shear rate	1/s
μ	Viscosity	Pa.s
μ_P	Bingham plastic viscosity	
λ	Linear concentration	-
ρ	Density	kg/m^3

τ	Shear stress	Pa
τ_0	Bingham yield stress	
ω	Spindle/vane speed	S^{-1}

Subscripts

0,floc	Floc at minimum condition	-
C	Coarse particles	-
cf	Carrier fluid mixture (Fine particle + water)	-
f	Fine particles mixture in water	-
floc	Floc	-
L	Pure Liquid (Water)	-
m	Maximum	-
max	Maximum packing concentration	-
mix	Final mixture (Coarse + Fines + Water)	-
T	Transition	-
V	Vane	-
w	Water	-
W	Wall	-

1. Problem Statement

Most mining industries in the world are experiencing ever growing pressure from the stakeholders and the regulatory bodies to minimize the ecological footprints of their operations. Accordingly, the Canadian oil sands industry continues to test and adopt new fine particle tailings treatment options as they work to minimize land disturbance and water consumption in the production of bitumen from mined oil sand. At present, companies use tailings treatment options that involve the combination of coarse sand with a highly non-Newtonian, fine-particle tailings stream to promote clay particle aggregation and water release. The target is to produce a tailings deposit which can be reclaimed while recycling increased amounts of water from the tailings streams so that fresh water intake can be reduced further.

The addition of coarse particles to a concentrated fine particle slurry increases the rheology of the resulting mixture, which can have a profound impact on the operation of downstream pumps and pipelines. As the mixture must remain non-segregated from the point of production to its final disposal at a tailings pond, an accurate prediction of the mixture rheology is vital for effective design and stable operation of the pipeline system required for transporting these complex mixtures. The problem is complicated by the absence of a correlation which can satisfactorily predict the Bingham yield stress of the resulting mixture.

The problem can be explained with the example of an industrial process as illustrated in Figure 1.1. Here, a fine particle mixture is obtained from a thickener, to which a coarse particle stream is added and the resulting mixture is transported to a tailings pond. The rheological properties of these mixtures must be determined for design and operation of the pipeline system.

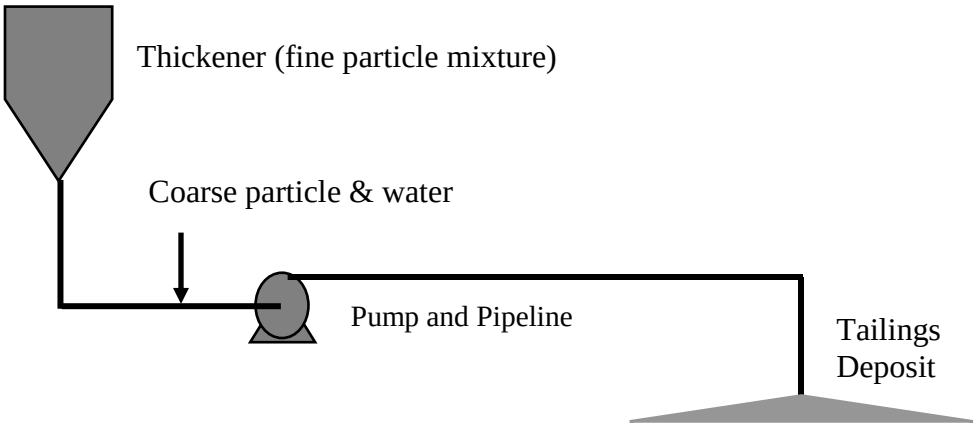

Figure 1.1: A typical preparation and transportation system for tailings.

The fine particle mixture consists of clay and water. It is a non-Newtonian mixture. There are several models available to predict the non-Newtonian behavior of such mixtures. Among them, the Bingham fluid model is the most popular and widely used for predicting the rheological behavior of this kind of mixtures (Slatter and Wasp, 2002). The Bingham fluid model has two parameters - plastic viscosity and yield stress. The yield stress originates from the flocculation of clay particles, the detailed mechanism of which will be discussed in Chapter 2 (Background). The mixture's plastic viscosity and the yield stress

increase with clay concentration and the increases can be predicted well with correlations provided Chapter 2.

When coarse particles are added to the fine-particle mixture, a sand-clay-water mixture is obtained. This mixture is non-Newtonian, and can be satisfactorily approximated with time-independent Bingham fluid model (Sumner, 2000). Both plastic viscosity and Bingham yield stress increases with sand concentration. The increase in plastic viscosity with sand concentration can be predicted satisfactorily with correlations discussed in the subsequent chapter. However, the increase in Bingham yield stress with sand concentration is subject to disagreement among researchers.

This research project is focused on the accurate prediction of Bingham yield stress of sand-clay-water mixtures, which is very important for stable pipeline operation. If the sand-clay-water mixture somehow becomes segregated at any point of transportation in the pipeline, the sand particle will settle down at the bottom of the pipe and eventually the pipeline can become plugged. Moreover, the settling of sand in the pipeline will deprive the tailings deposit of sand. Then the tailings deposit may not have the required geotechnical characteristics.

For most slurry pipelines carrying high yield stress mixtures of coarse sand and clay, it is crucial to operate in turbulent flow. The relation of sand deposition with laminar to turbulent transition velocity and the dependence of transition velocity

on Bingham yield stress can be explained with the help of Figure 1.2 and Figure 1.3 respectively. Figure 1.2 shows data collected at Saskatchewan Research Council in 2002 for a sand-clay-water mixture containing 50% solids. In the left plot of Figure 1.2, it is seen that when the velocity is sufficiently high, the solids concentration at the bottom of the pipe is 50% and that is equal to the average solids concentration throughout the pipe, which means no significant deposition has occurred at high velocities. However, if the velocity is lower than what can be called the deposition velocity, the solids concentration at the bottom of the pipe is 65% and that is higher than the rest of the pipe, which confirms significant deposition of sand particles.

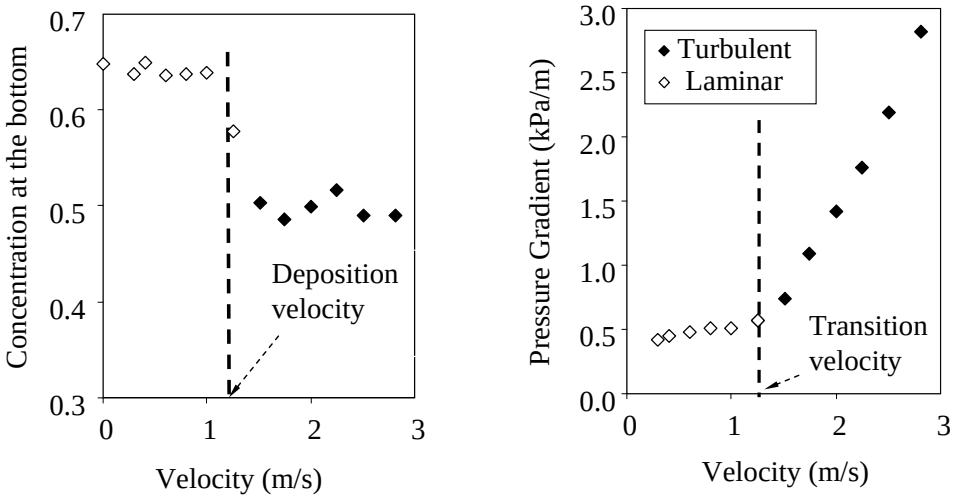

Figure 1.2: Sand deposition at laminar flow condition (Source: Saskatchewan Research Council, Canada).

In the other plot of Figure 1.2, pressure gradient is considered against the bulk velocity of the same mixture. This graph shows that as long as the flow remains turbulent, sand particles are kept suspended by the turbulent eddies. When there is a transition from turbulent flow regime to a laminar flow regime, the turbulent eddies are no longer there and the sand particles settle down.

Figure 1.3 shows the increase in transition velocity with Bingham yield stress. The plot is obtained using Equations 2.5, 2.8, 2.13-2.14 and 2.23-2.27, which are presented in the following chapter. It should be recognized that the ability of some of these equations to accurately predict relevant mixture properties are not immune from questions; however, they can still be used for illustrating the problem in the absence of better correlations. It has already been mentioned that Bingham yield stress increases with sand concentration, meaning that the addition of sand increases the Bingham yield stress, which in turn increases the transition velocity of the mixture. Thus a pipeline which is operating at a velocity slightly higher than the transition velocity can experience deposition of sand particles if sand concentration is increased. Similarly, a fluctuation of the operating velocity from its steady-state value may result in hitting the laminar flow region, even though the sand concentration remains unchanged. Either of the events can take place due to weakness of the design originated from the lack of a correlation which can accurately predict changes in Bingham yield stress with sand concentration. As a result, a satisfactory prediction of transition velocity is not

possible as long as the changes in Bingham yield stress with sand concentration in not accurately determined.

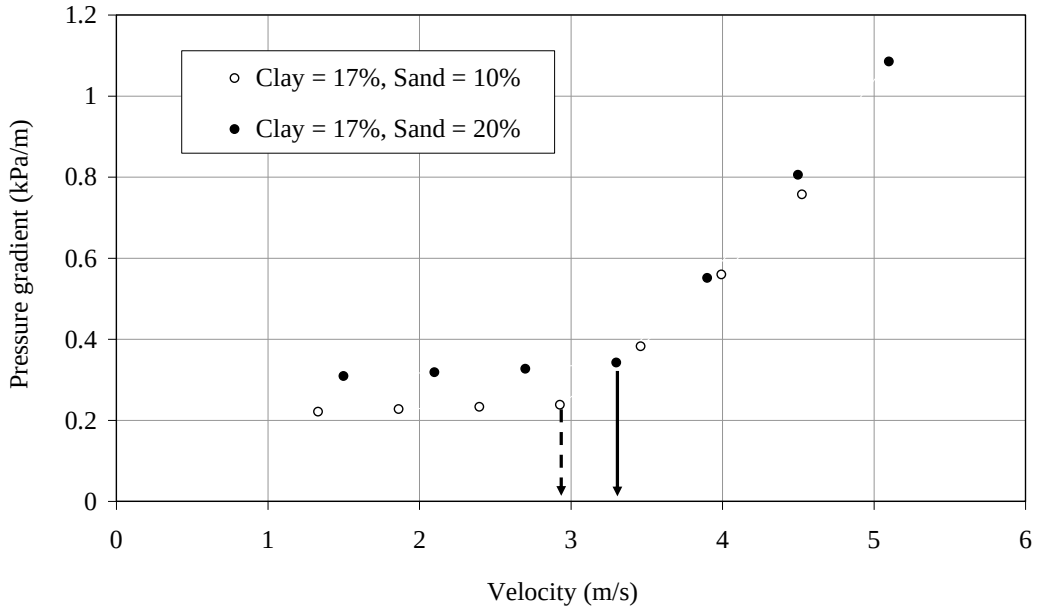

Figure 1.3: Change in transition velocity with sand concentration of a sand-clay-water mixture in a 10" ID pipe with a roughness of 45 micron.

Here it is worth to note that economic considerations do not allow a pipeline to be operated at a velocity which is far higher than the transition velocity. Yet, the industries want to transport as much solids as practically possible. This results in operating the pipeline at a velocity which is not far from the transition velocity. Hence, it is very important to determine the effect of sand concentration on Bingham yield stress accurately, so that an optimum operating velocity can be selected, which is not only sufficiently higher than the transition velocity, but also capable of meeting cost requirements.

Therefore, the objectives of this research project are to

- Investigate the change in Bingham yield stress with sand concentration in high-density sand-clay-water mixtures.
- Determine the effect of coarse particle (sand) diameter on the Bingham yield stress of these mixtures.

2. Background

2.1. Newtonian and Bingham fluid model

Newton described the relation between shear stress (τ) and shear rate ($\dot{\gamma}$) for one dimensional flow of a fluid as:

$$\tau = \mu \dot{\gamma} \qquad \textbf{2.1}$$

This is the famous Newton's law of viscosity (Bird et al., 1960). The proportionality constant 'μ' is independent of both shear stress and shear rate, and is known as Newtonian viscosity or simply, viscosity. Hence, the rheogram of a Newtonian fluid is a straight line which passes through the origin, as shown in Figure 2.1. The slope of the straight line gives the viscosity of that particular fluid.

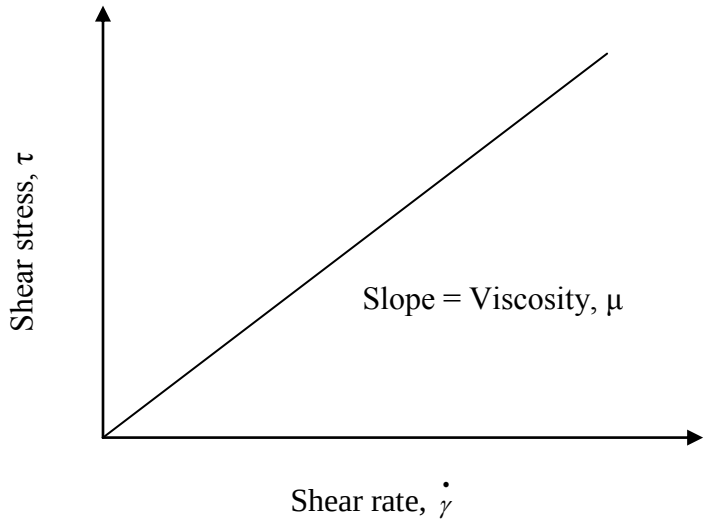

Figure 2.1: Rheogram of a Newtonian fluid.

However, there are many fluids and mixtures that do not obey Newton's law of viscosity. A Newtonian fluid requires only one parameter, namely viscosity, to characterize its rheological behavior. On the other hand, a non-Newtonian fluid require more than one parameter for the same purpose. It is important to note that the viscosity of a Newtonian fluid is a physical property, i.e. for a particular Newtonian fluid at a given temperature, there is a particular viscosity; however, a non-Newtonian fluid can be modeled with more than one non-Newtonian fluid model.

The present study uses fine particles which, when mixed with water, form flocs. These flocs can form larger groups known as aggregates. When at rest, the interactions among aggregates can lead to a continuous structure throughout the mixture that is responsible for yield stress of the mixture (Michaels and Bolger, 1962). If a shear stress greater than the yield stress is applied, the mixture starts to flow (except at very low shear rates) and will exhibit a linear relationship between the shear stress and the shear rate. The Bingham fluid model contains a yield stress term and a linear viscosity term, and is therefore selected for approximating the behavior of all mixtures containing flocculating fine particles in this project. It is worth mentioning that a number of researchers, including Michaels and Bolger (1962), Thomas (1999), Litzenberger (2004) and Paulsen (2007), found the Bingham plastic model suitable for similar mixtures.

The rheological equation for Bingham plastic model is

$$\tau = \tau_0 + \mu_p \dot{\gamma} \qquad \textbf{2.2}$$

The two parameters of the model are Bingham yield stress 'τ_0', and Bingham plastic viscosity 'μ_p'. The rheogram of this fluid model is provided in Figure 2.2. From the figure it is seen that the shear stress versus shear rate relation is represented by a straight line which does not go through the origin; rather it intersects the Y-axis at a point which gives the yield stress of the mixture, and the plastic viscosity is obtained from the slope of the curve.

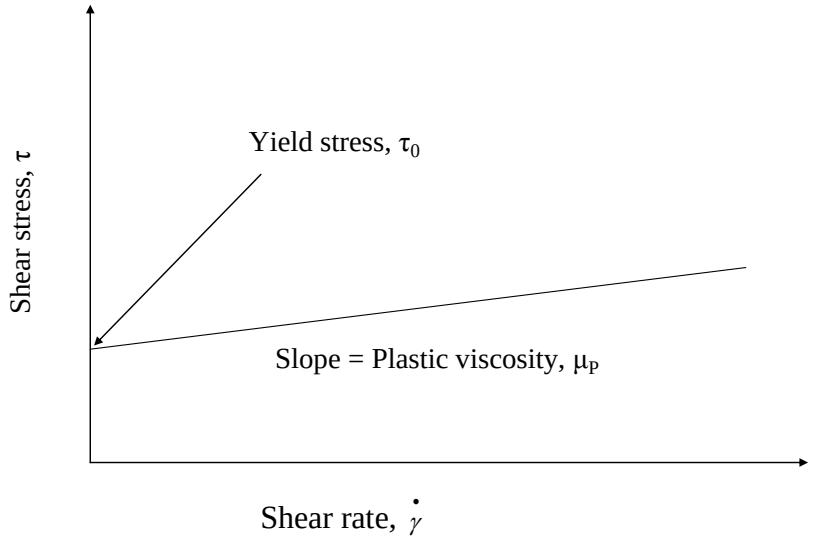

Figure 2.2: Rheogram of a Bingham fluid.

2.2. Effect of particle concentration

2.2.1. Fine particles in water

There is no sharp boundary between coarse and fine particles in terms of their size. The typical size of a fine particle is 10 micron or less. These particles form a homogeneously dispersed mixture when mixed with water or any other fluid, as described by Shook et al. (2002). Due to their small size, they are greatly affected by the Brownian motion of the fluid they are mixed with. According to Litzenberger (2004) and Coussot (1997), the effects of electrostatic repulsive and Van der Waals attractive forces outweigh any effects due to hydrodynamic forces, because of the high surface area to mass ratio of fine particles. The relative magnitudes of these two opposing forces – electrostatic repulsive and Van der Waals attractive - determine the rheology of the fine particle mixture in water, along with the size and concentration of the fine particles. However, which colloidal force term will dominate depends on surface charge of the particle and the pH, ionic strength and ionic species in water.

Michaels and Bolger (1962) described fine particle interactions in detail. According to them, when electrostatic repulsive forces dominate over van der Waals attractive forces, the fine particles will not form flocs with one another and the mixture will then exhibit Newtonian behavior. When Van der Waals attractive forces dominate over the electrostatic repulsive forces, the particles form flocs. The flocs can form larger groups, known as aggregates, depending on the balance of forces acting on them. A floc can thus be viewed as a basic unit which is

formed due to strong attraction among its constituent particles; whereas the strength of attraction among the flocs in an aggregate is much lower.

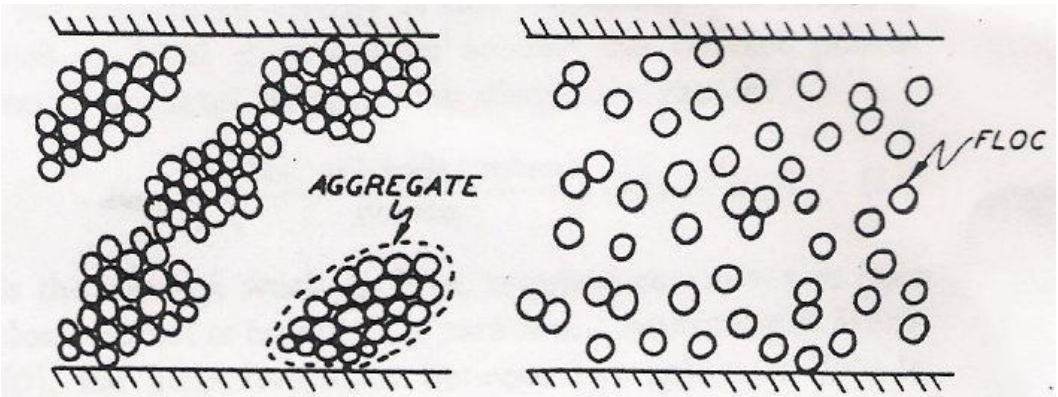

Figure 2.3: Effect of shear on aggregation of flocs (Michaels & Bolger, 1962).

Van Olphen (1977) found that kaolin particle has a plate-like shape; so it has two basal planes (or faces), both of which are negatively charged. Based on the ionic species and their strength in water, these particles can stay dispersed or associate with each other in different ways.

The edge-to-face and edge-to-edge modes of association, as shown in Figure 2.4, lead to the formation of flocs. As evident from the nature of these associations, they entrap a significant amount of water inside the flocs, which reduces the amount of free water in the mixture and thereby increases the viscosity of the mixture.

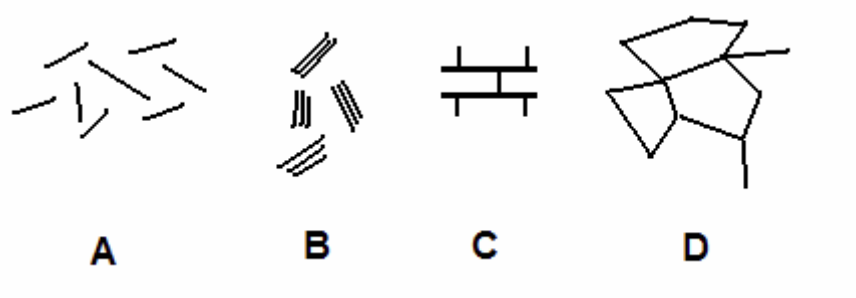

Figure 2.4: Plate like kaolin particle and their association (from Van Olphen, 1977) – A) Dispersed, B) Face-to-face, C) Edge-to-face, and D) Edge-to-edge.

Litzenberger (2004) carried out an experimental program to investigate the effect of flocculant and dispersant on the rheological parameters of kaolin-water mixture. He found that, the addition of a flocculant to the mixture supplied additional positive ions which helped the van der Waals attractive forces to exert more influence over the electrostatic repulsive forces. As a result, flocculation was promoted and mixture yield stress was increased. On the other hand, when a dispersant was added in adequate amount, it formed a complex with the positive ion and thereby reduced the concentration of positive ion from aqueous phase. Then electrostatic repulsive forces dominated over the Van der Waals attractive forces and flocs were destroyed, causing a decrease in yield stress.

Thomas (1961) investigated twenty different fine particle mixtures and showed that Bingham yield stress and Bingham plastic viscosity is primarily dependent on size (d_p) and concentration (C_f) of the fine particles. Based on this work, Thomas (1963) proposed the following relation:

$$\tau_f = A\frac{C_f^3}{d_p^2} \qquad \textbf{2.3}$$

Here, A is an empirical constant which needs to be determined by fitting the data.

Michaels and Bolger (1962) experimented with differently treated kaolin-water mixtures and related the changes in rheological parameters to the volume concentration of flocs (C_{floc}), in stead of fine particles such as kaolin. He proposed that the Bingham yield stress increases with the square of floc volume concentration, and a network strength term which includes $(C_{floc} - C_{0,floc})^3$, where '$C_{0,floc}$' is the minimum concentration of flocs necessary for network formation.

Thomas (1999) mentioned that, the change in Bingham yield stress with fine particle concentration can be approximated with the equation:

$$\tau_f = AC_f^n \qquad \textbf{2.4}$$

Shook et al. (2002) fitted oil sand Mature Fine Tailings data obtained from three tailings pond with the following equation:

$$\tau_f = \exp(13C_f) \qquad \textbf{2.5}$$

Coussot and Piau (1995) suggested a correlation having two empirical coefficients:

$$\tau_f = A\exp(BC_f) \qquad \textbf{2.6}$$

More recently, Thomas (1999) suggested a correlation to determine the plastic viscosity, although it contained an empirical coefficient (B).

$$\mu_f = \exp(BC_f) \qquad \textbf{2.7}$$

Shook et al. (2002) obtained a best fit of their data with a similar expression:

$$\mu_f = \exp(12.5C_f) \qquad \textbf{2.8}$$

The presence of empirical constants in the correlations discussed in this section underscores the fact that the best way to determine the rheology of a fine particle mixture is to carry out experiments with it.

2.2.2. Coarse particles in water

Schaan et al. (2000) suggested that the flow properties of particles which have an average diameter greater than 10 micron are governed mainly by hydrodynamic forces. A mixture containing inert coarse particles in a Newtonian fluid exhibits Newtonian behavior if the particles remain suspended in the fluid and they are too large to be significantly influenced by inter particle attraction forces. The addition of coarse particles to a Newtonian fluid increases the Newtonian viscosity of the resulting mixture. The rheology of such mixtures can be governed by the different types of hydrodynamic forces. Based on excluded volume effect only, Einstein (Michaels and Bolger, 1962 and Thomas, 1963) proposed a relation describing how the mixture viscosity is affected by the coarse particle concentration:

$$\frac{\mu_C}{\mu_L} = 1 + 2.5C_C \qquad \textbf{2.9}$$

Here, μ_C and μ_L are the viscosities of the mixture and the pure fluid, and C_C is the volume concentration of the particles.

The relation applies well to $C_C < 0.05$. In order to extend the applicability of the equation to higher concentrations, attempts were made to incorporate other hydrodynamic effects such as wake effects and lubricated contacts and particle-particle interaction effects including direct contacts, collisions and jamming (Ancey, 2001). For this purpose, Thomas (1965) proposed addition of two terms to Einstein's original equation.

$$\frac{\mu_C}{\mu_L} = 1 + 2.5C_C + 10C_C^2 + 0.00273\exp\left(16.6C_C\right) \qquad \textbf{2.10}$$

Based on the concept originally proposed by Landel et al. (1963), Thomas (1999) emphasized the importance of particle shape and size distribution, and attempted to take account of these effects by including the maximum solids concentration 'C_{max}' in the analysis, which will be discussed further in the context of coarse particle addition to non-Newtonian mixtures. Chong et al. (1971) developed an empirical correlation by successfully fitting the data of various mixtures having a wide range of coarse particles' concentration:

$$\frac{\mu_C}{\mu_L} = \left[1 + 0.75\left(\frac{C_C/C_{\max}}{1 - C_C/C_{\max}}\right)\right]^2 \qquad \textbf{2.11}$$

Schaan et al. (2000) used three different types of coarse particles of similar size but with different sphericity to develop a semi-empirical correlation:

$$\frac{\mu_C}{\mu_L} = 1 + 2.5C_C + 0.16\lambda^2 \qquad \textbf{2.12}$$

Here λ is linear concentration, and is defined as

$$\lambda = \left[\left(\frac{C_{\max}}{C_C}\right)^{1/3} - 1\right]^{-1}$$

2.2.3. Both fines and coarse particles in water

The rheological characteristics of two types of mixtures - flocculating fine particles in water and non-flocculating coarse particles in water – were discussed separately in previous sections. It was emphasized that they exhibit non-Newtonian and Newtonian behavior respectively. A number of researchers including Coussot (1995), Thomas (1999), Sumner et al. (2000), Ancey (2001) and Paulsen et al. (2010) used Bingham plastic model to approximate the rheological behavior of such mixtures. In each case, an increase in Bingham yield stress and Bingham plastic viscosity was observed when coarse particles were added to fine particles' mixtures.

Sumner et al. (2000) showed that the increase in Bingham plastic viscosity with increasing coarse particle concentration follows expected trends. However, the

effect on Bingham yield stress is not well understood, and researchers including Michaels & Bolger (1962), Thomas (1963), Thomas (1999), Sumner et al. (2000) and Paulsen et al. (2010) have not reached any agreement.

Those researchers have proposed several "potential" effects that are responsible for the increase in yield stress upon the addition of a coarse particle fraction. These effects can be useful when interpreting the findings of the present work. However, it should be kept in mind that all of these effects may not apply to the cases studied here.

1. Unless water chemistry is modified in a way that causes electrostatic repulsive forces to dominate over attractive van der Waals forces, fine particles form flocs in a mixture with water and entrap a significant amount of water inside the flocs. The water that is left outside the floc structure at large is known as "free water". If coarse particles are added to an already flocculated fine particle mixture, then some of the free water will be adsorbed on the surface of the coarse particles and form layers of water surrounding the particles (Iler, 1979). According to Grim and Cuthbert (1945), these layers have a typical thickness of 3-10 molecules of water. If significant amount of water is adsorbed on the particles' surfaces, it will not only increase the effective solids concentration, but also reduce the distance among the flocs and aggregates. As a result, the mixture yield stress will go up.

2. When coarse particles are added to a fine particle mixture, it increases the total solids concentration and thus reduces the spacing among the flocs and aggregates. Depending on the size of the coarse particles relative to the mean aggregate size, two things can happen:

(i) If the ratio of coarse particle diameter to aggregate diameter is very large, the theory proposed by Thomas (1963) should hold and yield stress should vary with the cube of coarse particle concentration. This is known as the "crowding effect".
(ii) When the ratio of coarse particles-to-aggregates diameter approaches one, then the coarse particles can disturb the interaction among the aggregates causing the yield stress to increase at a rate which is lower than the cube of coarse particle concentration (Sumner et al., 2000). This is referred to the "shielding effect". This phenomenon may actually occur due to the rearrangement of flocs within the aggregates, rather than due to the so called shielding effect (Sanders, 2010).

3. When the coarse particle component is sand, there is a chance of an attractive force occurring between the flocs and the sand particles due to the similarity of their surface composition. This is in addition to the already established attractive forces among the aggregates. In this case, the sand particles may actually become a part of the aggregates, rather than just reducing the distance among the aggregates as mentioned in 2(i). As a result, the yield stress can increase at a rate which is higher than the cube of sand volume concentration. However, it is not clear yet whether the attraction between coarse particles and aggregates is

significant enough to impact the rheology of the mixture. Additional details about this type of network formation can be found in Ancey (2001).

As mentioned earlier, a number of researchers tried to determine the effect of coarse particles' addition on Bingham yield stress of a fine particle mixture. Sumner et al. (2000) considered a cubic relation, $1/(1-C_C)^3$, to predict the change in Bingham yield stress with coarse particles' concentration (C_C). However, the equation under-predicted the Bingham yield stress at high values of coarse particle concentration. They suggested that the non-spherical shape of the coarse particles makes the effective particle volume greater than the actual volume as they rotate in a shear field, which enhances the effect originated from the crowding of particles. They also discussed the possibility of coarse particles taking part in the floc formation process.

Thomas (1999) experimented with two mine tailings slurries and four differently sized sands, and described the effect of coarse particle concentration on Bingham yield stress of a slimes slurry using the following semi-empirical correlation:

$$\frac{\tau_{0,mix}}{\tau_{0,cf}} = \left(1 - \frac{C_C}{AC_{\max}}\right)^{-2.5} \qquad \textbf{2.13}$$

The relation was found to be in reasonable agreement with experimental data when he used $AC_{max} = 0.9$ in place of $C_{max} = 0.75$, which was originally proposed by Landel et al. (1963) in an analogous correlation for viscosity. It is worth noting that Thomas (1999) considered only two fine particle mixtures, although the range

of coarse particle concentrations he considered was large. Since he used mine tailings slurries directly for mixture preparation without any form of treatment, it was not possible for him to ensure identical water chemistry for all the mixtures he tested. Hence the result was surely affected by different flocculation behavior arising from variation in water chemistry in the mixtures. Additionally, he did not mention if all the experiments were carried out at the same temperature.

Based on the similarity of surface chemistry between the kaolin flocs and sand particles, Paulsen et al. (2010) proposed that sand-floc interactions can be considered to be similar to weak floc-floc interactions, which means the effect due to presence of coarse particles can be substituted by that of an equivalent volume fraction of kaolin flocs. The mixture can be modeled with any of the correlations described in Section 2.2.1.

Fewer correlations were proposed to predict the effect of adding coarse particles on the Bingham plastic viscosity of a fine particle mixture. Thomas (1999) considered the effect using a correlation which is similar to the one he proposed for predicting Bingham yield stress of the same kind of mixture.

$$\frac{\mu_{p,mix}}{\mu_{p,cf}} = \left(1 - \frac{C_C}{AC_{\max}}\right)^{-2.5} \qquad \textbf{2.14}$$

Good agreement with experimental data was obtained using values of AC_{max} in the range of 0.6 to 0.9.

Sumner et al. (2000) used a modified version of Equation 2.10 which incorporated the potential effect of the non-spherical shape of sand particles.

$$\frac{\mu_{p,mix}}{\mu_{p,cf}} = 1 + 2.5C_C + 10C_C^2 + 0.0019\exp(20C_C) \qquad \textbf{2.15}$$

The correlation qualitatively agreed with his experimental findings. However, they used municipal tap water and hence could not maintain a constant state of water chemistry, which might have changed the floc size and affected the accuracy of their results. The applicability of the findings of Sumner et al. (2000) is limited by the fact that all of their kaolin mixtures in water had kaolin concentrations of 9.7% or lower.

2.3. Effect of particle size

Thomas (1961) discussed the effect of particle diameter on Bingham yield stress and Bingham plastic viscosity in detail. The average particle diameter strongly affects the extent of flocculation in a mixture because the diameter is directly related to the surface area available for particles to attach with one another, which is responsible for floc formation in favorable conditions. When particle diameter decreases, an increased number of fine particles take part in the flocculation process and thereby entrap increased amount of water inside the flocs. As a result, the amount of free water decreases, which ultimately causes the mixture yield stress and plastic viscosity to increase. He proposed that the yield stress of a fine particle mixture is inversely proportional to the square of the average diameter of

fine particles. Zhou et al. (1999) also postulated the same type of dependence of yield stress on average diameter of fine particles. Since the present work considered only one type of kaolin particles, it was not possible to investigate the effect of the average diameter of fine particles on the rheological parameters of the mixture.

Based on experiments with coal particles, Sengun and Probstein (1989) said that if the ratio of the diameter of the added coarse particles to the original fine particle diameter was greater than 10, then an increase in coarse particle concentration led to an increase in apparent viscosity which was found to be similar to that of a Newtonian suspension.

Since the effect of particle diameter on Bingham yield stress originates from the flocculation behavior of particles, and since sand particles do not form flocs with one another, there should be no effect of the average diameter of sand particle on Bingham yield stress. This project selected two type of sand with two different average diameters – one is double in size of the other – to find out the influence of sand diameter, if any.

2.4. Couette flow viscometer

Concentric cylinder viscometers are often used to determine mixture rheology. In this device, the mixture is sheared in the gap between two cylinders different diameters. The resulting flow is known as Couette flow. The advantage of using

concentric cylinder viscometer is that it requires a small amount of sample when compared to other viscometers typically used for similar purpose, for example, tube viscometer. In addition to that, the tests are comparatively inexpensive.

The present study used a concentric cylinder viscometer where the inner cylinder (spindle) rotated inside the stationary outer cylinder (cup). A schematic diagram of the geometry of the device used in this research project is given in Figure 2.5. Here, the diameters of the inner and outer cylinder are 'R_1' and 'R_2' respectively and the inner cylinder has the length 'L'.

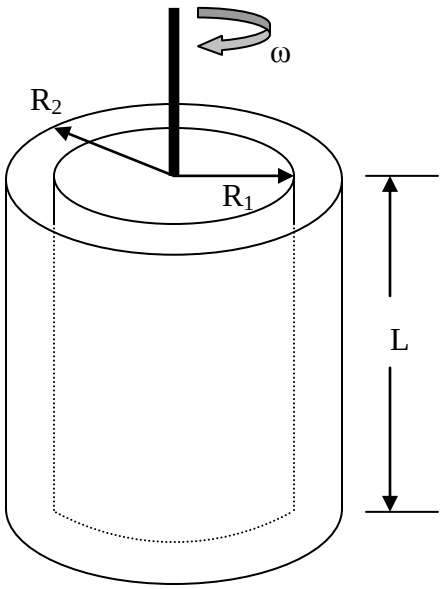

Figure 2.5: Schematic diagram of Couette flow viscometer.

The integrated relationship between the torque and the spindle speed for laminar Couette flow of Bingham fluid mixture is given by the following relationship (Shook et al., 2002):

$$\omega = \frac{T}{4\pi L\mu_p}\left[\frac{1}{R_1^2}-\frac{1}{R_2^2}\right]-\frac{\tau_0}{\mu_p}\ln\left(\frac{R_2}{R_1}\right) \qquad \textbf{2.16}$$

Consider a non-Newtonian mixture whose rheology can be best described by Bingham plastic model. If a set of "torque versus spindle speed" data for a this mixture is plotted in a linear scale, then it is possible to draw a straight line through the data points. The line will not pass through the origin; rather it will intercept the y-axis at a point. The intercept and the slope of the curve will then be read and used for calculating Bingham yield stress 'τ_0'and Bingham plastic viscosity 'μ_p'. For this purpose, Equation 2.16 is reorganized in the following form:

$$\frac{T}{4\pi L\mu_p}\left[\frac{1}{R_1^2}-\frac{1}{R_2^2}\right]=\omega+\frac{\tau_0}{\mu_p}\ln\left(\frac{R_2}{R_1}\right) \qquad \textbf{2.17}$$

Then,

$$Slope=\frac{4\pi L\mu_p}{\left[\frac{1}{R_1^2}-\frac{1}{R_2^2}\right]} \qquad \Rightarrow \mu_p = Slope\times\frac{1}{4\pi L}\times\left[\frac{1}{R_1^2}-\frac{1}{R_2^2}\right]$$

$$Intercept=\frac{4\pi L\mu_p}{\left[\frac{1}{R_1^2}-\frac{1}{R_2^2}\right]}\times\frac{\tau_0}{\mu_p}\ln\left(\frac{R_2}{R_1}\right) \qquad \Rightarrow \tau_0=\frac{Intercept\times\left[\frac{1}{R_1^2}-\frac{1}{R_2^2}\right]}{4\pi L\times\ln\left(\frac{R_2}{R_1}\right)}$$

If the mixture is Newtonian, then there is no yield stress. In that case Equation 2.16 reduces to:

$$\omega = \frac{T}{4\pi L\mu}\left[\frac{1}{R_1^2} - \frac{1}{R_2^2}\right] \qquad \textbf{2.18}$$

The viscosity of the Newtonian mixture (μ, not to be confused with μ_p) is obtained from the slope of the "torque versus spindle speed" curve and is given by:

$$\mu = Slope \times \frac{1}{4\pi L} \times \left[\frac{1}{R_1^2} - \frac{1}{R_2^2}\right]$$

Equation 2.16 is developed based on the condition that the mixture is completely sheared in the concentric cylinder assembly. At a low spindle speed, it is possible that sufficient energy in the form of torque is not applied to shear all the fluid layers inside the gap between the spindle and the cup. In that case, applied shear stress would reduce in strength while transmitting through the layers, and would become lower than the yield stress of the mixture even before it reaches the inside wall of the cup. There will be no shearing in those layers where applied shear stresses are lower than the yield stress of mixture, and those layers will behave as a solid material. This phenomenon is known as incomplete shearing of the mixture. In order to make sure that all the fluid layers across the gap are sheared, the applied shear stress at the cup must be higher than the yield stress of the mixture, as expressed by the following relation:

$$\frac{T}{2\pi R_2^2 L} > \tau_0 \qquad \textbf{2.19}$$

Hence the data which corresponds to incomplete shearing must be rejected from the analysis and determination of mixture's rheological properties.

2.5. Vane viscometer

As discussed earlier, the Bingham yield stress is obtained indirectly by drawing a best-fit straight line through a set of torque versus spindle speed data and extrapolating that line backward so that it intersect y-axis at a point. The same thing can be accomplished in a plot of shear stress versus shear rate, which is nothing but a modified form of a plot of torque versus spindle speed. However, an inherent drawback of Bingham plastic model is that it does not recognize the curvature of the rheogram at the very low spindle speeds. As a result, Bingham yield stress of a mixture is calculated to be higher than what can be called as "True yield stress" of the mixture.

The true yield stress is the minimum shear stress which is required to overcome the attractive Van der Waals forces among the flocs and initiate the flow of the mixture. A vane can be used to make a direct determination of true yield stress; hence it is also known as "Vane yield stress". A qualitative comparison of Bingham yield stress and Vane yield stress are given in Figure 2.6.

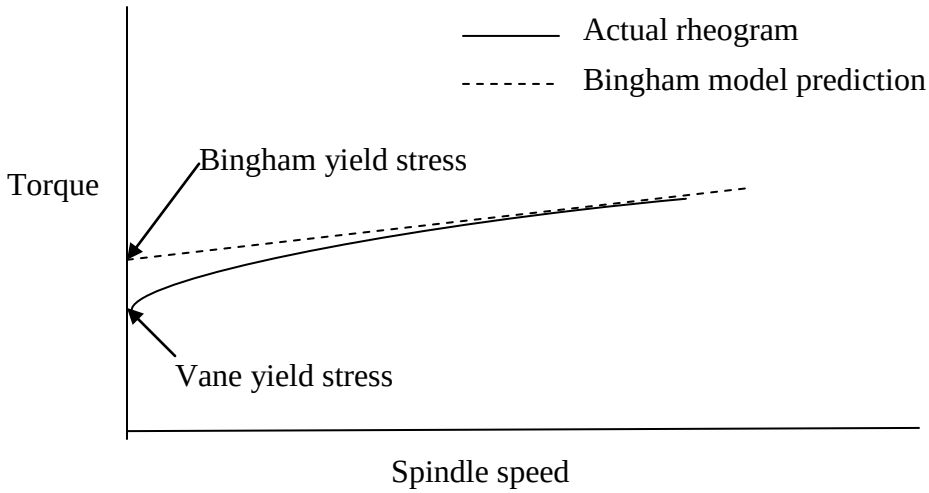

Figure 2.6: Relative position of Bingham and Vane yield stress in a rheogram.

It should be noted that Bingham yield stress is a fitted parameter. On the other hand, Vane yield stress is a true material property which is independent of any fluid model for its determination.

A vane has a number of thin blades of identical length and width, and all of them are connected to a cylindrical shaft at equal angles as shown in Figure 2.7.

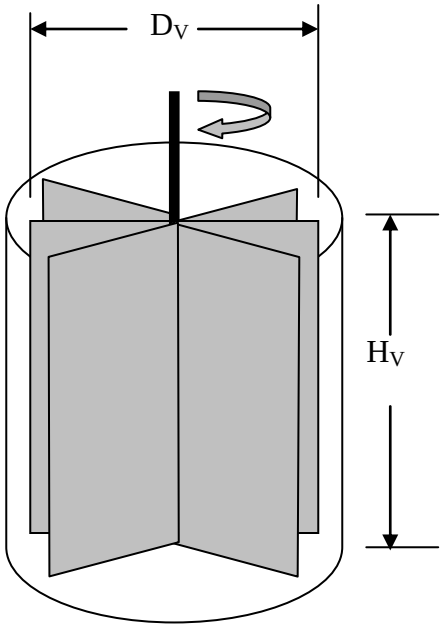

Figure 2.7: Schematic diagram of a vane.

According to Nguyen and Boger (1983), this geometrical shape not only eliminates any possibility of wall slip, but also it minimizes the potential effect of disturbance due to insertion of vane into the sample. The authors recommend that the vane must be fully immersed into the sample, and additionally the following conditions must be met in order to minimize any effect caused by the rigid boundaries of vessel holing the sample:

- Mixture depth = 2 × Vane height (H_V)
- Vessel diameter = 2 × Vane diameter (D_v)

A torque versus time response is used to determine the maximum torque obtained when the vane is rotated at a very low yet constant spindle speed, as shown in Figure 2.8.

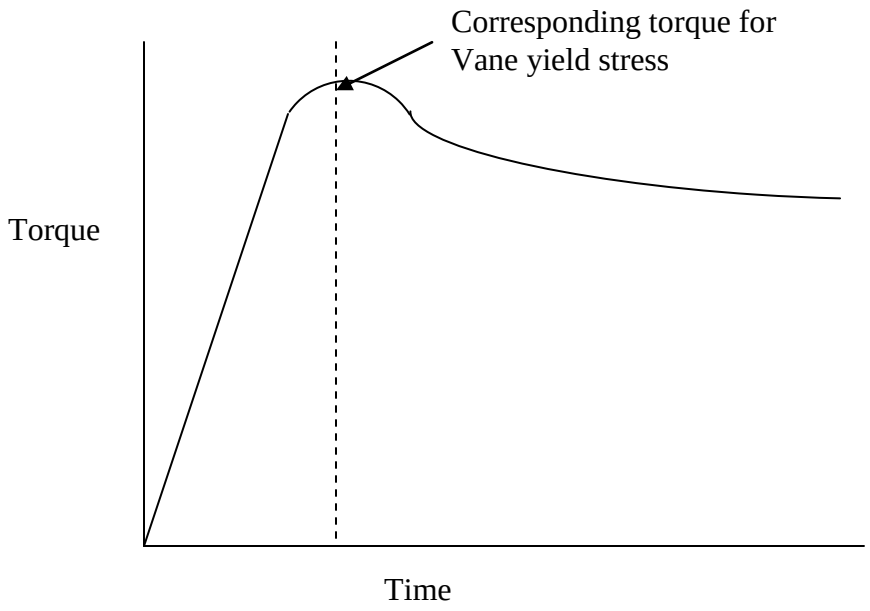

Figure 2.8: Torque versus time curve for vane measurement.

Nguyen and Boger (1983) developed a relation for calculating Vane yield stress from the maximum torque recorded:

$$T_m = \frac{\pi D_V^3}{2}\left[\frac{H_V}{D_V} + \frac{1}{3}\right]\tau_V \qquad \textbf{2.20}$$

or, $$\tau_V = \frac{T_m}{\frac{\pi D_V^3}{2}\left[\frac{H_V}{D_V} + \frac{1}{3}\right]} \qquad \textbf{2.21}$$

2.6. Pipe flow

Consider the horizontal section of a pipeline shown in Figure 2.9. It has a constant cross-sectional area ‘A’ and a constant diameter ‘D’ throughout its entire length of ‘L’. A steady-state operation of the pipeline is assumed with a fluid or mixture whose rheological parameters are also constant over the length.

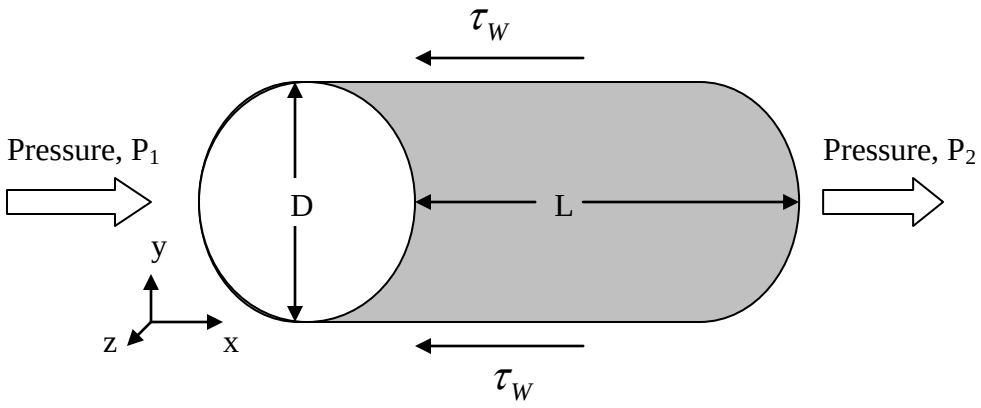

Figure 2.9: Schematic diagram of pipe flow.

A simple force balance over the section produces the following relation:

$$\frac{4\tau_w}{D} = -\frac{dp}{dx} \qquad \textbf{2.22}$$

$$\frac{4\tau_w}{D} = -\frac{\Delta P}{L} \qquad \textbf{2.23}$$

The average velocity 'V' of the mixture is found by dividing the total flow rate 'Q' with the cross-sectional area of the pipe,

$$V = \frac{Q}{A} = \frac{Q}{\frac{\pi}{4}D^2} = \frac{4Q}{\pi D^2} \qquad \textbf{2.24}$$

If the Bingham yield stress and Bingham plastic viscosity of a mixture is known, then Buckingham equation (Shook et al., 2002) can be used to obtain the wall shear stress generated by that mixture when the flow condition is laminar:

$$\frac{8V}{D}=\left(\frac{\tau_w}{\mu_p}\right)\left[1-\frac{4}{3}\left(\frac{\tau_0}{\tau_w}\right)+\frac{1}{3}\left(\frac{\tau_0}{\tau_w}\right)^4\right] \qquad \textbf{2.25}$$

However, the absence of a mechanistic analysis for approximating the turbulent flow behavior of mixtures having yield stresses necessitates the use of an appropriate model. The Wilson and Thomas (1985) model is the most widely used for this purpose, as it does not have any experimentally determined coefficients and also it can be conveniently used for Bingham plastic as well as other non-Newtonian fluids. If turbulent flow of a Newtonian fluid in a pipe is considered, the viscous effects dominate momentum transfer in the viscous sub-layer near the pipe wall, and inertial turbulent mixing is responsible for momentum transfer in the turbulent core. According to Wilson and Thomas (1985), if the fluid is replaced by a non-Newtonian one in the same flow condition and geometry, the viscous sub-layer increases in thickness. If the model is used for a fluid which has an yield stress, the velocity profile exhibit a flattening near the center of the pipe. Overall, there is a less dissipation of energy due to fluid friction when compared to similar situation of a Newtonian fluid. For turbulent flow of a Bingham fluid they provided an equation for calculating the wall shear stress:

$$\frac{V}{\left(\frac{\tau_w}{\rho_{mix}}\right)^{0.5}}=\left[2.5\ln\frac{\rho_{mix}D\left(\frac{\tau_w}{\rho_{mix}}\right)^{0.5}}{\mu_p}+2.5\ln\frac{1-\left(\frac{\tau_0}{\tau_w}\right)^2}{1+\frac{\tau_0}{\tau_w}}+\left(\frac{\tau_0}{\tau_w}\right)\left(14.1+1.25\frac{\tau_0}{\tau_w}\right)\right]$$

2.26

Here, ' ρ_{mix} ' is the mixture density, which can be obtained from the following relation:

$$\rho_{mix} = \sum \rho_i C_i \qquad \textbf{2.27}$$

The density and volume concentration of i^{th} component of the mixture is denoted by ' ρ_i ' and ' C_i ' respectively.

The wall shear stresses obtained from either Buckingham equation or Wilson and Thomas model (1985) can be converted into pressure gradient by using Equation 2.23.

Once the Bingham yield stress and Bingham plastic viscosity of a mixture is provided, two plots of pressure drop ' $\frac{\Delta P}{L}$ ' against average velocity 'V' – one for laminar flow and another for turbulent flow conditions – can be obtained using the correlations discussed above. If these two curves are combined in a single plot, they will intersect each other at a point and the x-coordinate of that point will give the velocity at which the transition from laminar to turbulent flow condition for this particular mixture takes place and the velocity is therefore known as transition velocity (V_T).

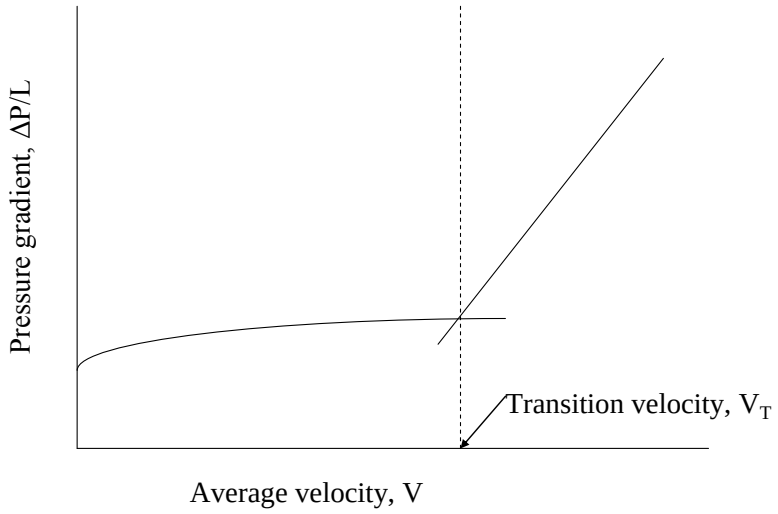

Figure 2.10: Determination of laminar to turbulent transition velocity.

3. Experimental methods

3.1. Materials

3.1.1. De-ionized water

All the experiments were performed using de-ionized water. Municipal tap water contains many mineral ions which can change the flocculation characteristics of fine particles to such an extent that, it affects significant changes in the rheology of the mixture tested. In addition to that, the amount of each of these ions can vary and therefore the chemistry of municipal tap water can not be regarded as constant or unchanged over time. Hence, it was decided to carry out all the experiments with de-ionized water. However, in order to mimic an industrial hard water source, and at the same time to keep control over the water chemistry, calcium chloride di-hydrate was added to de-ionized water at a fixed mass ratio of - calcium chloride di-hydrate : kaolin = 0.001. The de-ionized water was collected from "Elix Advantage Water Purification System" (Millipore SAS, France). The discharged water always had a resistivity greater than 5 MΩ.cm.

3.1.2. Pioneer Kaolin

Kaolin is a component in oil sand along with other types of clays (Masliyah, 2008). Also, numerous other studies have been done using kaolin slurries as idealized fine tailings slurries (Sumner, 2001; Litzenberger, 2003 and Paulsen 2007). The kaolin used in this study was obtained from Kentucky Tennessee Clay Company, USA and supplied by Plainsman Pottery, Edmonton, Canada. According to the supplier, the mean particle size of the kaolin is 1.0 – 1.2 micron.

Saskatchewan Research Council has been using this kaolin for various purposes for a long time. According to their database, which has been developed over the last eight years, the density of the kaolin is 2696 kg/m^3.

It is possible that some ions like calcium, magnesium or sodium are present in kaolin because it might have undergone a weathering process when mineral came into contact with hard water sources. Since the amount of these ions can vary from batch to batch over different production cycles, it was decided to collect all the kaolin from a single bag in order to maintain consistency of the experimental findings.

3.1.3. Lane Mountain (LM) sand

Lane Mountain (LM) sand is one of the two sands used in these experiments. It is produced by Lane Mountain Company, Valley, Washington, USA. Saskatchewan Research Council measured average particle diameter and bulk density of the sand and found them to be 90 micron and 2650 kg/m^3 respectively. Schaan (2000) reported the maximum solids concentration of the sand as 0.505 in his thesis. A size distribution of the sand can also be found in Schaan (2000) thesis.

3.1.4. Granusil Silica (GS) sand

The other sand used in the experiment was Granusil Silica (GS) sand, produced by Unimin Corporation, New Canaan, Connecticut, USA. The sand is also known as Unimin sand. Saskatchewan Research Council supplied the average particle

diameter, bulk density and maximum solids concentration of the sand as 190 micron, 2650 kg/m^3 and 0.6, respectively. A size distribution of the sand is available in Spelay's (2007) thesis.

3.2. Apparatus

3.2.1. Concentric cylinder viscometer

Most of the rheology measurements were conducted with a concentric cylinder viscometer (HAAKE VT550, Thermo Fisher Scientific, Waltham, MA, USA). The viscometer operation is based on the principles of Couette flow, the details of which were described in the previous chapter. The cup-and-rotor assembly of the viscometer is encircled by a temperature control vessel. The temperature of the assembly is controlled by sending a liquid substance through the temperature control vessel. The liquid is supplied from the temperature control unit at the desired temperature. For the purpose of this project, de-ionized water was found to be sufficient as the temperature control liquid. Figure 3.1 shows a photograph of the viscometer and its temperature control unit.

Three different combinations, commonly known as sensor systems, of one cup and three rotors can be employed separately in this viscometer. A photo of the cup and three rotors is given as Figure 3.2. The concentric cylinder tests were performed with the MV1 sensor system. However, each of the three sensor systems was used for calibrating the viscometer at the beginning of this project. The geometry of these sensor systems is provided in Table 3.1.

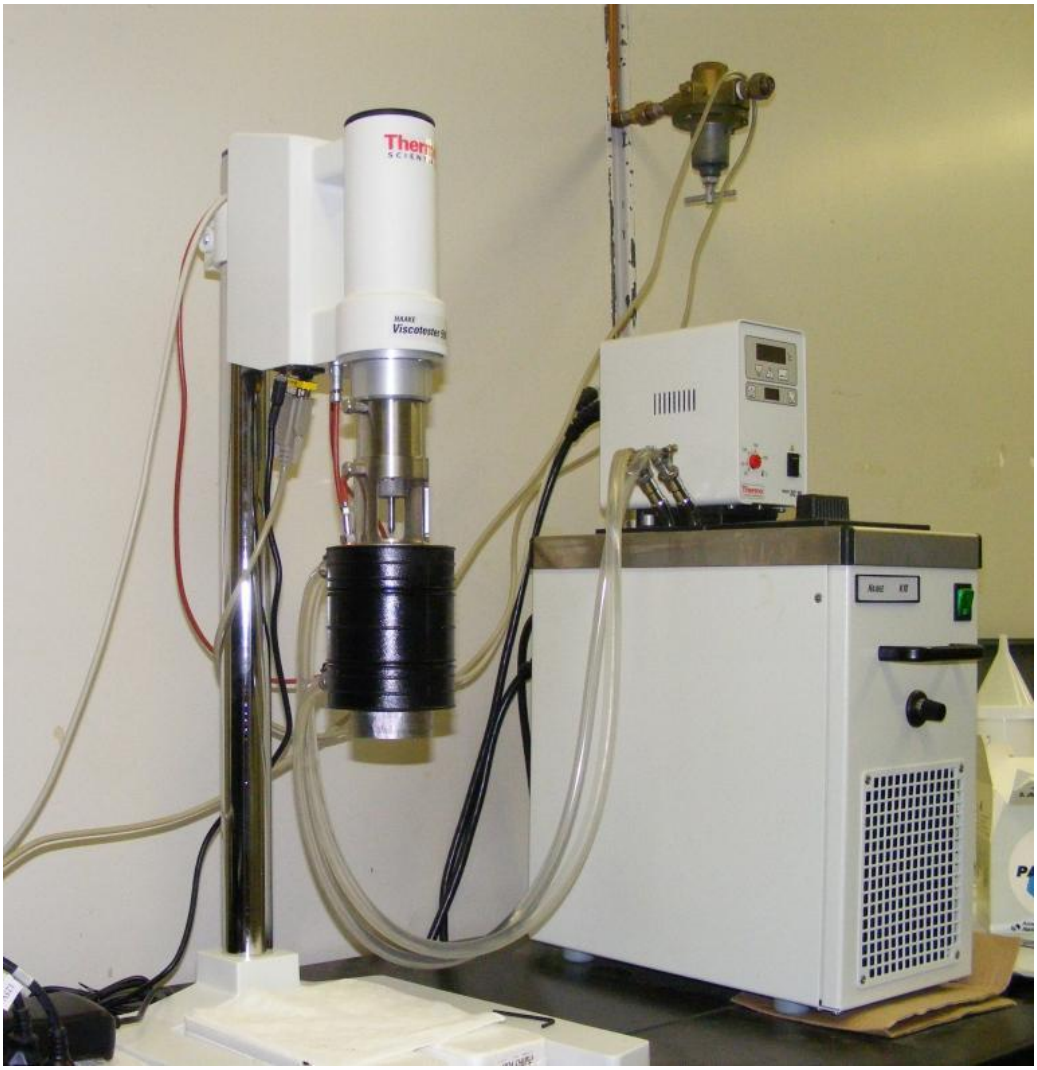

Figure 3.1: The HAAKE VT 550 viscometer and its temperature control unit.

Figure 3.2: The cup and the rotors.

Table 3.1: Sensor systems of Viscotester 550.

Sensor System	**MV1**	**MV2**	**MV3**
Rotor radius (mm)	20.04	18.4	15.2
Rotor height (mm)	60	60	60
Cup radius (mm)	21	21	21
Gap width (mm)	0.96	2.6	5.8
Sample volume (cm^3)	34	46	66

The maximum rotational speed of the viscometer is 800 RPM (revolutions per minutes). The full scale torque (FST) is 0.03 N.m in the range of 0 to 400 RPM, and then it decreases linearly until it become 0.02 N.m at 800 RPM, as shown in Figure 3.3.

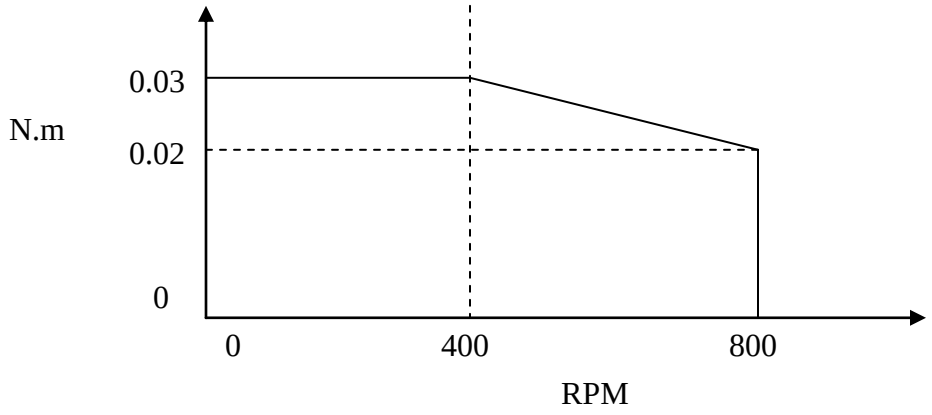

Figure 3.3: Torque-speed characteristics curve of the HAAKE VT 550.

The viscometer was calibrated with three Newtonian standard oils (Cannon Instrument Company, State College, Pennsylvania, USA). The relevant properties of these oils are given in Table 3.2. The objective was to calibrate the device at three operating ranges - low end, intermediate and high end - of the torque scale, and this can be inferred from the variation of viscosities of these oils. Each oil was tested at 20^0C and 25^0C. The sensor system was selected based on its range and the known viscosity of the standard. Actual measurements were compared with predictions obtained using the given viscosity of the standard. A typical calibration result is shown in Figure 3.4.

A partial recalibration was done after a year in operation of the viscometer to confirm the initial calibration. One standard was tested at a single temperature with each of the sensor systems. The results are reported in appendix 1.

Table 3.2: Properties of viscosity standard oil.

	Temperature (^{0}C)	Density (kg/m^3)	Viscosity (mPa.s)
N100	20	881.4	277.7
	25	878.3	200
S200	20	839.6	449
	25	836.5	332.3
N1000	20	849.5	2855
	25	846.5	2008

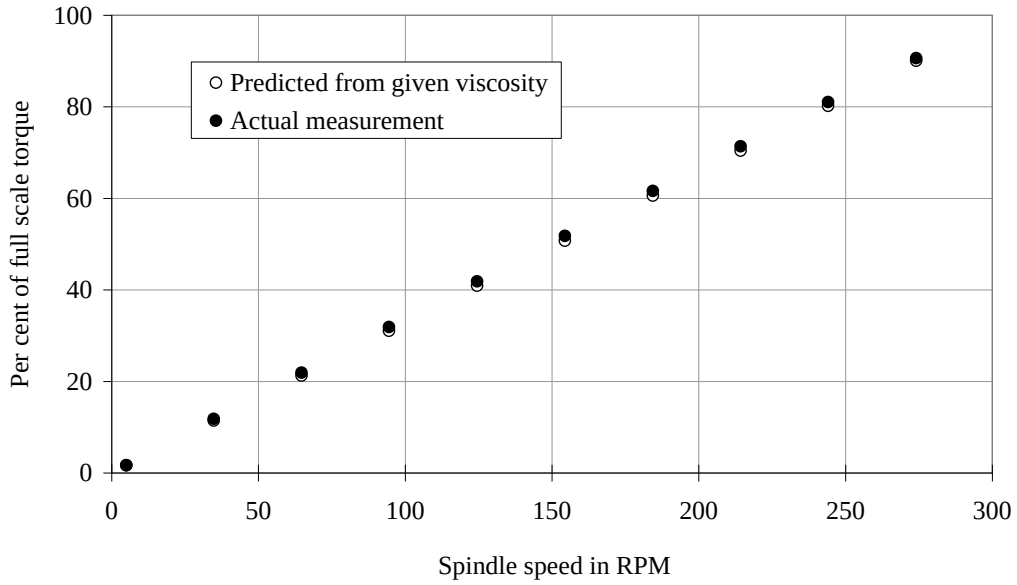

Figure 3.4: Calibration with N100 using MV1 at 20^{0}C.

3.2.2. Vane viscometer

The same viscometer utilized for the concentric cylinder experiments was adapted to be used as a vane viscometer. For this purpose, the cup-and-rotor assembly along with its temperature control vessel was removed, and a vane was attached to the viscometer where the rotor was previously connected. It can be recalled from the principles of vane measurement described in Chapter 2 that the rotational speed of the vane is so low that it generates almost no heat due to shearing, and hence there is no need for a temperature control system during vane measurements. Since the viscometer had already been calibrated for concentric cylinder measurements, no calibration was necessary before conducting experiments with the vane. The FL10 vane was used in this project. It has a diameter of 40 mm and a height of 60 mm. It has six blades connected to a shaft. A photograph of the vane is provided as Figure 3.5.

Figure 3.5: The FL 10 vane.

3.2.3. Mixture preparation equipment

A mixer was used to mix kaolin with water (EUROSTAR power control-visc, IKA Werke GmbH & Company, Germany). The mixer can operate from 50 to 2000 RPM, and can be conveniently used with a wide variety of stirrers. A radial-flow-disk-turbine stirrer entrains less amount of air than a pitched-blade turbine (PBT) stirrer; however, it can not provide good mixing in the upper portion of the mixture. Since a step to remove entrained air from the mixture was included in the experimental procedure, a 45^0 PBT stirrer was selected for all mixing activities.

A vacuum pump (NALGENE Vacuum Pump (aspirator type), Nalge Company, Rochester, New York, USA) was used to liberate the air entrained in the kaolin-water mixtures, the importance of which will be discussed in the Section 3.3.2. A schematic diagram of the pump is provided in Figure 3.6 to illustrate its operating principles. Point '1' is connected to a water source, and when required, water enters the pump through Point '1' and discharges through Point '3'. A continuous flow of water creates a vacuum at Point '2', which is connected to a container where vacuum is applied.

In order to obtain time and shear independent mixture for the experiments, the kaolin-water mixtures were sheared between two concentric cylinders as part of the experimental procedure. Although the shearing could be done in the cup-and-rotor assembly of the viscometer, the MV1 sensor system is capable of shearing only 34 cm^3 mixture at a time.

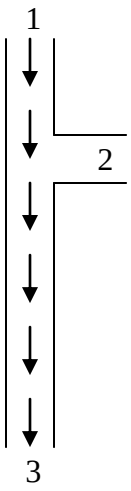

Figure 3.6: Schematic illustration of the principles of operations of a vacuum pump.

Some experiments, including those involving vane, required about 600 cm^3 sheared mixture. A custom-built Couette cell was used for shearing large mixture volumes. It has a rotor made of plastic, which rotates inside a glass-made cylinder. The rotor has a diameter and height of 50 mm and 400 mm respectively. The glass cylinder, which acts as the cup, has a diameter of 59 mm. A photo of the device is given as Figure 3.7.

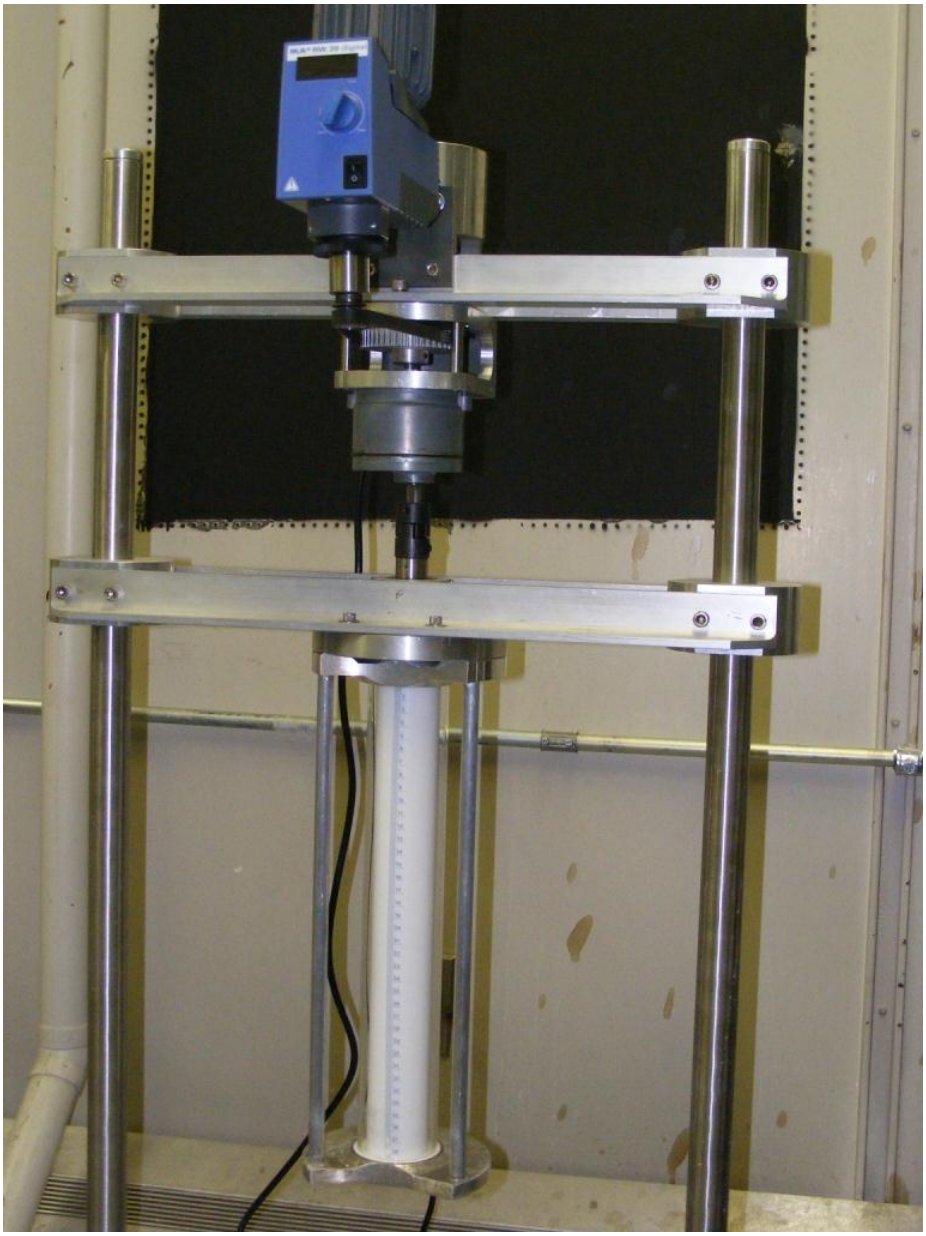

Figure 3.7: The Couette cell.

3.3. Mixture sensitivities

3.3.1. Shear sensitivity

When a freshly prepared mixture is subjected to shear, the flocs rearrange themselves in response to the flow, which can be detected from a trace of measured torque with time for a constant spindle speed. During initial shearing, the mixture experiences irreversible changes and ultimately reaches an equilibrium state, which is different from the initial state when the fresh mixture was at rest. Hence, if the mixture is not sheared for an extended period of time to allow the equilibrium state to be attained, the determination of rheological properties is bound to be affected by the shear sensitive nature of the mixture. According to Schaan et al. (2004), the time required to reach the equilibrium state is a function of shear rate: higher shear rates can be used to more rapidly produce a time-independent mixture.

Figure 3.8 shows the shear dependency of a kaolin-water mixture that was sheared for 60 minutes in the concentric cylinder viscometer. Here the curve stabilized after twenty-five minutes of shearing; hence constant and reproducible results could only be obtained if rheological measurements were done after 25 minutes. A shearing time of 30 minutes was selected for all kaolin-water mixtures. Thus it was ensured that time and shear independent mixtures were used for all the tests conducted during the project.

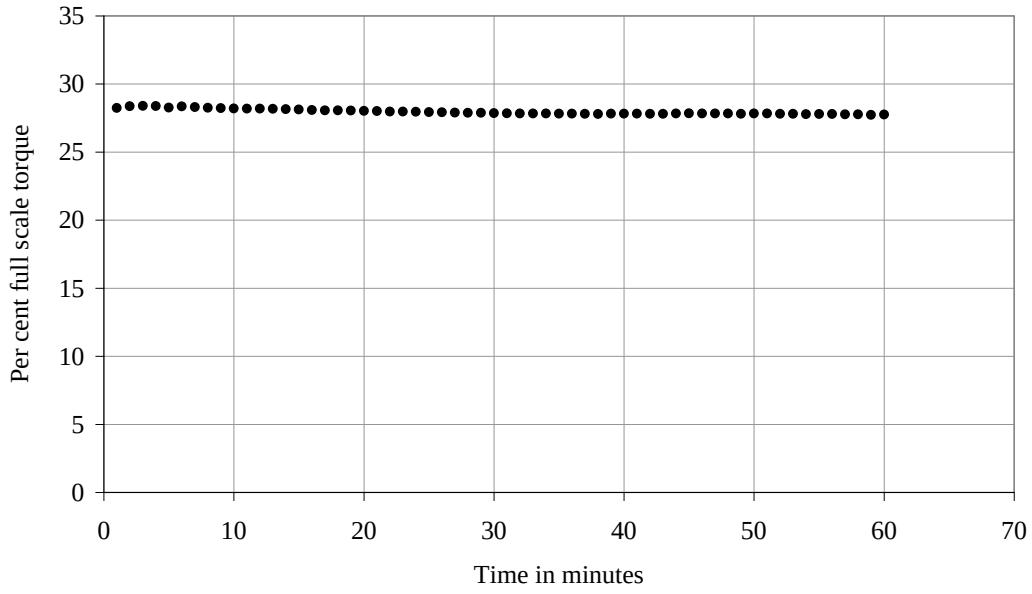

Figure 3.8: Shear sensitive behavior of 19% kaolin-water mixture with a $CaCl_2.2H_2O$: Kaolin (mass ratio) = 0.0028 at 400 RPM.

3.3.2. Entrained air

When kaolin is added to water, a significant amount of air is entrained into the mixture. If the addition is carried out very slowly, less air will be entrained. However, it is not possible to prevent some air entrainment during mixing, no matter how slow the addition is.

If the concentration of the kaolin is high enough such that the slurry exhibits a yield stress, the entrained air bubbles can not escape and therefore remained entrapped inside the mixture. These bubbles occupy spaces which could have been occupied by the mixture, and thus it can affect the density of the mixture. Moreover, the presence of a lot of such bubbles in the small gap between the

spindle and the cup of the concentric cylinder viscometer can change the rheology of the sample. Hence, it is very important to remove those air bubbles to ensure reproducible, stable rheological properties of the kaolin-water mixture.

A vacuum can be applied on the mixture, which can help the air bubbles to overcome the yield stress of the mixture. The limitation of the vacuum is that it is applied on the free surface of the mixture and may be effective for the upper portion of the mixture. Additionally, a magnetic bar can be stirred at the bottom of the mixture container, which can help the bubbles in the lower portion to rise toward the free surface of the sample. Hence, the experimental procedure used in this project included vacuuming the mixture for a specified time while stirring the magnetic bar for the latter 50% of that time. For example, for a 25 minutes vacuum period, there will be no magnetic stirring for the first 12.5 minutes to let air bubbles in the upper portion of the sample to escape the mixture, and then magnetic stirring will be done for the rest of time to help liberate the air bubbles in the bottom part of the sample.

3.3.3. Coarse particles settling

A non-Newtonian mixture having a sufficiently high yield stress can prevent the coarse particles from settling out of the mixture and accumulating at the bottom of the container, as long as the mixture is in a stationary state (Gillies et al., 2002). However, when the mixture is sheared, the effect of the yield stress is considerably diminished and the coarse particles will settle. There are several

methods available in the literature to calculate the “hindered settling velocity” of coarse particles settling in a Newtonian fluid at its stationary state, including the one proposed by Wilson et al. (2003). However, a method which takes into account the presence of a yield stress of a Bingham fluid subjected to shearing in a concentric cylinder assembly is yet to be proposed. Hence, instead of calculating the hindered settling velocity to determine the extent of mixture segregation, an indirect method of finding the effect of sand settling on mixture rheology was utilized. For this purpose, torque versus time responses for the highest sand concentration tested with each kaolin concentration were recorded for the planned duration of the experiment. If the difference between the highest torque and the lowest torque value after stabilization of any response curve was found to be lower than 3% in terms of maximum torque of the viscometer, it was inferred that significant amount of sand would not settle for the duration of the experiment. In addition to that, if settling was not a problem for the highest sand concentration considered with a particular kaolin concentration, then it would not be a problem for other sand concentrations tested with this particular kaolin-water mixture. This indirect method of determining the impact of sand settling on mixture rheology actually set the lower limit of kaolin concentration which can be satisfactorily tested with sand particles.

3.4. Procedures and matrices

3.4.1. Concentric cylinder viscometer tests

A general procedure for mixture preparation and measurement in the concentric cylinder viscometer was developed for a sand-kaolin-water mixture; however, the procedure can be conveniently adapted for testing a kaolin-water mixture by ignoring a number of steps. The main goal of the procedure was to eliminate, or at least minimize, the negative effects of different sensitivities of the mixture, and at the same time, maximize the reliability and reproducibility of the experimental data. All concentric cylinder viscometer tests were performed at a constant temperature of 20^0C. The fine fraction (< 75 micron) of the sand was sieved out before adding it to the kaolin-water mixture, to avoid any potential changes in fines concentration in the mixture. Moreover, the fine sand can affect the flocculation characteristics of the mixture.

The procedure is as follows:

1. Take required amount of de-ionized water in a beaker with baffles placed inside, with a target to produce 500 cm^3 of kaolin-water mixture in total.
2. Submerge the mixer in the water and begin mixing at 200 RPM. This RPM does not promote air entrainment.
3. Add the pre-weighed amount of kaolin very slowly.
4. Add required amount of $CaCl_2.2H_2O$, such that $CaCl_2.2H_2O$: kaolin (w/w) = 0.001.

5. Mix for 30 minutes at an RPM, which is sufficient for good mixing, but not strong enough to induce air entrainment. This RPM depends on the kaolin concentration of the mixture.
6. Vacuum 200 cm^3 mixture for 25 minutes, while using magnetic stirrer simultaneously for the last 12.5 minutes.
7. Shear a 34 cm^3 sample of mixture in the viscometer for 30 minutes, at a spindle speed which is higher than the highest spindle speed planned for the kaolin-water experiments. For example, a spindle speed of 400 RPM was used to shear all the kaolin-water mixtures for 30 minutes, as the highest spindle speeds used in rheological measurements of kaolin-water mixtures were always lower than 400 RPM.
8. Conduct a series of tests where the torque is measured as a function of spindle speed.
9. Transfer the mixture from the viscometer to a beaker.
10. Place a second sample in the viscometer and repeat step 7. Add this sample to the same beaker of step 9.
11. Add a pre-weighed amount of sand to the beaker and mix by hand.
12. This step is for mixtures having GS sand only. Shear the sand-kaolin-water mixture in the viscometer for 2 minutes at a spindle speed which is higher than the highest spindle speed planned for the sand-kaolin-water experiments.
13. Test the sand-kaolin-water mixture in the concentric cylinder viscometer.
14. Determine the kaolin volume concentration in the kaolin-water mixture.

15. Determine the sand volume concentration in the sand-kaolin-water mixture.

When testing a kaolin-water mixture, steps 9-13 and 15 are not required.

In order to determine if the settling of coarse particles could significantly affect the accuracy of the measurement, a torque versus time response can be taken for the highest sand concentration considered with each of the kaolin concentration described in the experimental matrix. In that case, step 12 should be removed and step 13 should be rewritten as, "Take a torque versus time response of the sand-kaolin-water mixture".

It is worth mentioning that

$$C_f = \frac{\overline{V}_f}{\overline{V}_f + \overline{V}_w}$$

and $$C_C = \frac{\overline{V}_C}{\overline{V}_C + \overline{V}_f + \overline{V}_w}$$

Here, C_C = Sand volume concentration in sand-kaolin-water mixture

C_f = Kaolin volume concentration in kaolin-water mixture

$\overline{V}_C$ = Volume of sand

$\overline{V}_f$ = Volume of kaolin

$\overline{V}_w$ = Volume of water

The experimental matrix used for both LM and GS sand is given in Table 3.3.

Table 3.3: Experimental matrix for concentric cylinder viscometer tests.

		Kaolin concentration (% vol.) in kaolin-water mixture				
		10	14	17	19	22
LM or GS Sand (% vol.) concentration in sand-kaolin-water mixture	0	×	✓	✓	✓	✓
	5	×	✓	✓	✓	✓
	10	×	✓	✓	✓	✓
	15	×	✓	✓	✓	✓
	20	×	✓	✓	✓	✓

3.4.2. Comparison tests of fresh and scalped kaolin-water mixture

Experiments were conducted to investigate if sand particles affect the water chemistry in any way, or if they adsorb significant amount of water on the surfaces which can affect the rheology of the mixture. It was decided to perform concentric cylinder viscometer tests on a kaolin-water mixture twice – one before the addition of sand and again after removing the sand particles. Paulsen (2007) followed a similar procedure for these tests.

However, the separation of kaolin-water mixture from a sand-kaolin-water mixture was found to be a difficult task. It was not possible to separate enough kaolin-water mixture for a single concentric cylinder viscometer test when a 75 micron mesh sieve was used, because any sand-kaolin-water mixture dealt in this project had its yield stress and plastic viscosity high enough to partially resist the

flow of kaolin-water mixture through that sieve. To facilitate the passage of kaolin-water mixture through the sieve, a 125 micron mesh sieve was taken. Since the opening of 125 micron mesh sieve was larger than the average diameter of LM sand particles used in this project, it was decided to perform the experiments with GS sand only.

If sand had any effect on water and its chemistry, then detecting the effect should be easier if the sand concentrations used in the experiments were relatively high. Hence, the two highest sand concentrations considered in this project – 15% and 20% - were selected for the comparison tests, against a kaolin concentration of 17%. As previous, all tests involving the concentric cylinder viscometer were performed at a constant temperature of 20^0C and the fine fraction was separated out from the sand to make sure that no fine sand joins the kaolin particles already present in the mixture and thereby affect floc structures.

The procedure for comparison tests are as follows:

1. Take required amount of de-ionized water in a beaker with baffles placed inside, with a target to produce 800 cm^3 of kaolin-water mixture in total.
2. Submerge the mixer in the water and begin mixing at 200 RPM. This RPM does not promote air entrainment.
3. Add the pre-weighed amount of kaolin very slowly.
4. Add required amount of $CaCl_2.2H_2O$, such that $CaCl_2.2H_2O$: kaolin (w/w) = 0.001.

5. Mix for 30 minutes at an RPM, which is sufficient for good mixing, but not strong enough to induce air entrainment. This RPM depends on the kaolin concentration of the mixture.
6. Vacuum 200 cm^3 mixture for 25 minutes, while using magnetic stirrer simultaneously for the last 12.5 minutes. Repeat this step 4 times to accumulate at least 700 cm^3 mixture.
7. Shear a 300 cm^3 mixture in the Couette cell for 60 minutes, at a rotor speed that is higher than the highest speed planned for the kaolin-water experiments. Repeat this step twice to accumulate approximately 600 cm^3 mixture.
8. Test the kaolin-water mixture in the viscometer.
9. Add a pre-weighed amount of sand to the beaker and mix by hand.
10. Test the sand-kaolin-water mixture in the viscometer.
11. Take the sand-kaolin-water mixture on a 125 micron sieve. The sieve is then covered with a lid and a pan is placed at the bottom. The lid-sieve-pan assembly is then put in a sieve shaker.
12. Operate the shaker for 15 minutes to separate kaolin-water mixture from the sand-kaolin-water mixture to be tested in the viscometer.
13. Determine the kaolin volume concentration in the fresh kaolin-water mixture.
14. Determine the sand volume concentration in the sand-kaolin-water mixture.

15. Determine the kaolin volume concentration in the scalped kaolin-water mixture.

3.4.3. Supernatant water chemistry

The effect of the addition of sand on the water chemistry of the kaolin-water mixture was determined by conducting an ion analysis of the supernatant water. Four identical mixtures containing 20% (by volume) LM sand in water were prepared in four identical beakers and left undisturbed for four different time periods – 1 day, 2 days, 3 days and 4 days. For each of the sample, all the sand particles settled to the bottom of the beaker, leaving a clear zone of supernatant water above. Two samples of the supernatant water were collected from each beaker. These eight samples were sent to the Syncrude Research Center (Edmonton, Alberta, Canada) for the determination of ionic contents in the supernatant water. They investigated the presence and amount of thirty-five ions, for example, chloride, sulfate, sodium, calcium, magnesium among others, for each of the sample. Additionally, the pH and conductivity of each of the sample were also determined. The results of the analysis are presented and discussed in Section 4.2.2.

3.4.4. Vane viscometer tests

The settling of coarse particles is not a problem for yield stress measurements with vane, since it is carried out at a very low RPM. Thus, a torque versus time response is not required to determine if coarse particle settling affects the

experimental results. The change in torque with time at a very low RPM reveals the "true" yield stress of the mixture, and hence it forms the core part of vane viscometer tests' procedure.

The amount of sample necessary for vane measurements depends on the type of vane used, the choice of which in turn is dependent on the rheology of the mixture. The FL10 vane was selected considering the combinations of sand and kaolin concentrations planned for vane measurement. This vane requires 600 cm^3 of sample for each test to fulfill the criteria recommended by Nguyen and Boger (1983), which were reported in Chapter 2.

As previous, the fine fraction (< 75 micron) of the sand was sieved out before adding it to the kaolin-water mixture.

The procedure for vane viscometer tests are as follows:

1. Take required amount of de-ionized water in a beaker with baffles placed inside, with a target to produce 800 cm^3 of kaolin-water mixture in total.
2. Submerge the mixer in the water and begin mixing at 200 RPM. This RPM does not promote air entrainment.
3. Add the pre-weighed amount of kaolin very slowly.
4. Add required amount of $CaCl_2.2H_2O$, such that $CaCl_2.2H_2O$: kaolin (w/w) = 0.001.

5. Mix for 30 minutes at an RPM, which is sufficient for good mixing, but not strong enough to induce air entrainment. This RPM depends on the kaolin concentration of the mixture.
6. Vacuum 200 cm^3 mixture for 25 minutes, while using magnetic stirrer simultaneously for the last 12.5 minutes. Repeat this step 4 times to accumulate at least 700 cm^3 mixture.
7. Shear a 300 cm^3 mixture in the Couette cell for 60 minutes, at a rotor speed that is higher than the highest speed planned for the kaolin-water experiments. Repeat this step twice to accumulate approximately 600 cm^3 mixture.
8. Test the kaolin-water mixture in the Vane viscometer at 0.01 RPM for 300 seconds.
9. Add a pre-weighed amount of sand to the beaker and mix by hand.
10. Test the sand-kaolin-water mixture in the Vane viscometer at 0.01 RPM for 300 seconds.
11. Determine the kaolin volume concentration in the kaolin-water mixture.
12. Determine the sand volume concentration in the sand-kaolin-water mixture.

When testing a kaolin-water mixture, steps 9-10 and step 12 are not required.

Four combinations arising from two kaolin concentrations, 17% and 19%, and two GS sand concentrations, 15% and 20%, were used for experimentation with Vane viscometer.

4. Results and discussion

4.1. Mixture deaeration tests

The application of vacuum helped entrained air bubbles to overcome the yield stress and eventually escape from the mixture. As the vacuum was applied on the surface of the mixture taken in a conical flask, the lower portion of the mixture was less influenced by the vacuum. A magnetic stirring bar was used during the latter half of the vacuuming process to facilitate the liberation of air bubbles from the lower region of the mixture. The procedure is described in Section 3.3.2.

In order to determine the most effective deaeration procedure, five identical kaolin-water mixtures containing 19% kaolin by volume and a $CaCl_2.2H_2O$ to kaolin mass ratio of 0.0028 were prepared. Each mixture was sheared at 400 RPM in the concentric cylinder viscometer for 60 minutes. The torque versus time response for each mixture is plotted in Figure 4.1. It is found that the mixture's shearing response for 25 minutes vacuum with stirring of 12.5 minutes did not vary significantly from that of 20 minutes vacuum with a stirring time of 10 minutes. Hence, the combination of 25 minutes vacuum with 12.5 minutes stirring was included in the procedure followed for all experiments carried out in this project.

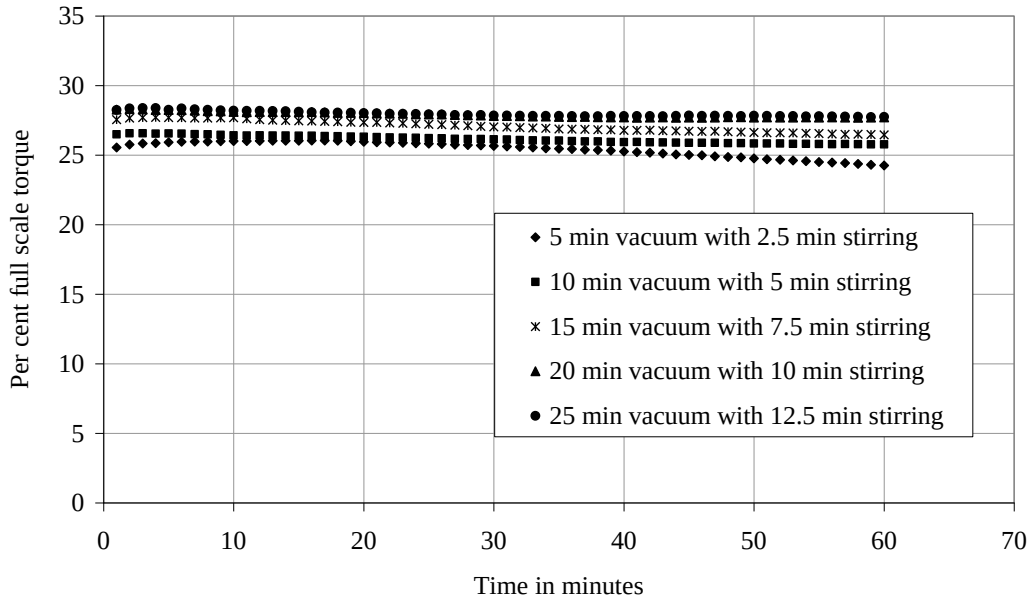

Figure 4.1: Torque versus time response for 19% kaolin-water mixture with a $CaCl_2.2H_2O$: Kaolin (mass ratio) = 0.0028 at 400 RPM, for different combinations of vacuum and stirring times.

4.2. Inertness of sand

4.2.1. Comparison of fresh and scalped fine-particle mixtures

If sand could significantly alter the amount and chemistry of water, then the true contribution of coarse particles to Bingham yield stress and plastic viscosity of the mixture could not be identified. Hence, the rheology of a kaolin-water mixture was determined twice – once before adding the sand and again after removing the sand. Before the addition of sand, the kaolin-water mixture is called as fresh mixture. When sand particles are separated from a sand-kaolin-water mixture, the resulting kaolin-water mixture is referred as scalped mixture. The rheology of these two mixture condition were compared to find any effect of coarse particles.

Figure 4.2 shows the torque response plot of comparison test conducted using 17% kaolin in kaolin-water mixture and 20% GS sand in sand-kaolin-water mixture.

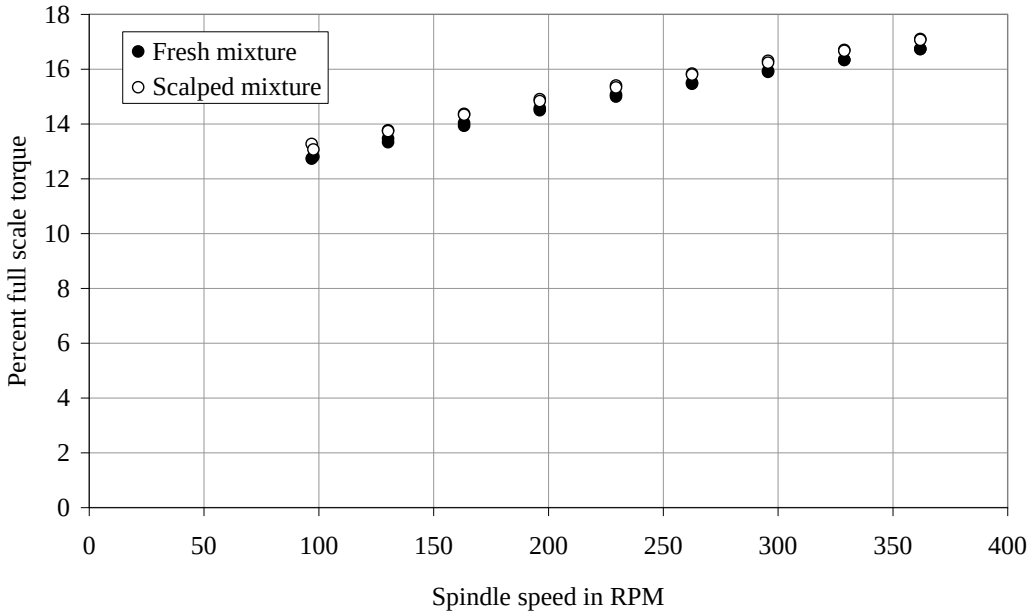

Figure 4.2: Concentric cylinder viscometer outputs for a fresh 17% kaolin-water mixture (before adding 20% sand) and a scalped mixture.

A similar test was carried out with another combination of kaolin and sand concentrations. The Bingham yield stress and plastic viscosity of each mixture, measured before sand addition and after the sand is removed, are provided in Table 4.1. No significant difference between the two conditions was found, which means sand particles neither altered the water chemistry nor adsorbed an appreciable amount of water. Hence it can be said that the change in Bingham yield stress and plastic viscosity when sand particles are added to kaolin-water mixture are related to the different mechanisms described Chapter 2, and not due

to any manipulation of water chemistry by sand particles. Moreover, the change in rheology caused by sand addition to a kaolin-water mixture is a reversible process in the sense that, when sand particles are removed, the kaolin-water mixture's rheology returns to its previous state.

Table 4.1: Comparison of the rheological properties of kaolin-water mixtures, before adding sand and after sieving it out.

Combinations tested	Mixture properties	Before adding sand	After sieving out sand
17% kaolin and 15% sand	Kaolin Concentration (% vol.)	16.9	17.1
	Bingham yield stress (Pa)	21.4	21.7
	Plastic viscosity (mPa.s)	12.7	12.4
17% kaolin and 20% sand	Kaolin Concentration (% vol.)	17.1	17.1
	Bingham yield stress (Pa)	21.8	22.5
	Plastic viscosity (mPa.s)	12.5	12.4

4.2.2. Chemical analysis of supernatant water

An ion analysis of supernatant water collected from a sand-water mixture can reveal if sand particles significantly changes the ionic content of the water used in the mixture, and thus affect the chemistry of water. For this purpose, four identical 20% sand-water mixtures were prepared and left undisturbed for different durations. Two samples of supernatant water were collected from each

of the mixtures. These eight samples were tested at Syncrude Research Centre (Edmonton, Alberta, Canada). The pH and conductivity of the samples are reported in Table 4.2, and the concentrations of the major ions are given in Table 4.3. The results for all 35 ions tested are available in Appendix 4. No significant difference was found among the eight samples for each of the ion tested. These findings reinforce the reasoning made in previous section that sand particles have no effect whatsoever on the water chemistry of the mixture.

Table 4.2: pH and conductivities of the supernatant water samples.

Contact time (day)	Samples	pH	Conductivity (mS/cm)
1	Sample A	7.9	0.06
	Sample B	7.8	0.06
2	Sample A	7.9	0.06
	Sample B	7.8	0.06
3	Sample A	8.2	0.05
	Sample B	8.0	0.05
4	Sample A	8.0	0.06
	Sample B	8.0	0.06

Table 4.3: Major ions of the supernatant water samples.

Contact time (day)	Samples	Na^{+} (ppm)	Ca^{++} (ppm)	Mg^{++} (ppm)	Si^{+4} (ppm)	Cl^{-} (ppm)
1	Sample A	6.5	3.4	1.2	1.6	4.4
	Sample B	6.2	3.3	1.2	1.9	4.7
2	Sample A	6.3	3.4	1.2	1.3	5.0
	Sample B	6.2	3.3	1.2	1.6	4.9
3	Sample A	5.9	3.2	1.1	1.4	4.2
	Sample B	4.6	3.3	1.2	1.4	4.6
4	Sample A	6.6	3.1	1.2	2.9	5.2
	Sample B	5.5	3.3	1.2	3.5	5.4

4.3. Settling of coarse particles

If the sand-kaolin-water mixture has a yield stress which is high enough to balance the stress generated by the weight of a sand particle, the sand will not settle as long as the mixture is in a stationary state. When the mixture is subjected to shear, the deposition of sand particles will occur (Gillies et al., 2002). However, if the concentration of kaolin in the mixture is high, the deposition of sand particles for the duration of a test may not be sufficient to induce significant error in measuring the rheology of that mixture. For this purpose, 20% sand was combined with mixtures containing 10%, 14%, 17%, 19% and 22% kaolin (by

volume) mixtures and a torque response curve was recorded for each mixture for a period of ten minutes, which is higher than the duration of any rheological test conducted in this project. The curves obtained for mixtures containing LM sand are shown in Figure 4.3, and those for GS sand and kaolin are given in Figure 4.4.

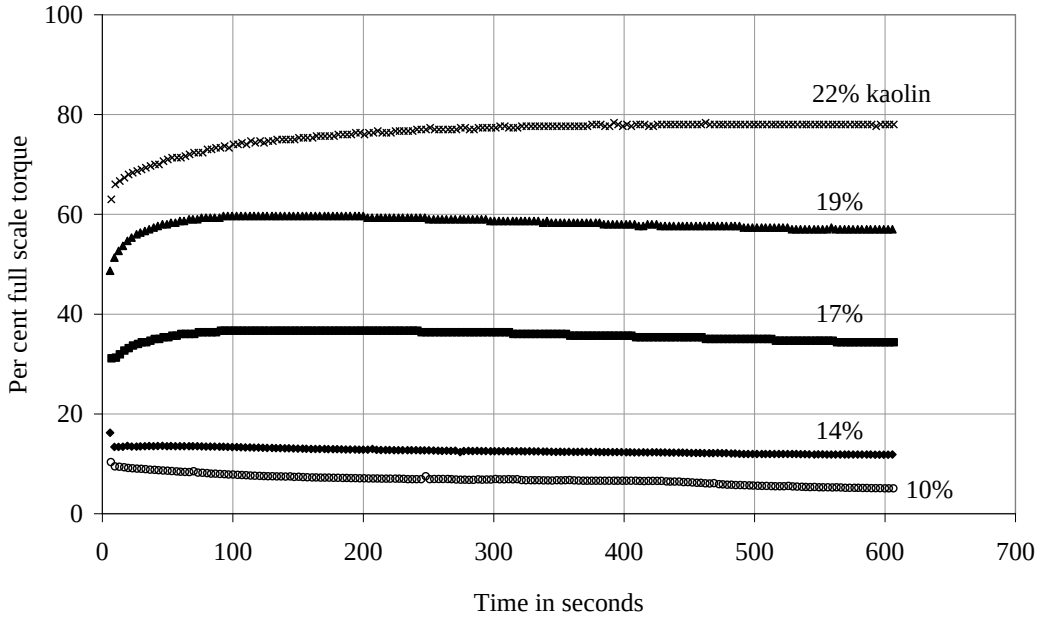

Figure 4.3: Torque response curves for different kaolin mixtures containing 20% LM sand (by volume) and a mass ratio of $CaCl_2.2H_20$:Kaolin=0.001. All readings recorded at 400 RPM, except those reported for 22% kaolin mixture, which were recorded at 75 RPM.

It is seen from the figures that both of the mixtures containing 10% kaolin experienced continued deposition of sand particles for the entire durations of the torque versus time response tests. Hence, it was decided not to conduct any rheological test that involved the addition of sand particles to a 10% kaolin-water mixture. For the mixtures having 14%, 17% and 19% kaolin concentration, there

are possible indications that sand deposition occurred. However, the difference between the measured torque at t=100s and that measured at t=600s was found to be less than 3% for each of these kaolin concentrations. This finding suggests that the magnitude of sand deposition is not high enough to affect the rheology measurements made for sand/kaolin mixtures containing 14%, 17% and 19% kaolin. For the mixtures containing 22% kaolin, there was no sign of sand deposition.

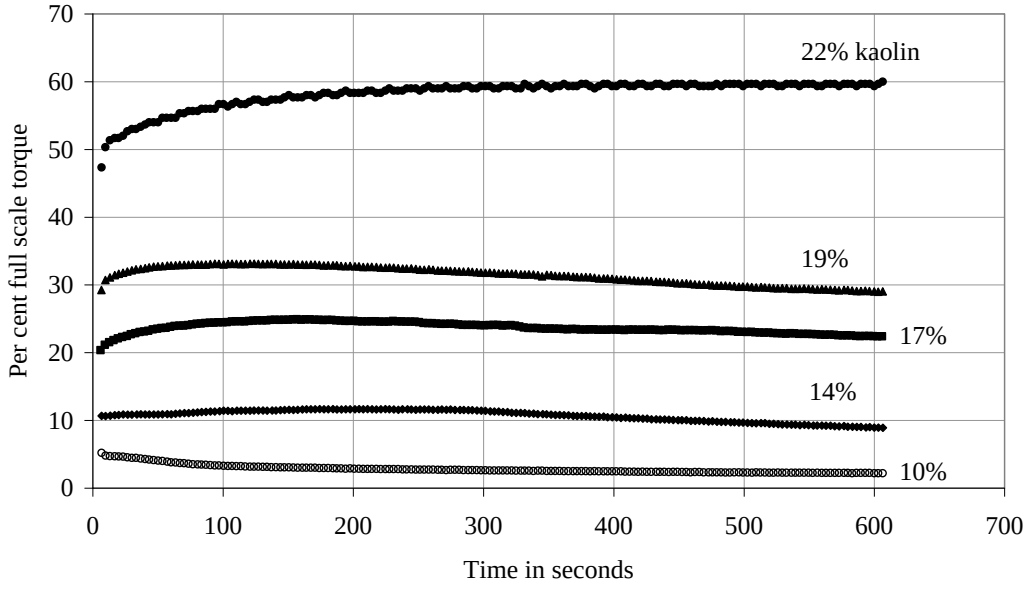

Figure 4.4: Torque-time response for different kaolin mixtures with 20% GS sand and a mass ratio of $CaCl_2.2H_20$:Kaolin=0.001. All readings recorded at 200 RPM, except those reported for 22% kaolin mixture, which were recorded at 75 RPM.

4.4. Kaolin-water mixture rheology

The Bingham fluid properties of the sand-free kaolin-water mixtures containing were first determined. These values are required to distinguish the actual contribution of sand particles to those parameters of the sand-kaolin-water mixture. The effect of kaolin volume concentration on the Bingham yield stress is shown in Figure 4.5 and 4.6, and the variation of plastic viscosity with kaolin concentration is shown in Figure 4.7. Error bars shown in the figures are determined from the yield stresses and plastic viscosities of four kaolin-water mixtures of same concentration reported in this thesis. Error bars are not shown for kaolin concentration, as they are negligible compared with those of Bingham yield stress or plastic viscosity.

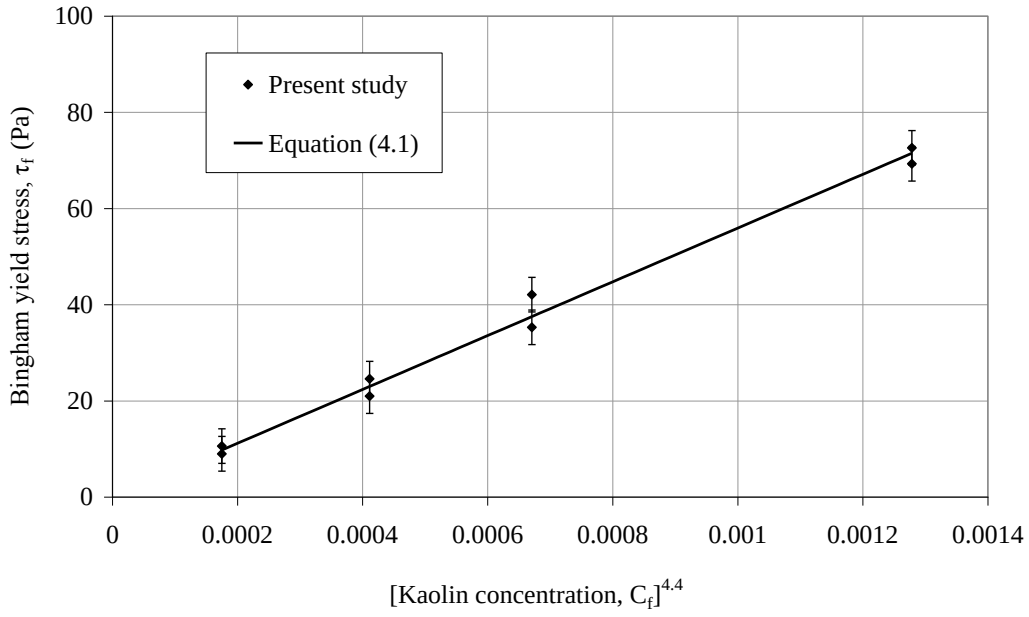

Figure 4.5: Bingham yield stress as a function of kaolin concentration for sand-free kaolin-water mixtures ($CaCl_2.2H_20$:Kaolin=0.001).

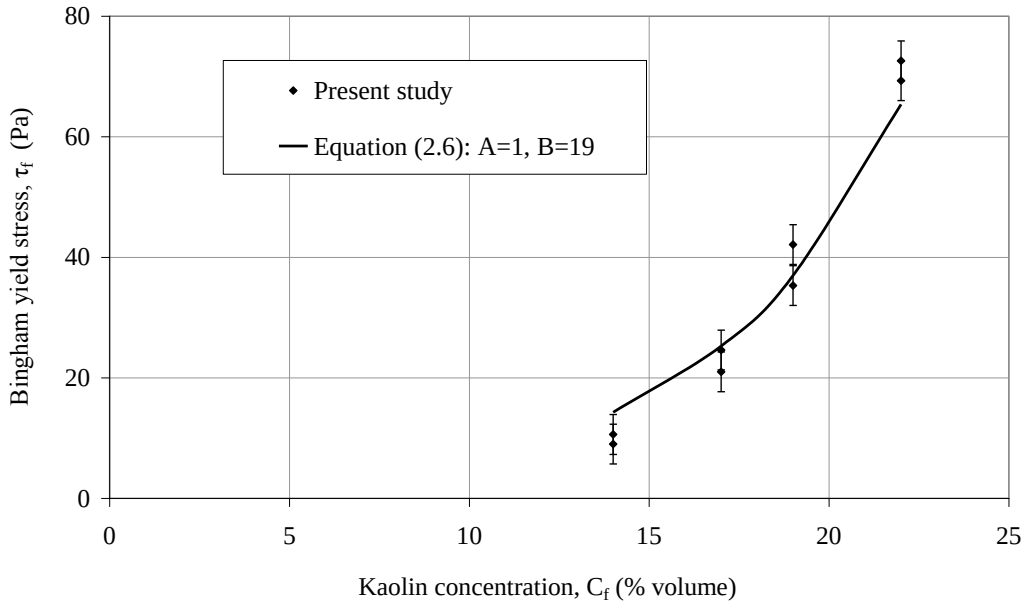

Figure 4.6: Bingham yield stress as a function of kaolin concentration for sand-free kaolin-water mixtures ($CaCl_2.2H_20$:Kaolin=0.001).

The experimental data presented in Figure 4.5 are fit with the following correlation:

$$\tau_f = 55937 C_f^{4.4} \qquad \textbf{4.1}$$

This correlation matches with Equation 2.4, which is the general form of correlation mentioned by Thomas (1999) for predicting Bingham yield stress with change in solids volume concentration. However, a somewhat inferior fit with experimental data can be obtained if Equation 2.6 is used, with values A=1 and B=19, as seen in Figure 4.6.

Similarly, the correlation used for approximating the data shown in Figure 4.7 is:

$$\mu_f = \exp(15C_f) \qquad \textbf{4.2}$$

This correlation is similar to the Thomas' (1999) general form, described by Equation 2.7, for predicting variation in Bingham plastic viscosity with solids volume concentration. Note that, if the coefficient '15' is replaced by '12.5', the correlation perfectly matches with Equation 2.8, which was found by Shook et al. (2002) in their experimentation with mature fine tailings.

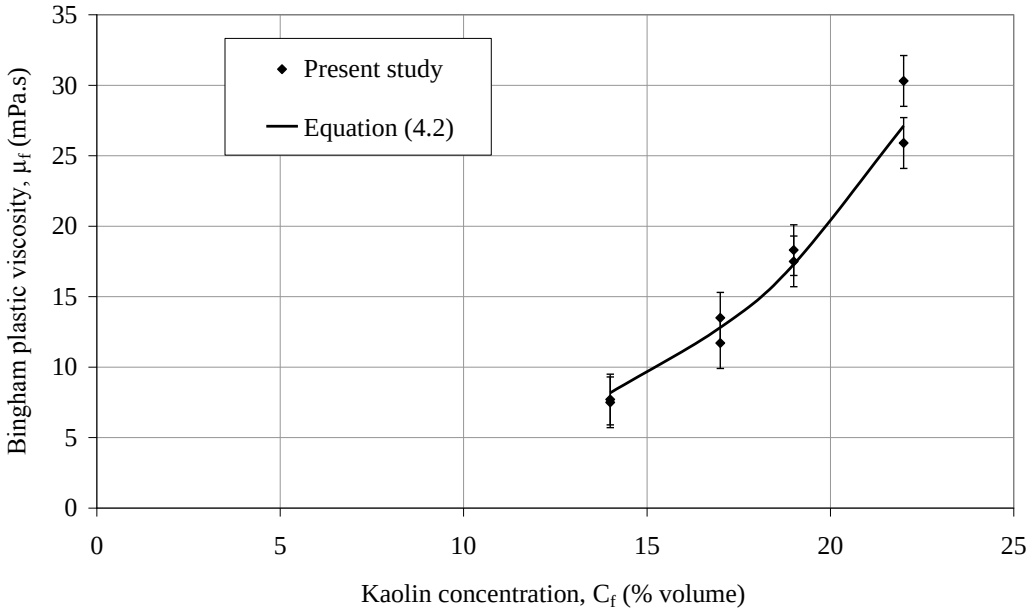

Figure 4.7: Bingham plastic viscosity as a function of kaolin concentration for sand-free kaolin-water mixtures ($CaCl_2.2H_20$:Kaolin=0.001).

The method of obtaining empirical coefficients of Equation 4.1 and 4.2 is consistent with the efforts of other researchers who worked with similar mixture in the past. Since the equations are empirical in nature, a change in either water chemistry or clay mineralogy would make those correlations invalid.

4.5. Rheology of sand-kaolin-water mixture

4.5.1. Effect of sand concentration on Bingham yield stress

The change in Bingham yield stress with sand volume concentration for different kaolin-water mixtures is presented in Figures 4.8 and 4.9 for LM and GS sand, respectively. The test for the combination of 22% kaolin in carrier fluid (kaolin + water) and 20% sand in total (sand + kaolin + water) mixture resulted in uncharacteristic high torque measurements. It is suspected that coarse particles formed a blockage in the annulus of the viscometer. Hence, the result of this test is reported in the Appendix but is not included as part of the data analyzed here.

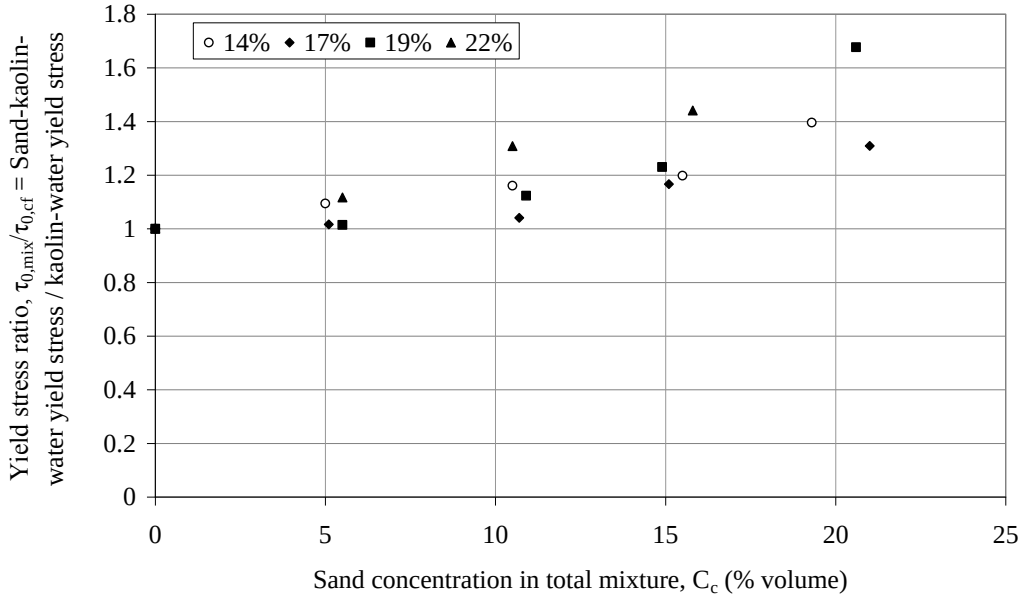

Figure 4.8: Effect of Lane Mountain (LM) sand addition on mixture Bingham yield stress.

Figures 4.8 and 4.9 show that the ratio of sand-kaolin-water mixtures yield stress to that of kaolin-water mixture increases with sand concentration for each kaolin mixture. Additionally, the effect of kaolin concentration on Bingham yield stress is more evident than that for any of the sand. It indicates that the mixture rheology is governed by fine particles and their flocculation characteristics. However, at the highest coarse sand concentrations, a significant increase in mixture yield stress was observed.

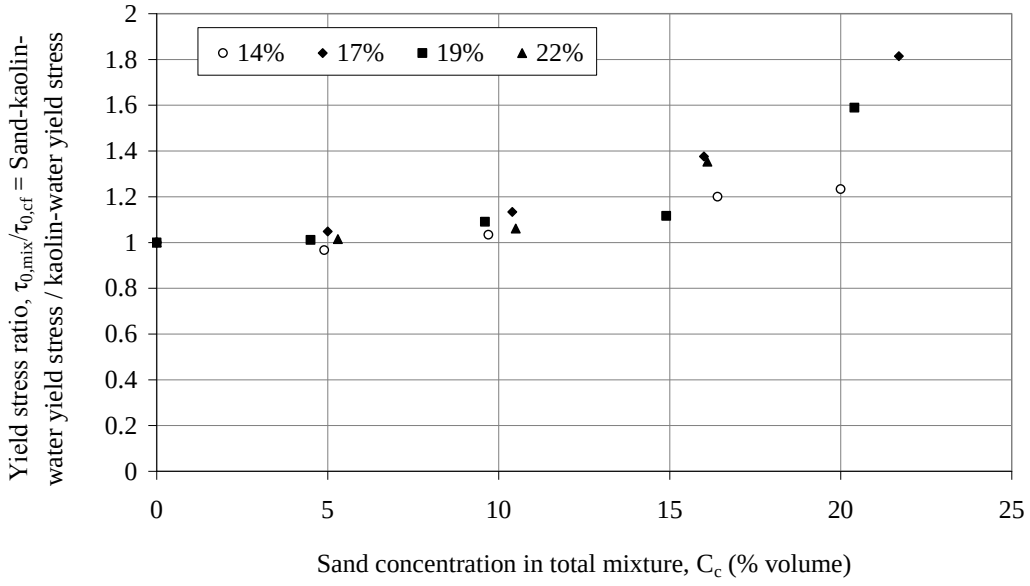

Figure 4.9: Effect of Granusil Silica (GS) sand addition on mixture Bingham yield stress.

Figure 4.10 shows the experimental findings with respect to different possible interaction mechanisms between sand particle and kaolin flocs, the details of which were discussed in Section 2.2.3. The data obtained by Paulsen (2007) and Thomas (1999) are also included in the figure. All these data show increasing

scatter as sand concentration goes higher. It is found that the data obtained from present study, and most of Thomas' (1999) and Paulsen's (2007) data fall within a region between what can be called "no effect" and "crowding effect" lines. In this region, the diameter of aggregates approaches the diameter of sand particles, and thus, the crowding effect is partially nullified by the rearrangement of flocs within the aggregates (Sanders, 2010).

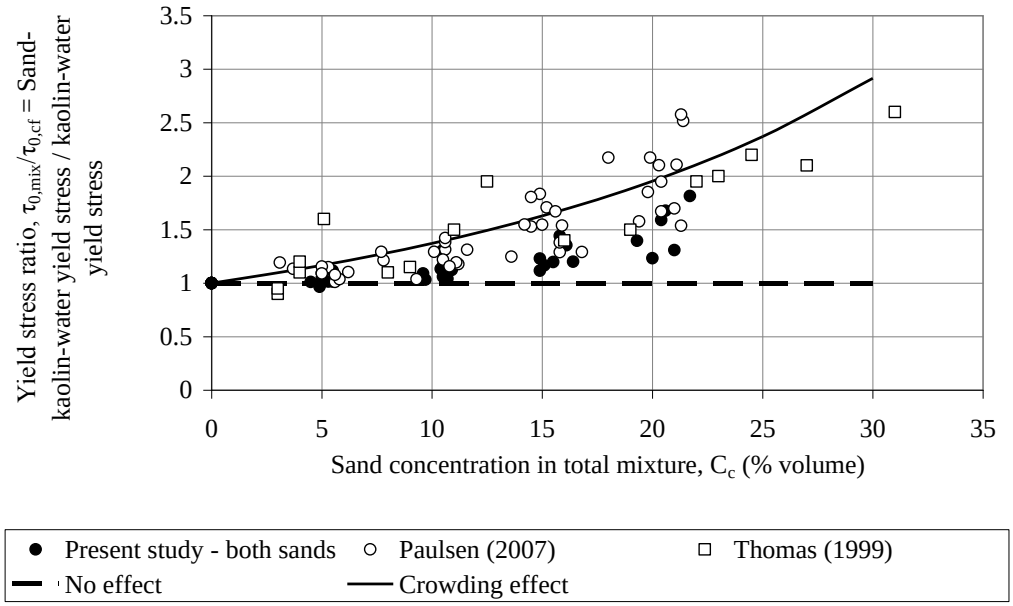

Figure 4.10: Experimental results shown bounded by lines representing inert sand behavior ("no effect") and particle floc crowding ("crowding effect").

The results obtained from present study indicate that the sand did not become a part of the kaolin floc network. The sand was truly inert and simply reduced the distance between the flocs, and thereby increased the probability of clay-floc interactions (Sumner, 2000). In other words, the tests conducted here (and most by others) show that sand promotes kaolin flocculation without becoming a part

of the kaolin flocs. Hence the increase in yield stress, when sand particles are added, is due to additional flocculation of clay particles only.

The yield stress ratios obtained from the present study are compared with those measured by Paulsen (2007) and Thomas (1999) in Figure 4.11. Thomas (1999) chose 1.5 as the value of coefficient 'A' to obtain the best fit of his data with his correlation:

$$\frac{\tau_{0,mix}}{\tau_{0,cf}} = \left(1 - \frac{C_C}{1.5C_{\max}}\right)^{-2.5} \qquad \textbf{4.3}$$

However, the value of 1.5 did not work well with Paulsen's (2007) data. The best fit of his data with the Thomas (1999) correlation was obtained when he replaced 1.5 with 1.943.

$$\frac{\tau_{0,mix}}{\tau_{0,cf}} = \left(1 - \frac{C_C}{1.943C_{\max}}\right)^{-2.5} \qquad \textbf{4.4}$$

Still then, Paulsen (2007) witnessed significant under-prediction of his data at high concentration ratio even with the new correlation, which means the usefulness of Equation 4.4 is limited to moderate and low concentration of sand.

The experimental data of present study is best fitted by selecting 2.869 as the value for the coefficient in the original equation proposed by Thomas (1999).

$$\frac{\tau_{0,mix}}{\tau_{0,cf}} = \left(1 - \frac{C_C}{2.869C_{\max}}\right)^{-2.5} \qquad \textbf{4.5}$$

The predicting ability of Equation 4.5 is much better when compared with other two correlations even at the highest sand concentration tested in this study.

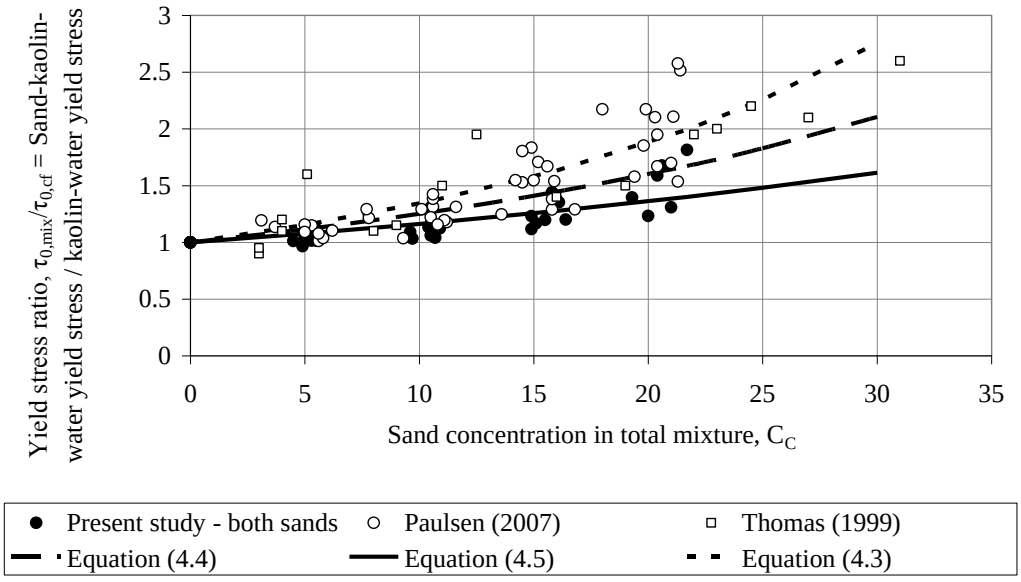

Figure 4.11: Comparison of yield stress ratios obtained from present study with those of previous studies.

The difference in the value of coefficient found in present study with that of Thomas (1999) and Paulsen (2007) can be attributed to several reasons. Although the structure of the correlation followed a logical approach by recognizing the importance of the ratio C_C/C_{max}, the selection of 1.5 as the coefficient was purely empirical, as it provided the best fit of the Thomas' (1999) experimental data. In addition the Thomas (1999) correlation was developed using only two mine tailings slurries as fine particle mixtures, although the range of coarse particle concentration was quite broad. It is well known that the Bingham yield stress of a fine particle slurry originates from the flocculation of fine particles in water and the flocculation characteristics is a strong function of water chemistry. Since he used mine tailings slurries directly for mixture preparation without any form of

treatment, it is highly likely that identical water chemistry was not maintained for all the mixtures, and if that is the case, then it is bound to affect the reliability of the result he obtained. Moreover, it was not clear if he performed all the experiments at the same temperature. This reasoning can be extended further to explain why the value of coefficient he found was different from that of either Paulsen (2007) or that found from the present study. Other contributing factors for the difference may include the ratio of coarse to fine particle size, the size distribution and shape of coarse particles and the mineralogy of kaolin clay.

It is important to note that an experimental procedure was developed in this project incorporating several steps of mixture treatment before rheological measurement, which were not considered by either Thomas (1999) or Paulsen (2007). The steps include removing entrained air bubbles and eliminating time and shear dependency of fine particle mixtures. The importance of these steps associated with the reliability and reproducibility of the measured data are discussed in details in Chapter 3. The absence of these steps in Thomas (1999) or Paulsen's (2007) work might have contributed to the interaction among particles and also the interaction between fine particle flocs and coarse particles, ultimately resulting in experimental results that differed considerably from those obtained here.

4.5.2. Effect of sand concentration on Bingham plastic viscosity

The change in Bingham plastic viscosity with LM and GS sand concentration for the same kaolin-water mixture discussed in previous section are shown in Figures 4.12 and 4.13, respectively. The effects of kaolin and sand concentration are found to be qualitatively similar to those observed in the case of Bingham yield stress. Again the effect of kaolin concentration is found dominant over that of any sand, reinforcing the governing role of fine particles in controlling mixture rheology.

The findings of present study are compared with those of Paulsen (2007) and Thomas (1999) in Figure 4.14. A correlation used to describe the effect of sand addition to a Newtonian mixture proposed by Thomas (1965) in the form of Equation 2.10 is also included in the figure. Thomas (1999) used 1.5 as the value of the coefficient in his correlation for plastic viscosity, which is identical to the value he used in his correlation for the effect of coarse particle addition on mixture yield stress:

$$\frac{\mu_{p,mix}}{\mu_{p,cf}} = \left(1 - \frac{C_C}{1.5 C_{\max}}\right)^{-2.5} \qquad \textbf{4.6}$$

Paulsen (2007) replaced 1.5 with 1.943 to obtain best fit of his data with Thomas (1999) correlation, but still experienced under-prediction of his data at higher values of coarse particle concentration:

$$\frac{\mu_{p,mix}}{\mu_{p,cf}} = \left(1 - \frac{C_C}{1.943 C_{\max}}\right)^{-2.5} \qquad \textbf{4.7}$$

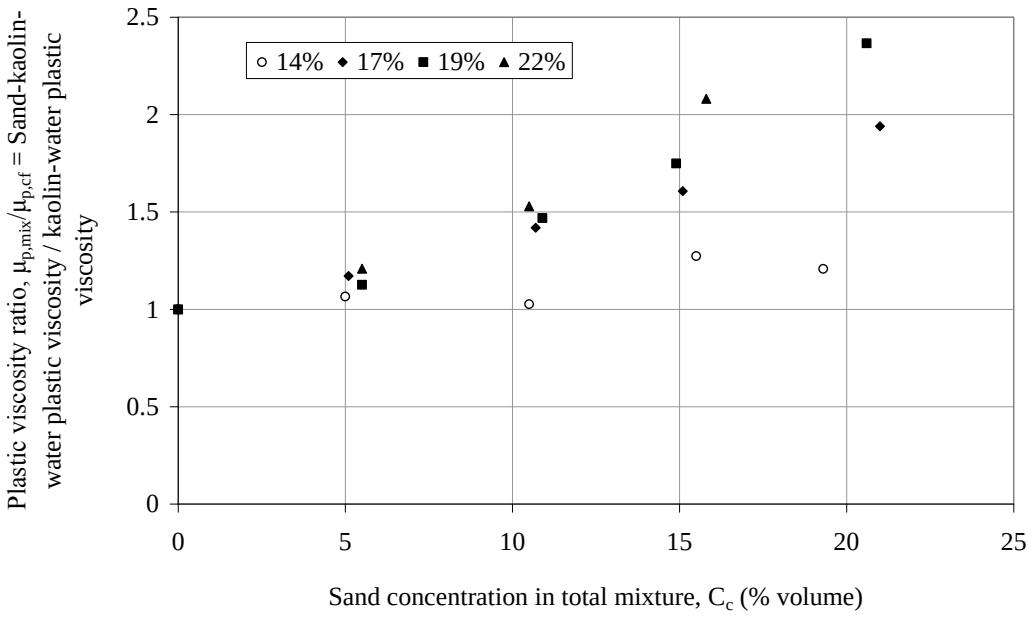

Figure 4.12: Effect of Lane Mountain (LM) sand addition on mixture Bingham plastic viscosity.

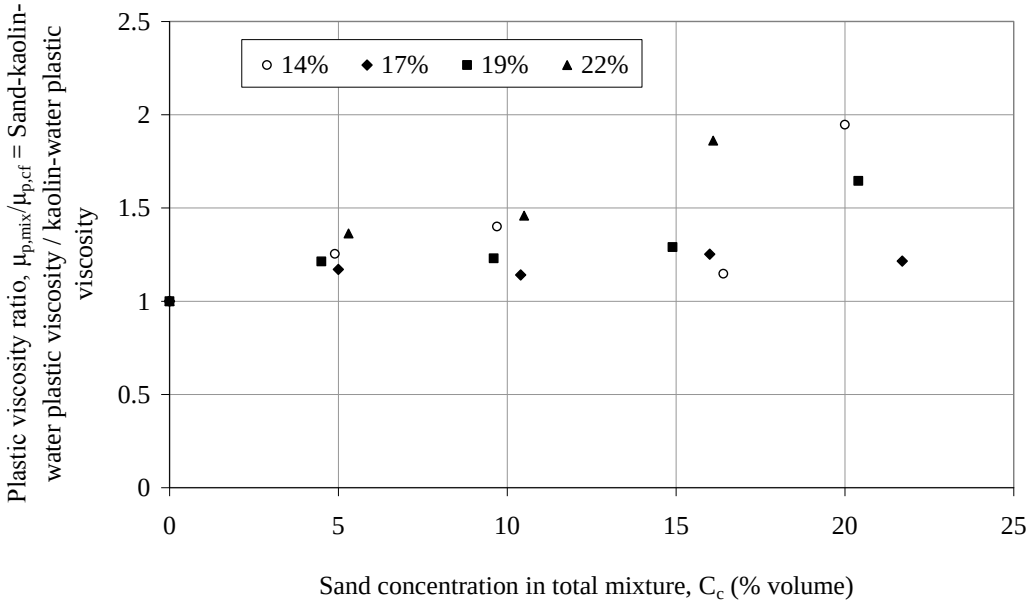

Figure 4.13: Effect of Granusil Silica (GS) sand addition on mixture Bingham plastic viscosity.

However, the value of coefficient which provided the best fit of the data obtained from present study is 1.841.

$$\frac{\mu_{p,mix}}{\mu_{p,cf}} = \left(1 - \frac{C_C}{1.841 C_{\max}}\right)^{-2.5} \qquad \textbf{4.8}$$

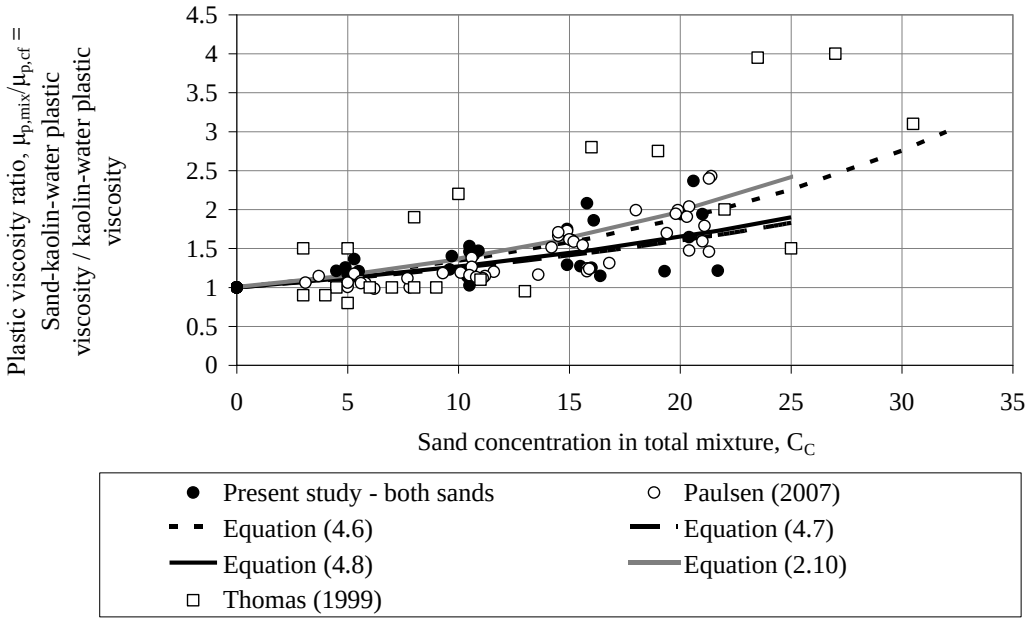

Figure 4.14: Comparison of plastic viscosity ratios obtained from present study with those of previous studies.

Since the effect of sand addition on plastic viscosity of non-Newtonian mixture can be considered as analogous to that of Newtonian mixture (Shook et al., 2002), the curve obtained from the correlation for Newtonian mixtures given by Equation 2.10 was to be close to other curves shown in the figure.

For relatively less concentrated mixtures of kaolin in water, it is believed that the high spindle speed used in the experiment caused sand particles to move away

from the spindle toward the cup. Therefore, a portion of the sample which was adjacent to the spindle experienced lower sand concentration than the rest of the mixture during the rheological measurement. This phenomenon might contribute to lower values of plastic viscosities which are reflected by the relatively lower plastic viscosity ratios obtained in Figure 4.14, especially at higher sand concentrations.

Note that the plastic viscosity ratios shown in Figure 4.14 are more scattered than the yield stress ratios shown in Figure 4.13. This happens partly due to the highly sensitive nature of plastic viscosity. When a set of torque versus spindle speed data is collected from a concentric cylinder viscometer test, the plastic viscosity is calculated from the slope of the curve of torque versus spindle speed plot and the Bingham yield stress calculated from the intercept of the curve. It has been found that if there is a minor change in the slope of the curve, it results in a fairly large variation in plastic viscosity compared to a variation in the corresponding Bingham yield stress.

The scattering of plastic viscosity ratios obtained in Figure 4.14 can be further explained with the help of Michaels and Bolgers' (1962) work. According to them, shear rate strongly affects the size of aggregates and thus the contents of water and kaolin inside the aggregate. A change in kaolin content inside the aggregates will change the ratio of aggregate concentration in the mixture to concentration of kaolin inside the aggregates. For any particular kaolin

concentration, a change in this ratio will cause a change in concentration of aggregates. A change in concentration of aggregates will cause a change in plastic viscosity of kaolin-water mixture. At the end, a change in plastic viscosity of kaolin-water mixture will cause a change in the ratio of plastic viscosities. However, this explanation is qualitative rather than quantitative. Because there is no correlation available in the literature which can adequately describe the change in aggregate size with shear rate, especially at high kaolin concentration. The problem is further complicated due to the presence of sand particles as it can affect the relation between shear rate and aggregate size. The exact mechanism of floc rearrangement within the aggregates in response to sand addition is also not known.

4.5.3. Effect of sand size on Bingham yield stress and plastic viscosity

The two sand types tested here were selected because the average diameter of one sand is nearly twice that of the other. It is worth recalling that the diameters of LM sand and GS sand were 90 micron and 190 micron, respectively. The comparison of yield stress ratio and plastic viscosity ratio of one sand with those measured upon addition of the other sand was expected to reveal the effect of coarse particle diameter on mixture rheology.

Figures 4.15 and 4.16 show the yield stress ratios and plastic viscosity ratios for both sands, respectively. Although the average diameter of GS sand was nearly

twice that of LM sand, the yield stress and plastic viscosity ratios obtained with GS sand are qualitatively similar to those obtained with LM sand.

According to Thomas (1963) and Zhou et al. (1999), the yield stress of the mixture should be inversely proportional to the square of the particle diameter. However, Figures 4.15 and 4.16 suggest that the sand particle diameter does not significantly affect either Bingham yield stress or plastic viscosity of the mixture. This is likely related to the fact that sand particles do not form flocs with one another and hence, the mechanism by which particle diameter affects flocculating behavior of fine particles as postulated by Thomas (1963) and Zhou et al. (1999) does not apply to sand particles.

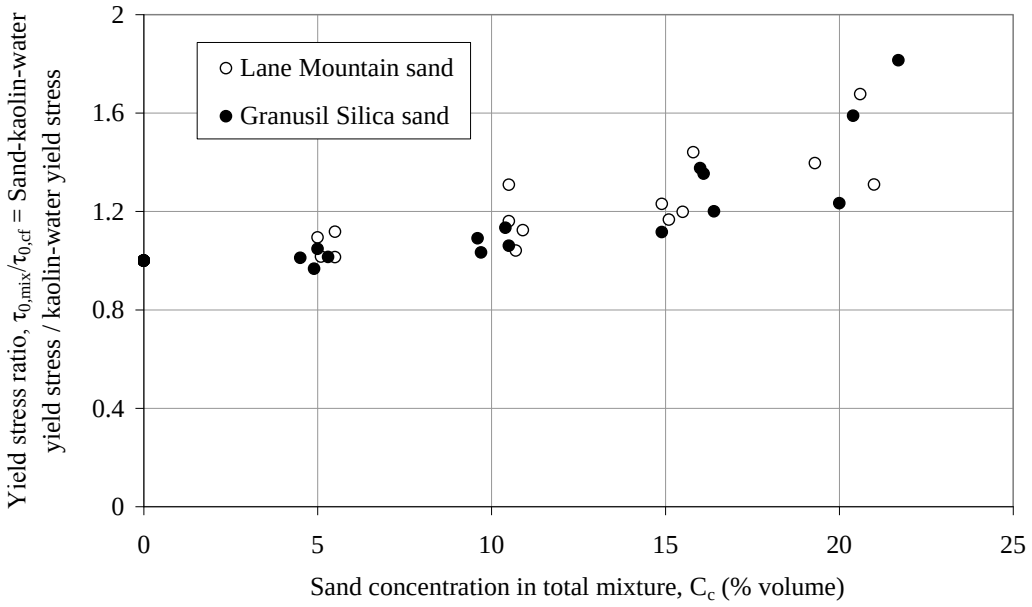

Figure 4.15: Effect of particle diameter on the ratio of mixture (sand-kaolin-water) to carrier fluid (kaolin-water) yield stress.

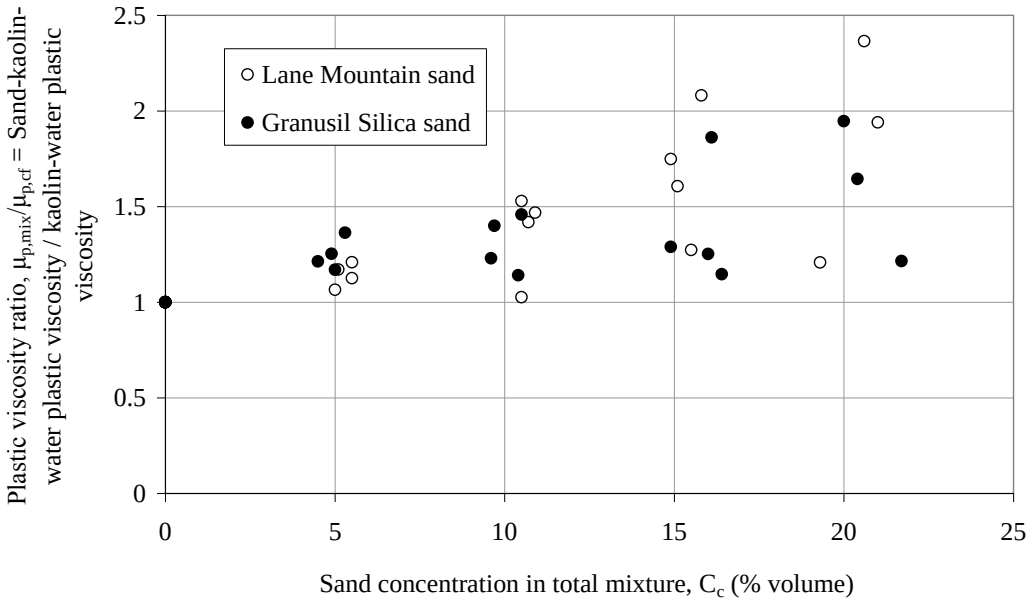

Figure 4.16: Effect of particle diameter on the ratio of mixture (sand-kaolin-water) to carrier fluid (kaolin-water) plastic viscosity.

4.6. Vane viscometer measurements

Four combinations of GS sand and kaolin concentrations were tested with the vane viscometer to find the "true" or vane yield stress of the mixture. The yield stress ratios were plotted with their counterparts for Bingham yield stresses, as shown in Figure 4.17.

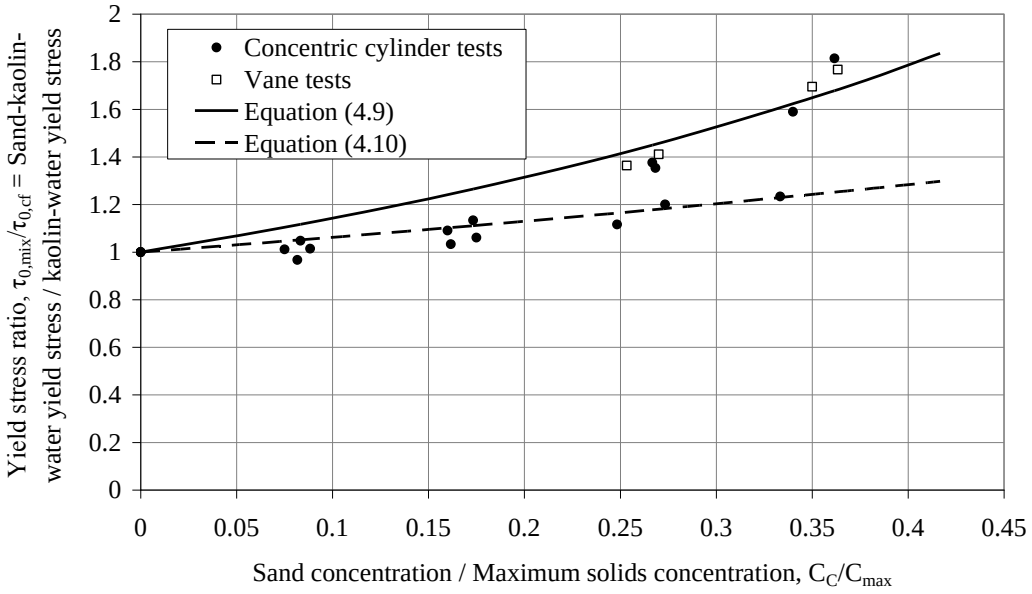

Figure 4.17: Comparison of Bingham yield stress ratio with Vane yield stress ratio for GS sand-kaolin-water mixture.

The data obtained from concentric cylinder viscometer tests are separated and approximated with 2 correlations, the general form of which is obtained from Thomas (1999) correlation:

$$\frac{\tau_{0,mix}}{\tau_{0,cf}} = \left(1 - \frac{C_C}{1.933 C_{\max}}\right)^{-2.5} \qquad \textbf{4.9}$$

$$\frac{\tau_{0,mix}}{\tau_{0,cf}} = \left(1 - \frac{C_C}{4.211 C_{\max}}\right)^{-2.5} \qquad \textbf{4.10}$$

It is seen from Figure 4.17 that Equation 4.9 and 4.10 forms the upper bound and the lower bound of the data obtained from concentric cylinder viscometer measurements, respectively. Note that the data found from Vane viscometer tests provide good agreement with the upper bound and there is a significant difference between the upper bound and the lower bound. However, due to limited amount of test data collected from Vane viscometer, it was not possible to come to a conclusion why the data in the lower bound fall below the findings of Vane viscometer tests. In other words, it is not possible to strongly suggest that future data will never follow the lower bound if additional tests are carried out with Vane viscometer.

5. Conclusions and recommendations

5.1. Conclusions

- The primary objective of the project was to determine the change in rheological properties of the sand-clay-water mixture with sand concentration, with a particular focus on Bingham yield stress. Additionally, the effect of sand size on the rheological properties was also tested.

- As a preliminary set of experiments, the same kaolin-water mixture was tested in two conditions – once before the addition of Granusil Silica (GS) sand particles and again after sieving them out. The similarity between kaolin concentrations, yield stresses and plastic viscosities of these two conditions proves that sand particles are truly inert and do not attempt to alter the chemistry of water. It also proves that the adsorption of water molecules on the surfaces of sand particles is not significant enough to affect any change in the rheology of the mixture.

- Lane Mountain (LM) sand particles were kept in contact of water undisturbed for four different durations and the supernatant water samples collected after each of the durations were tested in Syncrude Research Centre (Edmonton, Alberta, Canada). No significant change in pH, conductivity and the concentrations of 35 ions considered in the test could

be identified from this analysis. This result confirms that water chemistry of the mixture could not be altered upon addition of the coarse sand.

- A torque versus time response for each kaolin concentration tested with the highest sand concentration was recorded. It was found that mixtures of 10% kaolin in water (by volume) experienced significant deposition of sand particles over the duration of the experiment. Hence, no rheological tests were performed at this kaolin concentration.

- The rheology of numerous kaolin-water mixtures was determined as part of this study. The change in Bingham yield stress and plastic viscosity of kaolin-water mixture with kaolin concentration was modeled with Equations 4.1 and 4.2, respectively. According to these equations, the yield stress varied with the 4.4^{th} power of kaolin concentration and plastic viscosity changed exponentially with kaolin concentration. The general forms of these correlations are obtained from Thomas (1999). It is interesting to note that the coefficients in these correlations had to be determined experimentally. This is consistent with all other previous attempts to predict the effect of clay concentration on yield stress and plastic viscosity of clay-water mixture.

- The effect of sand concentration on the Bingham yield stress and plastic viscosity of sand-kaolin-water mixture was determined. The result was

compared with the findings of Thomas (1999) and Paulsen (2007). It was found that the data produced in this project, and most of Thomas' (1999) and Paulsen's (2007) data belong to a condition where the crowding effect of sand particles is partially nullified by the rearrangement of flocs inside the aggregates. At this condition, the diameter of aggregates approached the diameter of the sand particles; however, the sand particles do not appear to become part of the flocs. The presence of sand particles is believed to facilitate additional contact among the flocs, which is responsible for an increase in yield stress.

- The results related to Bingham yield stress was modeled with a semi-empirical correlation (Equation 2.13) originally proposed by Thomas (1999):

$$\frac{\tau_{0,mix}}{\tau_{0,cf}} = \left(1 - \frac{C_C}{AC_{\max}}\right)^{-2.5}$$

He obtained the best fit of his data by setting A=1.5. The value of the same coefficient was obtained as 1.943 and 2.869 by Paulsen (2007) and present study respectively. Thomas' (1999) data experienced tremendous scatter for all the sand concentrations he considered. As a result, the usefulness of his correlation is severely undermined. Paulsen's (2007) correlation under predicted Bingham yield stress ratios at high sand concentrations and thus the usefulness of his correlation is limited to low and moderate concentrations of sand. The correlations obtained by fitting

data of present study showed least amount of scatter and its predicting ability is better when compared with other two correlations even at the highest sand concentration tested in this project. The difference in coefficients between present study and others can be attributed to the effect of additional steps included in mixture preparation and thus the interaction between sand and kaolin particles.

- It is suspected that high spindle speed might have moved away coarse particle from the vicinity of the spindle, which is evident from the low values of plastic viscosity ratios obtained especially from mixtures having relatively low kaolin concentrations.

- The plastic viscosity ratios showed more scatter than the yield stress ratios. This is partly due to fact that small changes in the torque versus spindle speed data result in large changes in the plastic viscosity. A qualitative explanation for the scatter in plastic viscosity ratios can be provided with the help of Michaels and Bolger's (1962) work. However, additional research is needed to exploit the usefulness of their analysis.

- The experimental procedure was developed with a hope to eliminate the inconsistency of results as experienced by previous researchers. However, no clear trend could be observed. It indicates that an important variable is yet to be identified and considered. The importance of floc rearrangement in response to coarse particle addition to the mixture was highlighted.

- The average diameter of the Granusil Silica (GS) sand was twice that of the Lane Mountain (LM) sand used in this project. Yet no significant difference was found between the rheology of the mixtures prepared with these two sands, which indicates that coarse particle diameter does not significantly affect either Bingham yield stress or plastic viscosity. Here it is important to note that the effect of coarse particle diameter on Bingham yield stress and plastic viscosity was not studied before.

- A few GS sand-kaolin-water mixtures were tested using the Vane viscometer. The yield stress ratios obtained from these tests were compared with the ratios found from concentric cylinder viscometer tests. The data generated from concentric cylinder viscometer tests was approximated with two functions which formed the upper bound and lower bound of the test data. The Vane viscometer data agreed with the upper bound. The reason why Vane viscometer findings did not match with the lower bound could not be determined due to the limited number of tests carried out with the Vane viscometer.

5.2. Recommendations

- Before conducting any experiments with shear-dependent mixtures containing inert coarse particles and flocculating fine particles, research must be carried out to address the limitation of understanding on the following:

- Quantitative analysis on rearrangement of flocs due to addition of coarse particles.

- Characterization of aggregate concentration and shear rate.

- Additional experiments should be carried out with Vane viscometer by following the procedure developed in this project.

References

Ancey, C. “Role of Lubricated Contacts in Concentrated Polydisperse Suspensions”, Journal of Rheology, 45, no. 6, 1421-1439, 2001.

Ancey, C., and Jorrot, H. “Yield Stress for Particle Suspensions Within a Clay Dispersion”, Journal of Rheology, 45, no. 2, 297-319, 2001.

Bird, R.B., Stewart, W.E, and Lightfoot, E.N., *Transport Phenomena*, Madison: John Wiley & Sons, 1960.

Chong, J.S., Christiansen, E.B., and Baer, A.D., “Rheology of Concentrated Suspensions”, Journal of Applied Polymer Science, 15, no. 8, 2007-2021, 1971.

Coussot, P., *Mudflow Rheology and Dynamics,* Rotterdam: A.A. Balkema, 1997.

Coussot, P., and Piau, J.M. “The effects of an addition of force-free particles on the rheological properties of fine suspensions”, Canadian Geotechnical Journal, 32, 263-270, 1995.

Gillies, R., Sun, R., Schaan, J., and Shook, C.A., “Pipeline flow of oilsand consolidating tailings slurries”, Hydrotransport 15, BHR Group, Cranfield, U.K., 865-878, 2002.

Grim, R.E., and Cuthbert, F.L., “Some Clay-Water Properties of Certain Clay Minerals”, Journal of American Society of Ceramics, 28, no. 3, 90-95, 1945.

Iler, R.K., *The Chemistry of Silica*, New York: Wiley-Interscience, 1979.

Landel, R.F., Moser, B.G., and Bauman, A.J., "Rheology of Concentrated Suspensions - Effect of a Surfactant", 4th International Congress on Rheology, Brown University, Proceedings Part 2, 663-692, 1963.

Litzenberger, C.G., and Sumner, R.J. "Flow Behavior of Kaolin Clay Slurries", Hydrotransport 16, BHR Group, Cranfield, U.K., 77-91, 2004.

Masliyah, J., *Course Notes - ChE 534 Fundamentals of Oilsands Extraction*, Department of Chemical and Materials Engineering, University of Alberta, Edmonton, AB, 2008.

Michaels, A.S., and Bolger, J.C. "The Plastic Flow Behaviour of Flocculated Kaolin Suspensions", Ind. & Eng. Chem. Fundamentals, 1, no. 3, 153-162, 1962.

Nguyen, Q.D., and Boger, D.V. "Yield Stress Measurement for Concentrated Suspensions." Journal of Rheology, 27, no. 4, 321-349, 1983.

Paulsen, E., *Investigating the Effect of Coarse Particle Addition on the Measured Rheological Parameters of Fine Clay Slurries,* M.Sc. Thesis, University of Stellenbosch, Stellenbosch, South Africa, 2007.

Paulsen, E., Sumner, R.J., and Sanders, R.S. "The effect of coarse particle addition on the rheology of fine clay slurries", Hydrotransport 18, BHR Group, Cranfield, U.K., 343-361, 2010.

Sanders, R.S., *Personal Communication,* 11 August 2010.

Schaan, J.J., *Pipeline Flow of Newtonian Fine Particle Slurries*, M.Sc. Thesis, University of Saskatchewan, Saskatoon, Canada, 2000.

Schaan, J., Sumner, R.J., Gillies, R.G., and Shook, C.A., "The effect of particle shape on pipeline friction for newtonian slurries of fine particles", Can. J. of Chem. Eng., 78, 717-725, 2000.

Schaan, J., Sanders, R.S., Gillies, R.G., McKibben, M.J., Litzenberger, C., Sun, R.J., and Shook, C.A., "Effects of shear history on flow properties of flocculant-dosed, thickened tailings slurries", Hydrotransport 16, BHR Group, Cranfield, U.K., 403-414, 2004.

Sengun, M.Z., and Probstein, R.F., "Bimodal model of slurry viscosity with application to coal-slurries. Part 1. Theory and experiment", Rheol. Acta 28, 382-393, 1989.

Shook, C.A., Gillies, R.G., and Sanders, R.S., *Pipeline Hydrotransport with Applications in the Oil Sand Industry*, Saskatoon: Saskatchewan Research Council, 2002.

Slatter, P.T., and Wasp, E.J., "The Bingham Plastic rheological model: friend or foe?", Hydrotransport 15, BHR Group, Cranfield, U.K., 315-328, 2002.

Spelay, R.B., *Solids transport in laminar, open channel flow of non-Newtonian slurries*, PhD Thesis, University of Saskatchewan, Saskatoon, Canada, 2007.

Sumner, R.J., Munkler, J.J., Carriere, S.M., and Shook, C.A., "Rheology of Kaolin Slurries Containing Large Silica Particles", Journal of Hydrology and Hydromechanics, 48, 110-124, 2000.

Thomas, A.D., "The Influence of Coarse Particles on the Rheology of Fine Particle Slurries", Rheology in the Mineral Industry II, 113-123, 1999.

Thomas, D.G., “III. Laminar-Flow Properties of Flocculated Suspensions” AIChE 7, no. 3, 431-437, 1961.

Thomas, D.G., “Transport Characteristics of Suspensions VII. Relation of Hindered-Settling Floc Characteristics to Rheological Parameters.” AIChE 9, no. 3, 310-316, 1963.

Thomas, D.G., “Transport Characteristics of Suspensions VII. A Note on the Viscosity of Newtonian Suspensions of Uniform Spherical Particles.” J. Colloid Sci. 20, 267-277, 1965.

Van Olphen, H., *An Introduction to Clay Colloid Chemistry, New* York: Wiley-Interscience, 1977.

Wilson, K.C., and Thomas, A.D., “A New Analysis of the Turbulent Flow of Non-Newtonian Fluids”, Can. J. Chem. Eng., 63, 539-546, 1985.

Wilson, K.C., Horsley, R.R., Kealy, T., Reizes, J.A., and Horsley, M., “Direct prediction of fall velocities in non-Newtonian materials”, Int. J. Min. Pro., 71, 17-30, 2003.

Zhou, Z., Solomon, M.J., Scales, P.J., and Boger, D.V., “The Yield Stress of Concentrated Flocculated Suspensions of Size Distributed Particles”, Journal of Rheology, 43, no. 3, 651-671, 1999.

Appendix 1: Calibration and recalibration tests

Calibration test 1

Calibration oil	N100
Standard viscosity (mPa.s)	277.7
Standard density (kg/m^3)	881.4
Temperature	20^{0}C

Sensor system	MV1
Spindle radius (mm)	20.04
Cup radius (mm)	21
Spindle length (mm)	60

Spindle speed in RPM	Predicted torque (% FST)	Measured torque (% FST)
5.004	1.644058	1.698
34.8	11.4335	11.84333
64.7	21.2571	21.91667
94.5	31.04786	31.89
124.5	40.90432	41.86667
154.4	50.72792	51.8
184.4	60.58439	61.63333
214.3	70.40799	71.36667
244.1	80.19875	81.03333
274.1	90.05521	90.63333

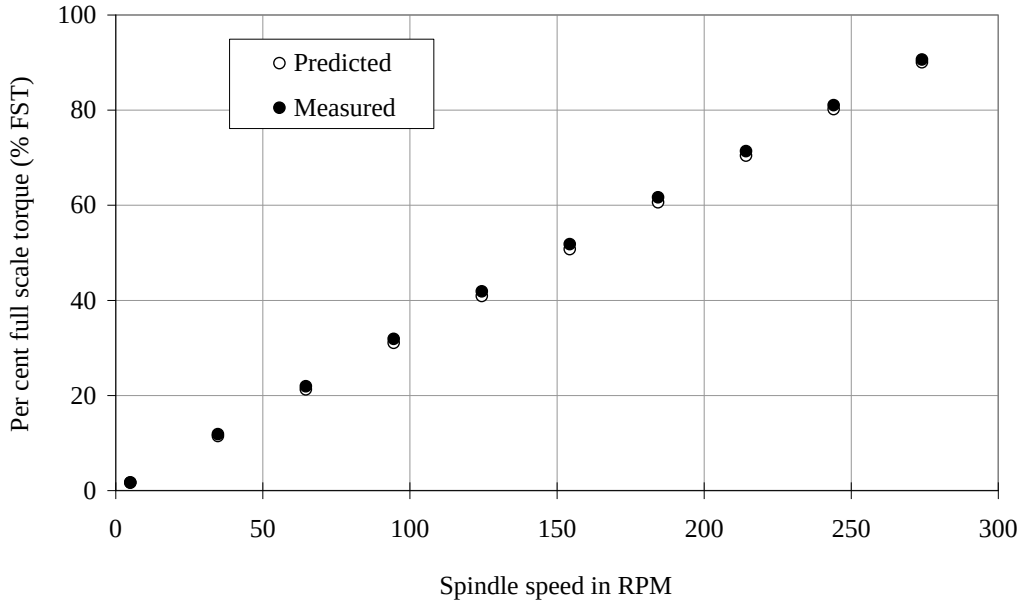

Calibration test 2

Calibration oil	N100
Standard viscosity (mPa.s)	200
Standard density (kg/m^3)	878.3
Temperature	25^{0}C

Sensor system	MV1
Spindle radius (mm)	20.04
Cup radius (mm)	21
Spindle length (mm)	60

Spindle speed in RPM	Predicted torque (% FST)	Measured torque (% FST)
5.004	1.184053	1.211
46.6	11.02655	11.48667
88.4	20.91733	21.71667
130	30.76077	31.75667
171.5	40.58056	41.73333
213.3	50.47133	51.7
255.1	60.3621	61.53333
296.7	70.20555	71.16667
338.3	80.049	80.83333
379.9	89.89245	90.66667

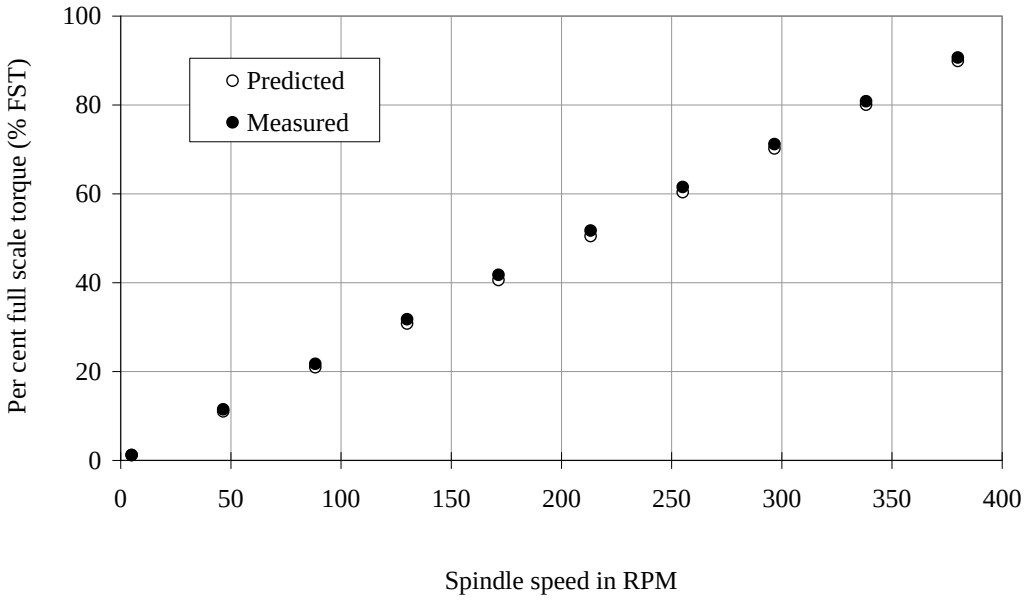

Calibration test 3

Calibration oil	N100
Standard viscosity (mPa.s)	277.7
Standard density (kg/m^3)	881.4
Temperature	20^{0}C

Sensor system	MV2
Spindle radius (mm)	18.4
Cup radius (mm)	21
Spindle length (mm)	60

Spindle speed in RPM	Predicted torque (% FST)	Measured torque (% FST)
5.004	0.533048	0.550333
77.6	8.266292	8.566667
150.2	15.99996	16.66667
222.9	23.74428	24.73333
295.7	31.49926	32.73
368.4	39.24358	40.6
440.9	48.62386	49.9698
513.7	60.44913	61.64043
586.4	73.95331	74.74349
659.1	89.54433	89.48879

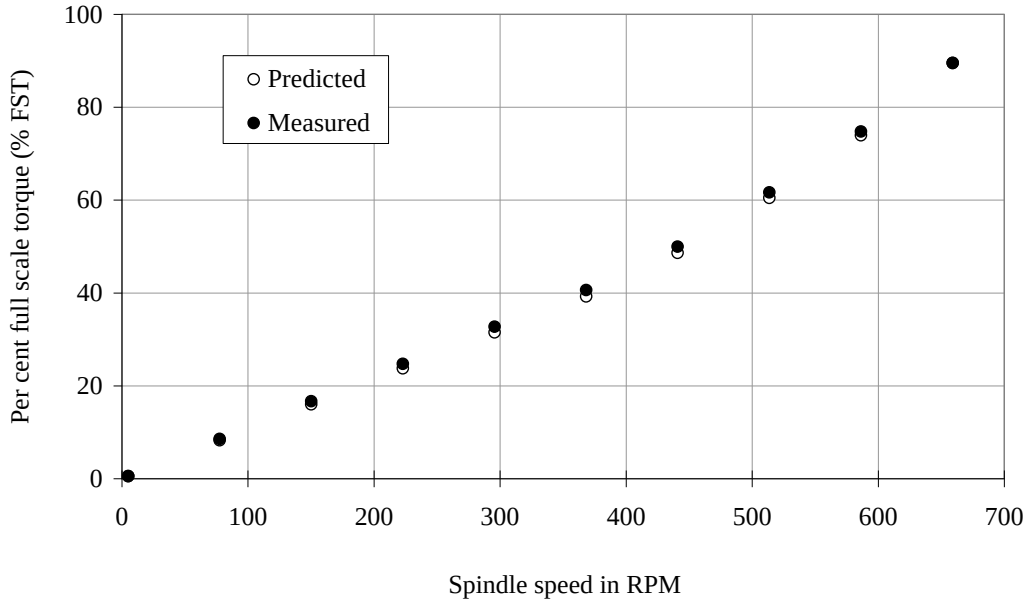

Calibration test 4

Calibration oil	N100
Standard viscosity (mPa.s)	200
Standard density (kg/m^3)	878.3
Temperature	25^{0}C

Sensor system	MV2
Spindle radius (mm)	18.4
Cup radius (mm)	21
Spindle length (mm)	60

Spindle speed in RPM	Predicted torque (% FST)	Measured torque (% FST)
5.004	0.383902	0.425667
91.2	6.996776	7.203333
177.2	13.59461	14.03333
263.3	20.20012	20.8
349.3	26.79796	27.5
435.5	34.42969	35.17389
521.6	44.52891	45.21513
607.8	56.39568	56.84338
693.8	70.48466	70.40388
779.6	87.48439	86.54315

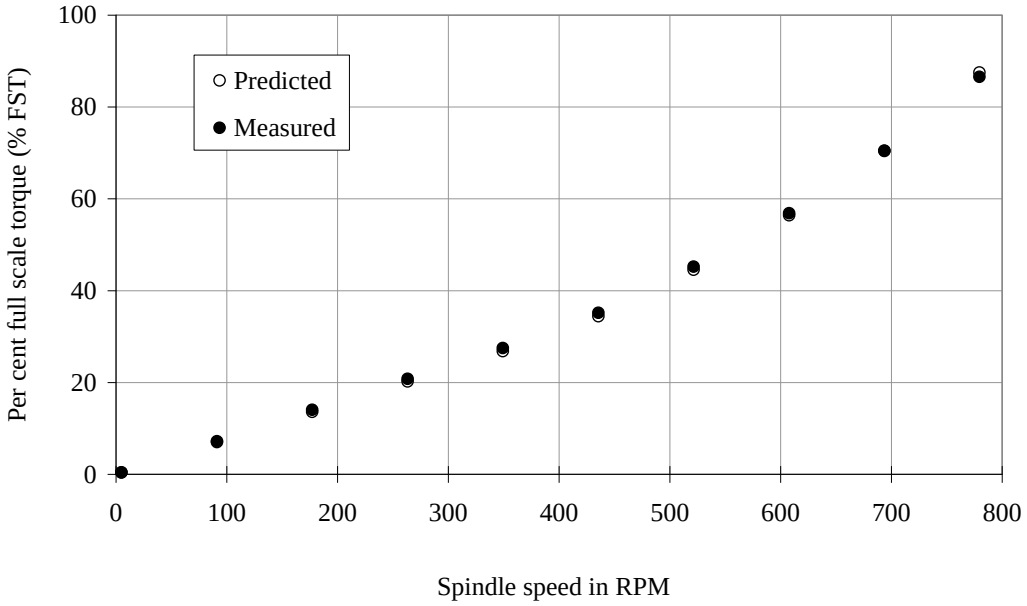

Calibration test 5

Calibration oil	N100
Standard viscosity (mPa.s)	277.7
Standard density (kg/m^3)	881.4
Temperature	20^{0}C

Sensor system	MV3
Spindle radius (mm)	15.2
Cup radius (mm)	21
Spindle length (mm)	60

Spindle speed in RPM	Predicted torque (% FST)	Measured torque (% FST)
5.004	0.177481	0.107667
91.2	3.234658	3.005667
177.2	6.284884	6.053333
263.3	9.338657	9.163333
349.3	12.38888	12.29
435.5	15.91708	15.96565
521.6	20.58603	20.79006
607.8	26.07212	26.43419
693.8	32.58555	33.01699
779.6	40.44464	40.82886

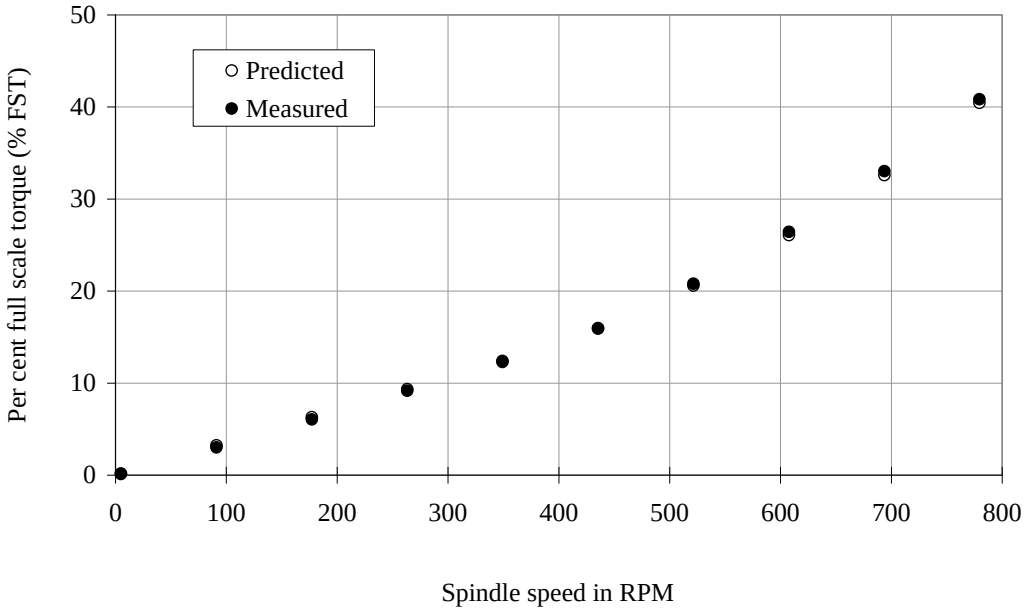

Calibration test 6

Calibration oil	N100
Standard viscosity (mPa.s)	200
Standard density (kg/m^3)	878.3
Temperature	25^{0}C

Sensor system	MV3
Spindle radius (mm)	15.2
Cup radius (mm)	21
Spindle length (mm)	60

Spindle speed in RPM	Predicted torque (% FST)	Measured torque (% FST)
5.004	0.127822	0.16
91.2	2.329606	2.334333
177.2	4.526384	4.593333
263.3	6.725716	6.833333
349.3	8.922494	9.06
435.5	11.46351	11.61013
521.6	14.82609	14.98516
607.8	18.77718	18.90748
693.8	23.46817	23.49592
779.6	29.1283	28.91273

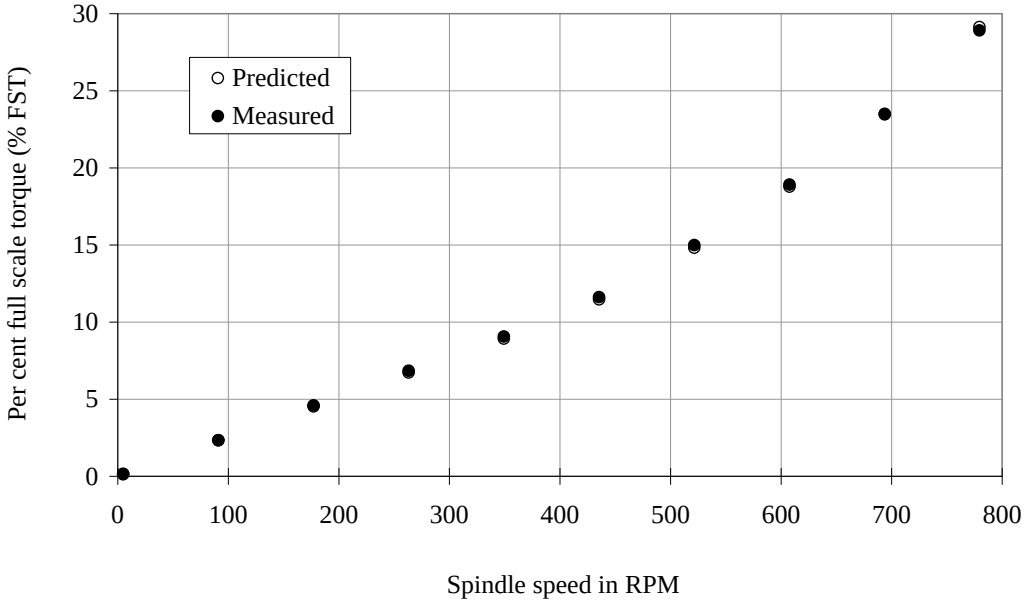

Calibration test 7

Calibration oil	S200
Standard viscosity (mPa.s)	449
Standard density (kg/m^3)	839.6
Temperature	20^{0}C

Sensor system	MV1
Spindle radius (mm)	20.04
Cup radius (mm)	21
Spindle length (mm)	60

Spindle speed in RPM	Predicted torque (% FST)	Measured torque (% FST)
5.004	2.658199	2.831333
23.3	12.37731	13.10333
41.6	22.09854	23.21
59.9	31.81977	33.2
78.4	41.64725	43.16667
96.5	51.26224	52.76667
115	61.08971	62.6
133.3	70.81095	72.06667
151.6	80.53218	81.6
170	90.30653	91.13333

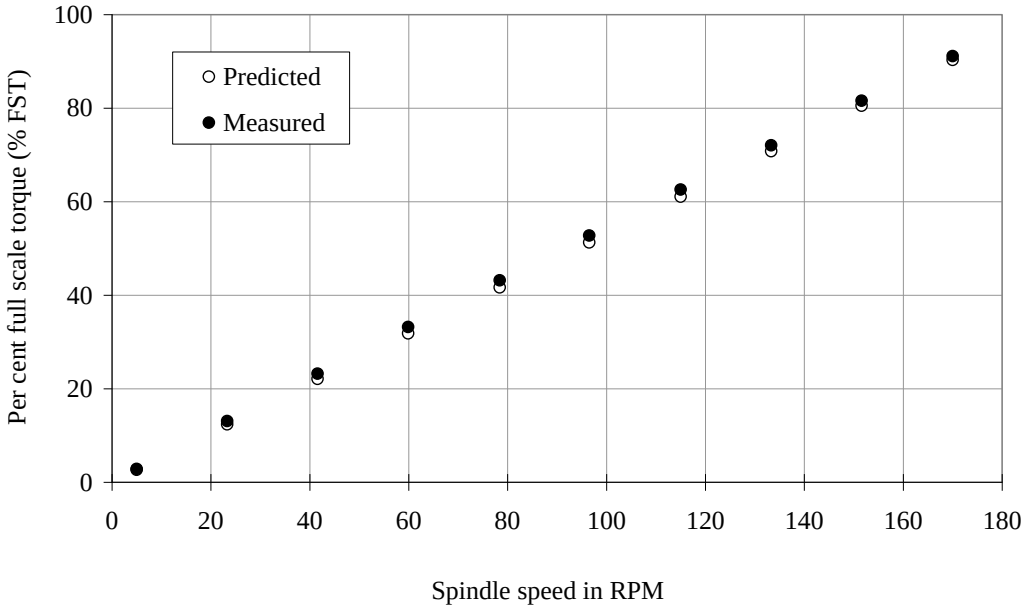

Calibration test 8

Calibration oil	S200
Standard viscosity (mPa.s)	332.3
Standard density (kg/m^3)	836.5
Temperature	25^{0}C

Sensor system	MV1
Spindle radius (mm)	20.04
Cup radius (mm)	21
Spindle length (mm)	60

Spindle speed in RPM	Predicted torque (% FST)	Measured torque (% FST)
5.004	1.967304	2.084
29.8	11.71576	12.53667
54.8	21.54442	22.8
79.7	31.33376	32.86667
104.5	41.08379	42.93333
129.4	50.87314	52.6
154.3	60.66248	62.33333
179.3	70.49114	72
204	80.20186	81.56667
228.9	89.9912	91.03333

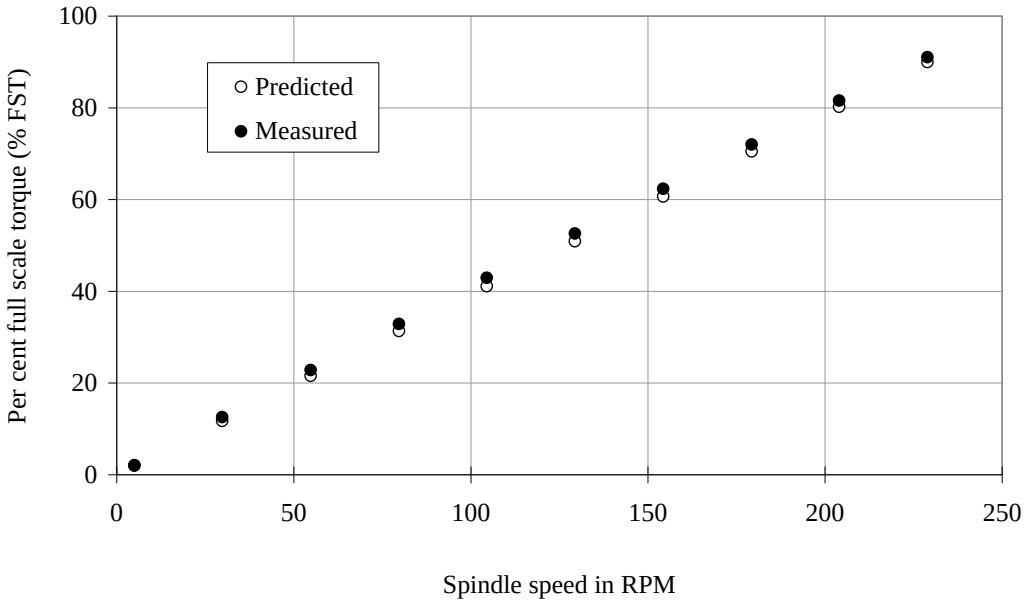

Calibration test 9

Calibration oil	S200
Standard viscosity (mPa.s)	449
Standard density (kg/m^3)	839.6
Temperature	20^{0}C

Sensor system	MV2
Spindle radius (mm)	18.4
Cup radius (mm)	21
Spindle length (mm)	60

Spindle speed in RPM	Predicted torque (% FST)	Measured torque (% FST)
5.004	0.86186	0.749333
58.3	10.04126	10.35
111.6	19.22134	19.88667
165.1	28.43587	29.49667
218.3	37.59873	38.96667
271.7	46.79604	48.36667
325	55.97613	57.63333
378.2	65.13899	66.7
431.5	76.32254	77.60377
485.1	89.92824	90.69872

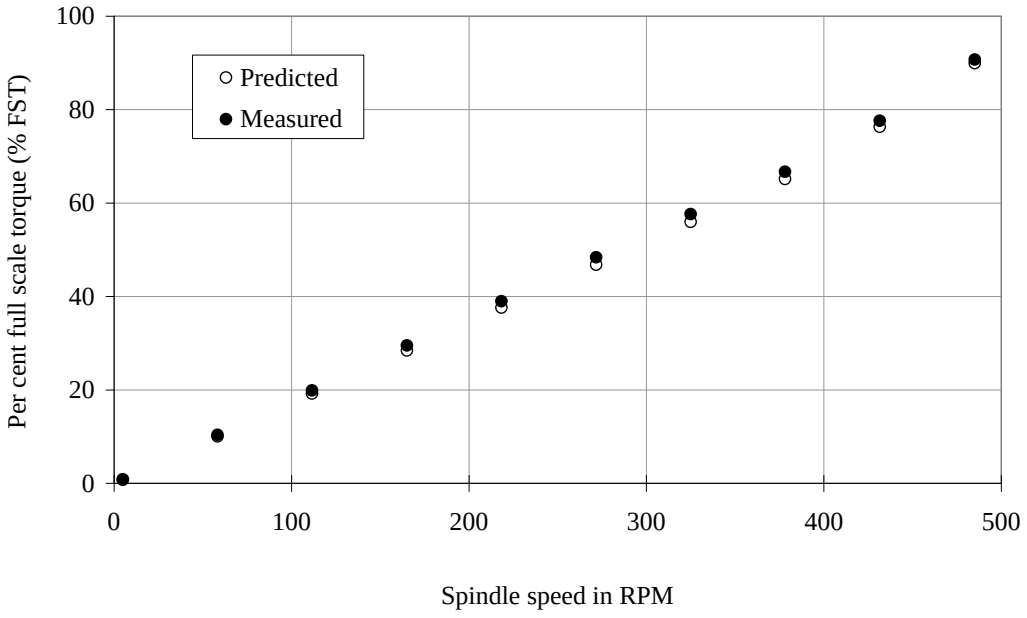

Calibration test 10

Calibration oil	S200
Standard viscosity (mPa.s)	332.3
Standard density (kg/m^3)	836.5
Temperature	25^{0}C

Sensor system	MV2
Spindle radius (mm)	18.4
Cup radius (mm)	21
Spindle length (mm)	60

Spindle speed in RPM	Predicted torque (% FST)	Measured torque (% FST)
5.004	0.637853	0.519
70.2	8.948301	9.116667
135.4	17.25926	17.71667
200.5	25.55747	26.23
266	33.90667	34.73333
331.1	42.20488	43.06667
396.2	50.50309	51.33333
461.5	62.00453	62.67896
526.7	75.06317	75.35638
591.9	89.81098	89.39589

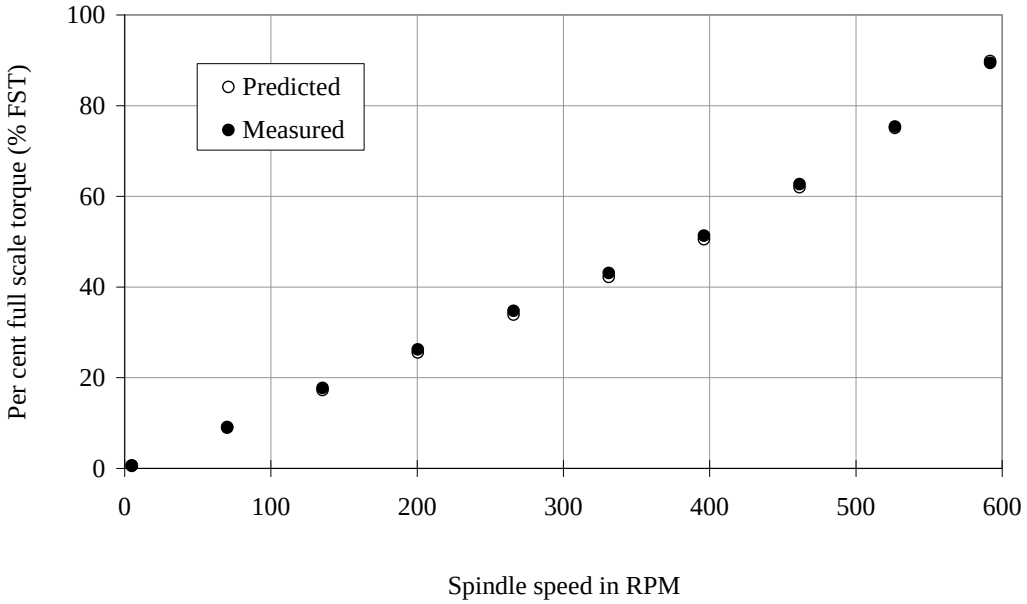

Calibration test 11

Calibration oil	S200
Standard viscosity (mPa.s)	449
Standard density (kg/m^3)	839.6
Temperature	20^{0}C

Sensor system	MV3
Spindle radius (mm)	15.2
Cup radius (mm)	21
Spindle length (mm)	60

Spindle speed in RPM	Predicted torque (% FST)	Measured torque (% FST)
5.004	0.28696	0.297333
91.2	5.229966	5.366667
177.2	10.16173	10.46667
263.3	15.09923	15.56667
349.3	20.031	20.60333
435.5	25.73558	26.38729
521.6	33.28457	33.94288
607.8	42.15477	42.65269
693.8	52.68603	52.79188
779.6	65.39303	64.70015

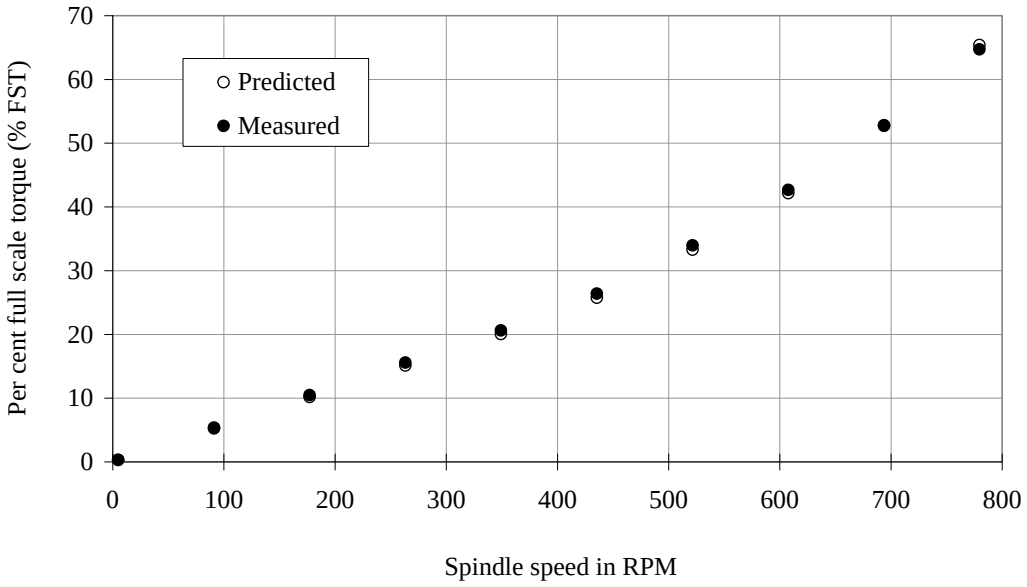

Calibration test 12

Calibration oil	S200
Standard viscosity (mPa.s)	332.3
Standard density (kg/m^3)	836.5
Temperature	25^{0}C

Sensor system	MV3
Spindle radius (mm)	15.2
Cup radius (mm)	21
Spindle length (mm)	60

Spindle speed in RPM	Predicted torque (% FST)	Measured torque (% FST)
5.004	0.212376	0.219
91.2	3.870641	4.033333
177.2	7.520587	7.866667
263.3	11.17478	11.7
349.3	14.82472	15.49
435.5	19.04662	19.85401
521.6	24.63355	25.55638
607.8	31.19829	32.13465
693.8	38.99236	39.80137
779.6	48.39667	48.90297

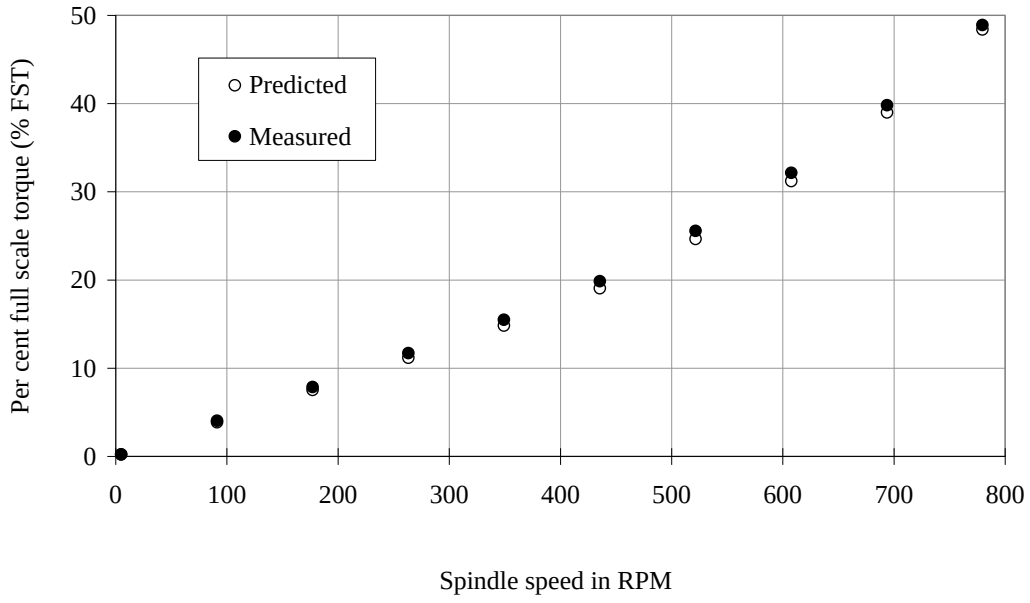

Calibration test 13

Calibration oil	N1000
Standard viscosity (mPa.s)	2855
Standard density (kg/m^3)	849.5
Temperature	20^{0}C

Sensor system	MV1
Spindle radius (mm)	20.04
Cup radius (mm)	21
Spindle length (mm)	60

Spindle speed in RPM	Predicted torque (% FST)	Measured torque (% FST)
1.003	3.387903	3.277333
3.801	12.8389	12.85333
6.704	22.64457	23.09667
9.597	32.41646	33.06667
12.5	42.22212	43.16667
15.4	52.01765	53.1
18.3	61.81318	63.16667
21.2	71.60872	73.03333
24.1	81.40425	82.86667
27	91.19978	92.63333

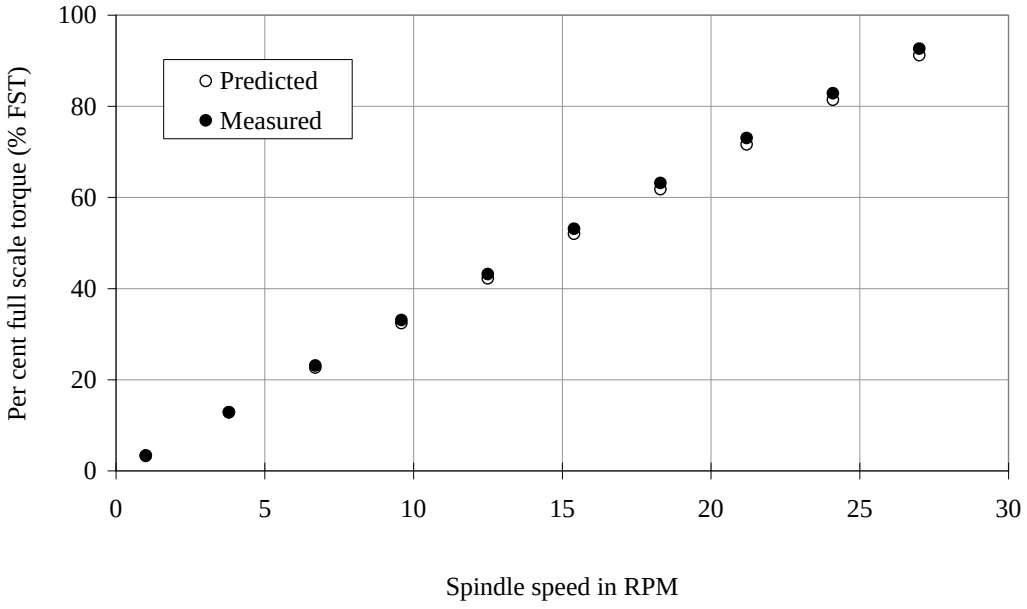

Calibration test 14

Calibration oil	N1000
Standard viscosity (mPa.s)	2008
Standard density (kg/m^3)	846.5
Temperature	25^{0}C

Sensor system	MV1
Spindle radius (mm)	20.04
Cup radius (mm)	21
Spindle length (mm)	60

Spindle speed in RPM	Predicted torque (% FST)	Measured torque (% FST)
1.003	2.382805	2.235333
5.099	12.11358	12.5
9.196	21.84674	22.77333
13.3	31.59652	32.82333
17.4	41.3368	42.73333
21.5	51.07708	52.6
25.6	60.81736	62.3
29.7	70.55764	72.13333
33.8	80.29793	82.06667
38	90.27577	91.93333

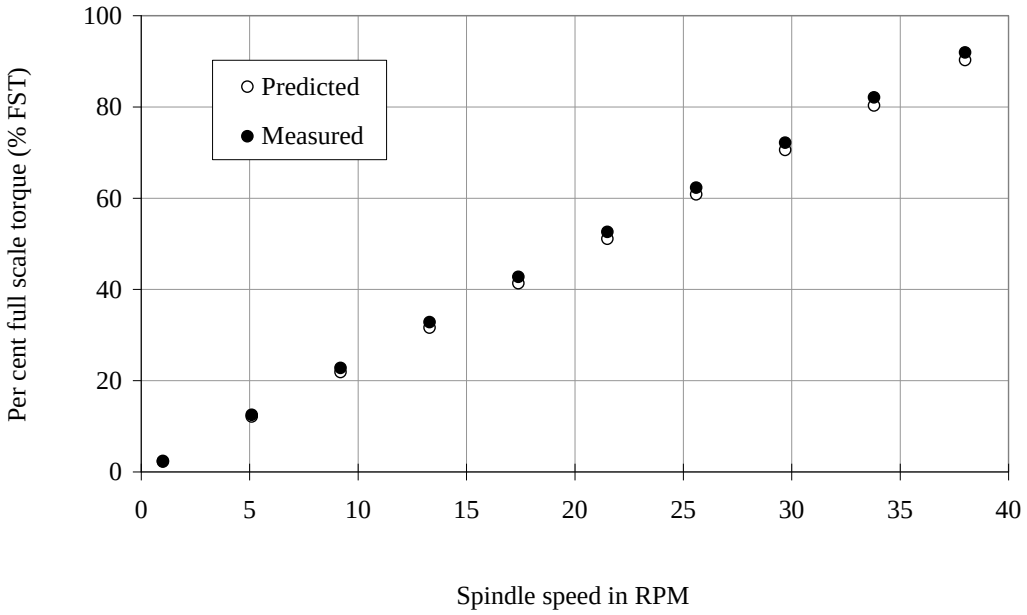

Calibration test 15

Calibration oil	N1000
Standard viscosity (mPa.s)	2855
Standard density (kg/m^3)	849.5
Temperature	20^{0}C

Sensor system	MV2
Spindle radius (mm)	18.4
Cup radius (mm)	21
Spindle length (mm)	60

Spindle speed in RPM	Predicted torque (% FST)	Measured torque (% FST)
5.004	5.480202	4.903333
13.5	14.78472	13.83667
22.1	24.20313	23.12333
30.6	33.51203	32.47333
39.2	42.93044	42.03333
47.7	52.23933	51.56667
56.3	61.65775	61.16667
64.7	70.85713	70.6
73.5	80.49457	80.33333
81.9	89.69395	89.83333

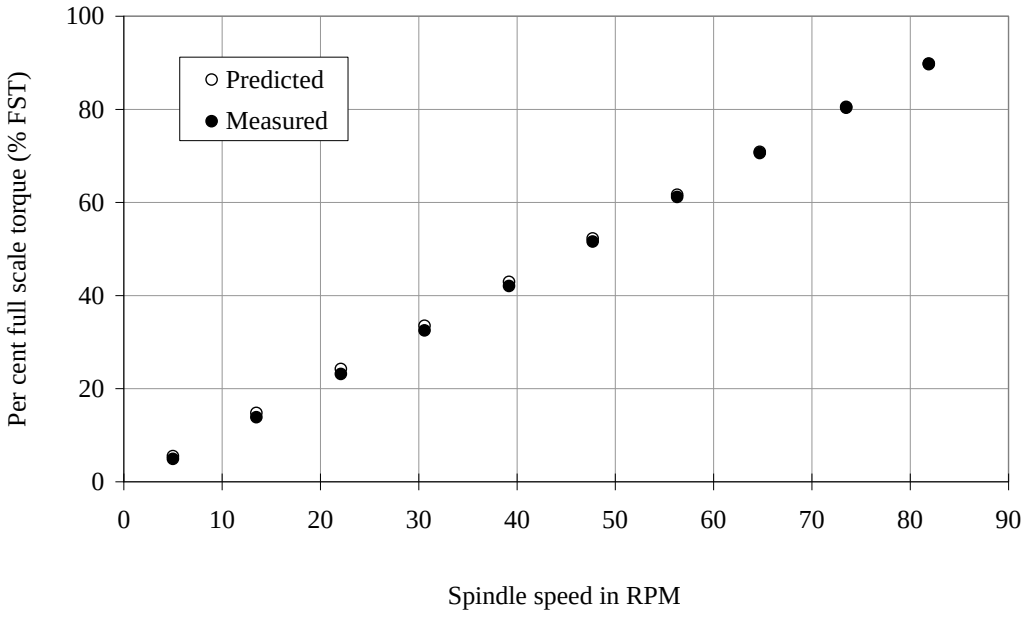

Calibration test 16

Calibration oil	N1000
Standard viscosity (mPa.s)	2008
Standard density (kg/m^3)	846.5
Temperature	25^{0}C

Sensor system	MV2
Spindle radius (mm)	18.4
Cup radius (mm)	21
Spindle length (mm)	60

Spindle speed in RPM	Predicted torque (% FST)	Measured torque (% FST)
5.004	3.854377	3.883333
17.3	13.32548	13.67
29.6	22.79967	23.44
42	32.35088	33.32
54.3	41.82507	43.06667
66.6	51.29926	52.8
78.9	60.77344	62.53333
91.2	70.24763	72.16667
103.6	79.79885	81.8
116	89.35006	91.36667

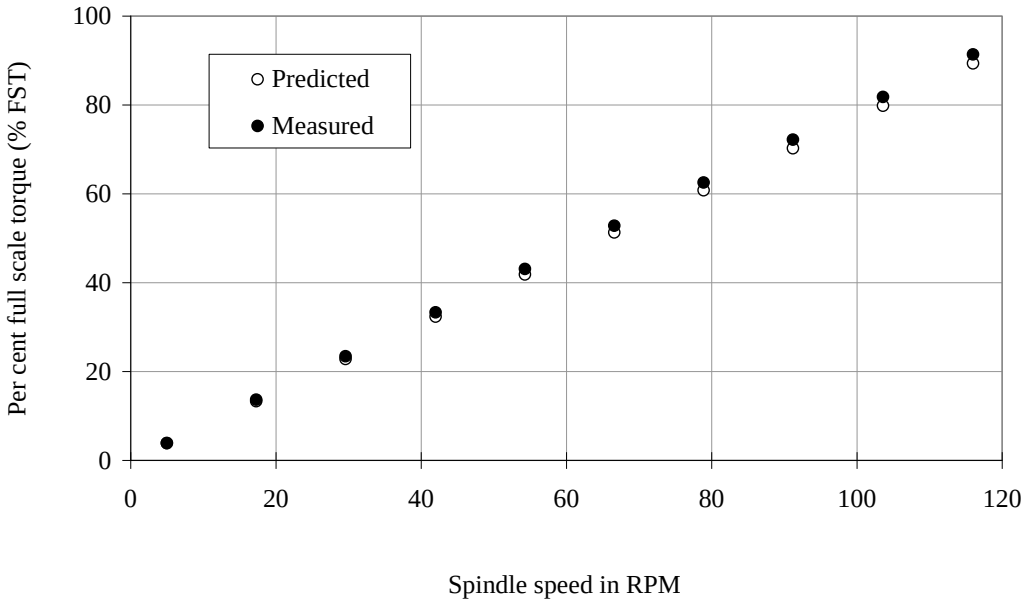

Calibration test 17

Calibration oil	N1000
Standard viscosity (mPa.s)	2855
Standard density (kg/m^3)	849.5
Temperature	20^{0}C

Sensor system	MV3
Spindle radius (mm)	15.2
Cup radius (mm)	21
Spindle length (mm)	60

Spindle speed in RPM	Predicted torque (% FST)	Measured torque (% FST)
5.004	1.824656	1.809333
31.7	11.55907	11.84667
58.4	21.29495	21.92667
85.2	31.06729	32.02333
112	40.83963	42.06667
138.8	50.61197	52.03333
165.6	60.38431	61.86667
192.3	70.12019	71.46667
219	79.85607	80.9
245.7	89.59194	90.03333

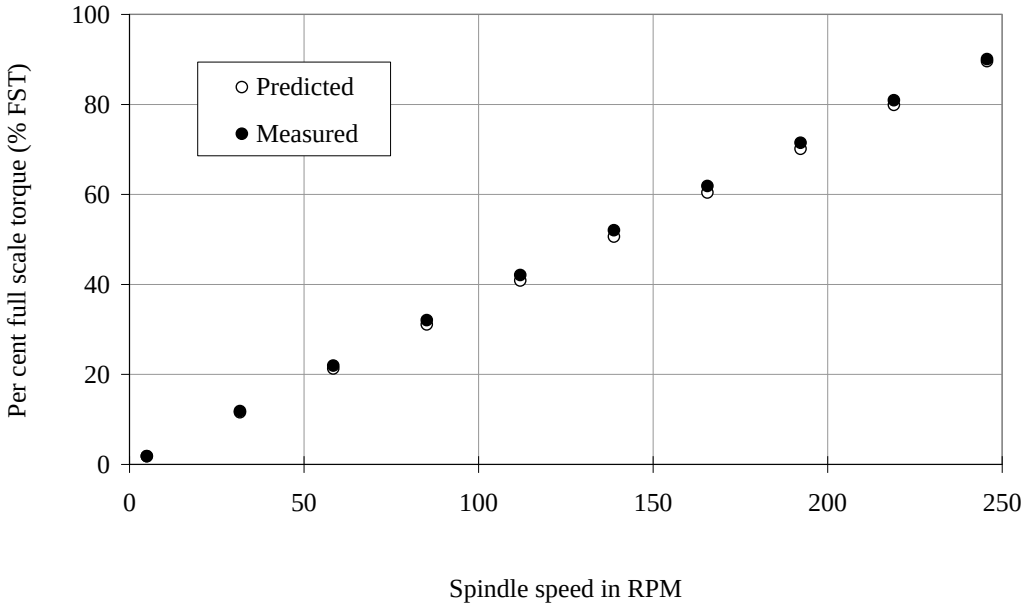

Calibration test 18

Calibration oil	N1000
Standard viscosity (mPa.s)	2008
Standard density (kg/m^3)	846.5
Temperature	25^{0}C

Sensor system	MV3
Spindle radius (mm)	15.2
Cup radius (mm)	21
Spindle length (mm)	60

Spindle speed in RPM	Predicted torque (% FST)	Measured torque (% FST)
5.004	1.283331	1.247
43.4	11.13041	11.72667
81.9	21.00416	22.19667
120.3	30.85226	32.51667
158.8	40.72601	42.76667
197.2	50.57412	52.8
235.6	60.42222	62.63333
274.1	70.29597	72.23333
312.6	80.16972	81.53333
351.1	90.04347	90.5

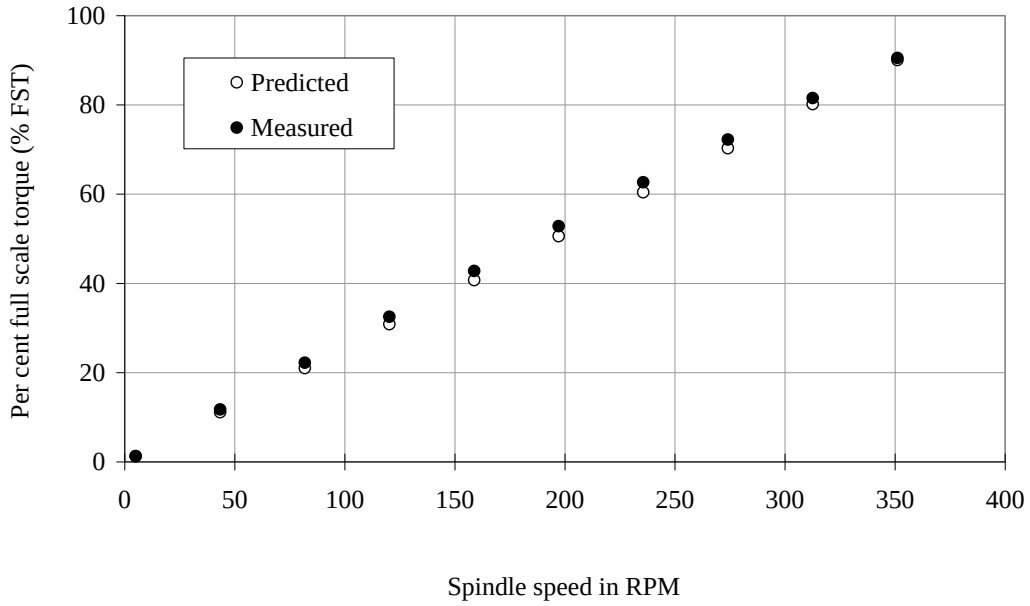

Recalibration test 1

Calibration oil	N100
Standard viscosity (mPa.s)	277.7
Standard density (kg/m^3)	881.4
Temperature	20^{0}C

Sensor system	MV1
Spindle radius (mm)	20.04
Cup radius (mm)	21
Spindle length (mm)	60

Spindle speed in RPM	Predicted torque (% FST)	Measured torque (% FST)
5.004	1.644058	1.645
34.8	11.4335	12.04
64.7	21.2571	22.47667
94.5	31.04786	32.73333
124.5	40.90432	42.9
154.4	50.72792	52.93333
184.4	60.58439	62.76667
214.3	70.40799	72.5
244.1	80.19875	82.06667
274.1	90.05521	91.53333

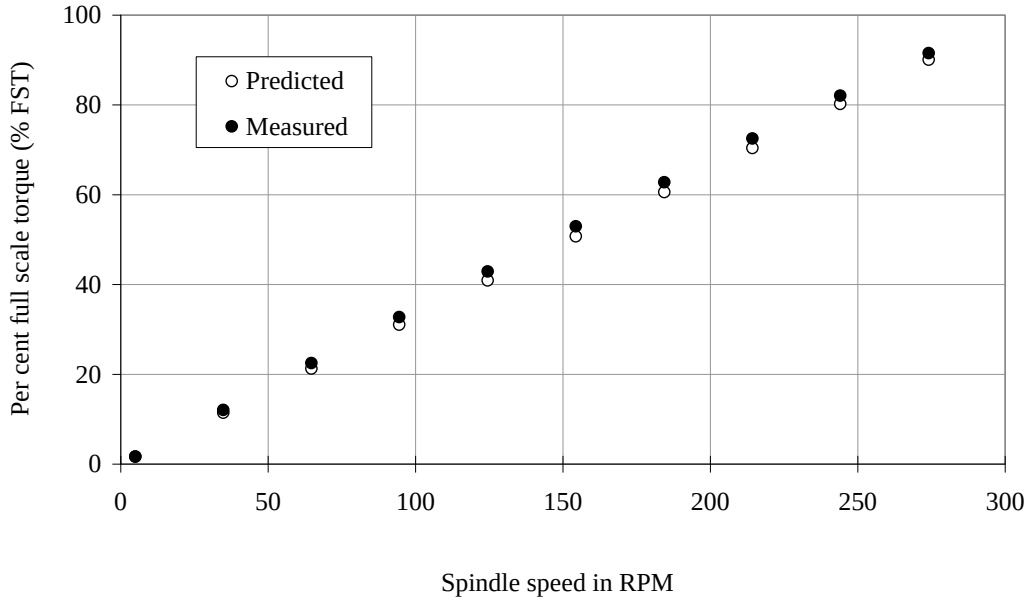

Recalibration test 2

Calibration oil	N100
Standard viscosity (mPa.s)	277.7
Standard density (kg/m^3)	881.4
Temperature	20^{0}C

Sensor system	MV2
Spindle radius (mm)	18.4
Cup radius (mm)	21
Spindle length (mm)	60

Spindle speed in RPM	Predicted torque (% FST)	Measured torque (% FST)
5.004	0.533048	0.456
77.6	8.266292	8.513333
150.2	15.99996	16.6
222.9	23.74428	24.66667
295.7	31.49926	32.67667
368.4	39.24358	40.56667
440.9	48.62386	50.03882
513.7	60.44913	61.7509
586.4	73.95331	74.86188
659.1	89.54433	89.70135

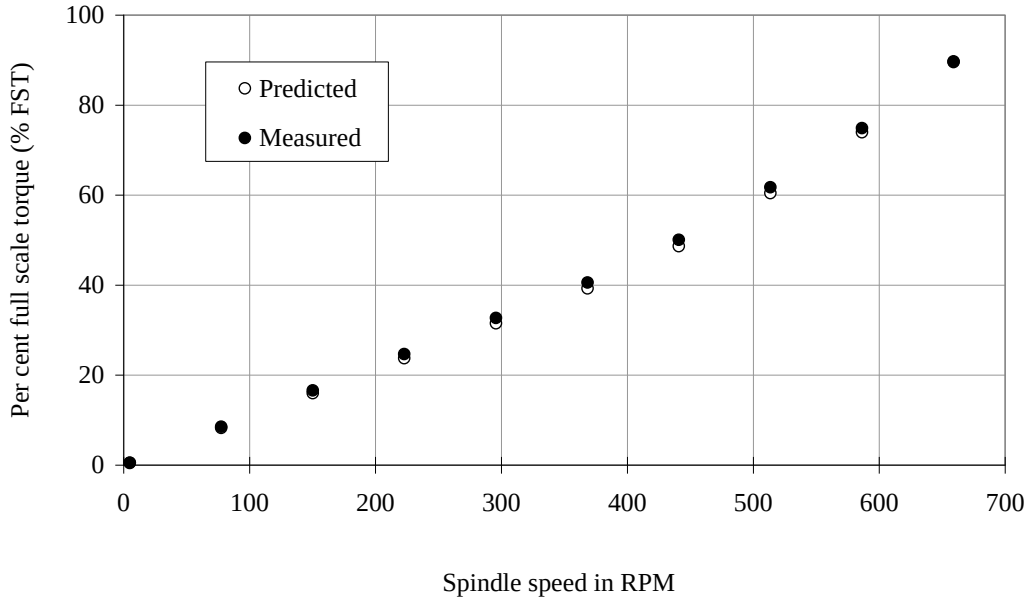

Recalibration test 3

Calibration oil	N100
Standard viscosity (mPa.s)	277.7
Standard density (kg/m^3)	881.4
Temperature	20^{0}C

Sensor system	MV3
Spindle radius (mm)	15.2
Cup radius (mm)	21
Spindle length (mm)	60

Spindle speed in RPM	Predicted torque (% FST)	Measured torque (% FST)
5.004	0.177481	0.154333
91.2	3.234658	3.204
177.2	6.284884	6.333333
263.3	9.338657	9.473333
349.3	12.38888	12.63333
435.5	15.91708	16.23358
521.6	20.58603	20.95697
607.8	26.07212	26.45434
693.8	32.58555	32.84926
779.6	40.44464	40.46319

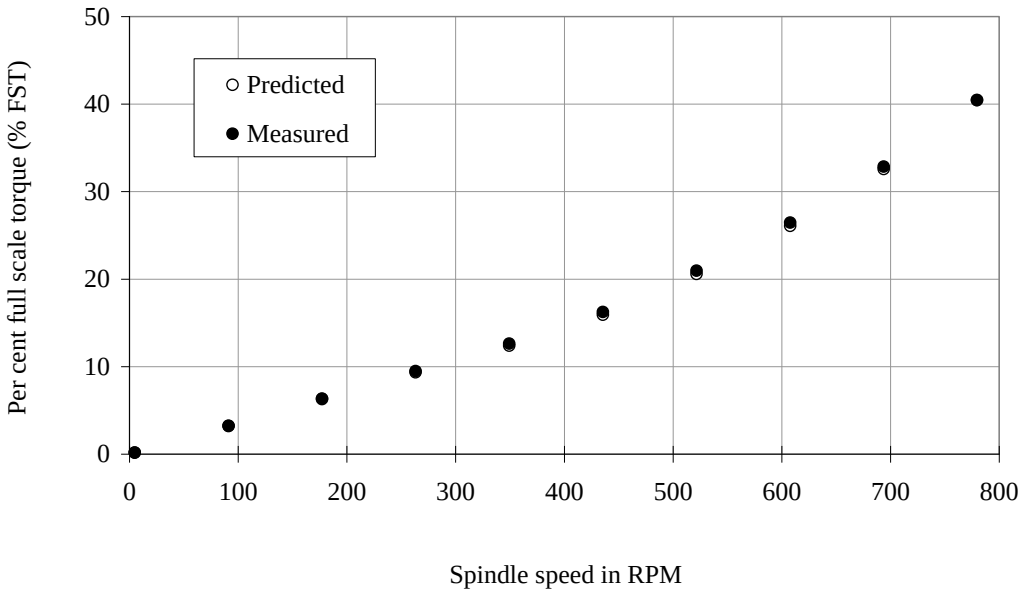

Appendix 2: Vacuum and stirring time selection tests

For all tests reported in this section:

Sensor system	MV1
Temperature	20^0C
Kaolin concentration (% volume)	19%
Sand concentration (% volume)	0%
$CaCl_2.2H_20$:Kaolin (w/w)	0.0028
RPM	400

Test with 5 minutes vacuum and 2.5 minutes of magnetic stirring

Time (min)	% FST	Time (min)	% FST	Time (min)	% FST
1	25.54972	21	25.92222	41	25.21
2	25.76444	22	25.90667	42	25.17667
3	25.83111	23	25.87778	43	25.11722
4	25.85278	24	25.84167	44	25.05222
5	25.91889	25	25.82278	45	25.01556
6	25.95833	26	25.80111	46	24.98333
7	25.96444	27	25.74944	47	24.91
8	25.97556	28	25.72389	48	24.86722
9	25.99556	29	25.70111	49	24.83278
10	26.005	30	25.65722	50	24.76833
11	26.00167	31	25.62056	51	24.70722
12	26.01389	32	25.58389	52	24.66833
13	26.02722	33	25.54278	53	24.615
14	26.035	34	25.49	54	24.56778
15	26.03778	35	25.46611	55	24.50222
16	26.03944	36	25.43722	56	24.46
17	26.03889	37	25.38944	57	24.42611
18	26.02722	38	25.35778	58	24.36222
19	25.98944	39	25.31833	59	24.30611
20	25.95667	40	25.26	60	24.25833

Test with 10 minutes vacuum and 5 minutes of magnetic stirring

Time (min)	% FST	Time (min)	% FST	Time (min)	% FST
1	26.48701	20	26.31389	41	25.94
2	26.56389	21	26.29778	42	25.92333
3	26.56222	22	26.27056	43	25.90722
4	26.54167	23	26.26167	44	25.89833
5	26.55944	24	26.24556	45	25.87944
6	26.53778	25	26.22111	46	25.88222
7	26.50778	26	26.205	47	25.87778
8	26.48833	27	26.16833	48	25.855
9	26.46	28	26.16167	49	25.85667
10	26.42389	29	26.15889	50	25.83222
11	26.40167	30	26.12889	51	25.82833
12	26.41222	31	26.11389	52	25.83222
13	26.40167	32	26.08556	53	25.81389
14	26.40167	33	26.05444	54	25.81333
15	26.39833	34	26.04833	55	25.79611
16	26.38722	35	26.04111	56	25.78833
17	26.36722	36	26.01	57	25.79778
18	26.35056	37	25.98833	58	25.78111
19	26.32556	38	25.97667	59	25.76611
20	26.31389	39	25.94833	60	25.77

Test with 15 minutes vacuum and 7.5 minutes of magnetic stirring

Time (min)	% FST	Time (min)	% FST	Time (min)	% FST
1	27.55254	21	27.35167	41	26.78
2	27.66722	22	27.30889	42	26.78889
3	27.69667	23	27.29222	43	26.75833
4	27.71722	24	27.24667	44	26.74333
5	27.7	25	27.21333	45	26.72
6	27.68944	26	27.19111	46	26.70333
7	27.66778	27	27.14722	47	26.71167
8	27.66778	28	27.11667	48	26.67333
9	27.67167	29	27.06778	49	26.65722
10	27.69	30	27.03056	50	26.63111
11	27.60778	31	27.01389	51	26.59944
12	27.54389	32	26.97611	52	26.59944
13	27.51722	33	26.95111	53	26.59222
14	27.48278	34	26.92167	54	26.56222
15	27.46389	35	26.87667	55	26.55611
16	27.44722	36	26.86667	56	26.51278
17	27.42389	37	26.85556	57	26.49667
18	27.4	38	26.82556	58	26.50556
19	27.36778	39	26.815	59	26.475
20	27.35611	40	26.78389	60	26.45111

Test with 20 minutes vacuum and 10 minutes of magnetic stirring

Time (min)	% FST	Time (min)	% FST	Time (min)	% FST
1	28.2678	21	27.99333	41	27.68889
2	28.30667	22	27.98833	42	27.69889
3	28.28389	23	27.96889	43	27.70667
4	28.24389	24	27.93222	44	27.68722
5	28.24222	25	27.92556	45	27.70389
6	28.22778	26	27.91833	46	27.69278
7	28.19389	27	27.88056	47	27.69556
8	28.165	28	27.86389	48	27.72389
9	28.14278	29	27.845	49	27.71944
10	28.11222	30	27.81333	50	27.70444
11	28.08056	31	27.81333	51	27.71389
12	28.09333	32	27.80444	52	27.69389
13	28.09778	33	27.77833	53	27.69833
14	28.09333	34	27.76889	54	27.71722
15	28.08611	35	27.74333	55	27.69889
16	28.09278	36	27.73333	56	27.70556
17	28.06667	37	27.74333	57	27.69833
18	28.03333	38	27.72444	58	27.68556
19	28.02889	39	27.71389	59	27.70111
20	28.01944	40	27.70556	60	27.71278

Test with 25 minutes vacuum and 12.5 minutes of magnetic stirring

Time (min)	% FST	Time (min)	% FST	Time (min)	% FST
1	28.2452	21	28.01167	41	27.81333
2	28.36111	22	27.97167	42	27.81167
3	28.38889	23	27.96667	43	27.80444
4	28.37778	24	27.96222	44	27.82722
5	28.26056	25	27.93111	45	27.84389
6	28.35833	26	27.92	46	27.82722
7	28.30111	27	27.89	47	27.83833
8	28.25278	28	27.87722	48	27.82611
9	28.22278	29	27.88278	49	27.81111
10	28.19889	30	27.85222	50	27.83111
11	28.185	31	27.84389	51	27.82722
12	28.18556	32	27.83833	52	27.80944
13	28.17	33	27.82778	53	27.80667
14	28.15556	34	27.82944	54	27.78556
15	28.12722	35	27.82556	55	27.79556
16	28.08722	36	27.81444	56	27.79
17	28.06278	37	27.80333	57	27.77389
18	28.06333	38	27.79778	58	27.76722
19	28.04389	39	27.81778	59	27.73667
20	28.02333	40	27.815	60	27.75278

Appendix 3: Fresh and scalped kaolin-water mixture comparison tests

For all tests reported in this section:

Sensor system	MV1
Temperature	20^0C
$CaCl_2.2H_20$:Kaolin (w/w)	0.001

Test combination: 17% kaolin and 15% sand

	Before adding sand	After sieving out sand
Kaolin concentration (% vol.)	16.9	17.1
GS Sand concentration (% vol.)	0	0
Bingham yield stress (Pa)	21.4	21.7
Plastic viscosity (mPa.s)	12.7	12.4

Before adding sand	
RPM	Torque (N.m)
96.9	0.00374
130.2	0.00396
163.3	0.00415
196.3	0.00431
229.5	0.00446
262.6	0.0046
295.7	0.00473
328.9	0.00486
362	0.00499
362	0.00499
328.9	0.00487
295.7	0.00475
262.6	0.00462
229.5	0.00448
196.3	0.00434
163.3	0.00418
130.2	0.004
97.7	0.0038

After sieving out sand	
RPM	Torque (N.m)
96.91	0.00381
130.2	0.00402
163.3	0.0042
196.3	0.00436
229.5	0.0045
262.6	0.00464
295.7	0.00476
328.9	0.00488
362	0.00499
362	0.00499
328.9	0.00487
295.7	0.00474
262.6	0.00461
229.5	0.00447
196.3	0.00432
163.3	0.00416
130.2	0.00399
97.68	0.0038

Test combination: 17% kaolin and 20% sand

	Before adding sand	After sieving out sand
Kaolin concentration (% vol.)	17.1	17.1
GS Sand concentration (% vol.)	0	0
Bingham yield stress (Pa)	21.8	22.5
Plastic viscosity (mPa.s)	12.5	12.4

Before adding sand	
RPM	Torque (N.m)
96.9	0.00382
130.2	0.004
163.3	0.00418
196.3	0.00435
229.5	0.0045
262.6	0.00464
295.7	0.00477
328.9	0.0049
362	0.00502
362	0.00502
328.9	0.0049
295.7	0.00478
262.6	0.00465
229.5	0.00452
196.3	0.00437
163.3	0.00421
130.2	0.00404
97.69	0.00384

After sieving out sand	
RPM	Torque (N.m)
96.9	0.00398
130.2	0.00413
163.3	0.00431
196.3	0.00447
229.5	0.00462
262.6	0.00475
295.7	0.00489
328.9	0.00501
362	0.00513
362	0.00512
328.9	0.005
295.7	0.00487
262.6	0.00474
229.5	0.0046
196.3	0.00445
163.3	0.0043
130.2	0.00412
97.3	0.00392

Appendix 4: Supernatant water ion-analysis

Note: BDL = Below detection limit.

Ions (ppm)	Day 1: Sample		Day 2: Sample		Day 3: Sample		Day 4: Sample	
	A	B	A	B	A	B	A	B
F	BDL	0.1	0.1	0.1	0.2	0.2	BDL	0.3
Cl	4.4	4.7	5.0	4.9	4.2	4.6	5.2	5.4
NO_2	BDL	BDL	BDL	BDL	BDL	BDL	BDL	BDL
NO_3	0.3	0.4	0.6	0.6	0.2	0.3	0.3	0.2
PO_4	BDL	BDL	BDL	BDL	BDL	BDL	BDL	BDL
SO_4	4.4	4.3	4.5	4.4	4.2	4.1	4.5	4.5
Br	BDL	BDL	BDL	BDL	BDL	BDL	BDL	BDL
Al	0.4	0.6	0.3	0.5	0.2	BDL	0.9	1.0
B	0.0	BDL	0.0	BDL	0.0	0.1	0.0	0.1
Ba	BDL	BDL	BDL	BDL	BDL	BDL	BDL	BDL
Ca	3.4	3.3	3.4	3.3	3.2	3.3	3.1	3.3
Cd	BDL	BDL	BDL	BDL	BDL	BDL	BDL	BDL
Co	BDL	BDL	BDL	BDL	BDL	BDL	BDL	BDL
Cr	BDL	BDL	BDL	BDL	BDL	BDL	BDL	BDL
Cu	0.2	0.2	0.2	0.3	BDL	BDL	0.1	0.1
Fe	0.2	0.3	0.1	0.2	BDL	BDL	0.4	0.5
K	BDL	BDL	BDL	BDL	BDL	BDL	BDL	BDL
Li	BDL	BDL	BDL	BDL	BDL	BDL	BDL	BDL
Mg	1.2	1.2	1.2	1.2	1.1	1.2	1.2	1.2
Mn	BDL	BDL	BDL	BDL	BDL	BDL	BDL	BDL
Mo	BDL	BDL	BDL	BDL	BDL	BDL	BDL	BDL
Na	6.5	6.2	6.3	6.2	5.9	4.6	6.6	5.5
Ni	BDL	BDL	BDL	BDL	BDL	BDL	BDL	BDL
P	BDL	BDL	BDL	BDL	BDL	BDL	BDL	BDL
Pb	BDL	BDL	BDL	BDL	BDL	BDL	BDL	BDL

Ions (ppm)	Day 1: Sample		Day 2: Sample		Day 3: Sample		Day 4: Sample	
	A	B	A	B	A	B	A	B
S	2.0	1.8	1.8	1.8	1.7	1.9	1.8	2.0
Sb	BDL	BDL	BDL	BDL	BDL	BDL	BDL	BDL
Se	BDL	BDL	BDL	BDL	BDL	BDL	BDL	BDL
Si	1.6	1.9	1.3	1.6	1.4	1.4	2.9	3.5
Sn	ENA	ENA	ENA	ENA	ENA	ENA	ENA	ENA
Sr	0.0	0.0	0.0	0.0	0.0	0.0	0.0	0.0
Ti	0.0	0.0	0.0	0.0	0.0	BDL	0.0	BDL
V	BDL	BDL	BDL	BDL	BDL	BDL	BDL	BDL
Zn	BDL	BDL	BDL	BDL	BDL	BDL	BDL	BDL
Zr	BDL	BDL	BDL	BDL	BDL	BDL	BDL	BDL

Appendix 5: Lane mountain sand settling tests

For all tests reported in this section:

Sensor system	MV1
Temperature	20^0C
$CaCl_2.2H_20$:Kaolin (w/w)	0.001
Sand concentration (% volume)	20%

Kaolin concentration (% volume) = 10% and Spindle speed 400 RPM

Time (sec)	% FST	Time (sec)	% FST	Time (sec)	% FST
6.61	10.33333	107	7.733333	207.7	7.033333
9.735	9.466667	110.3	7.7	210.9	7.033333
13.08	9.4	113.6	7.633333	214.2	7
16.84	9.3	117	7.6	217.6	7
19.87	9.133333	120.7	7.566667	220.9	7
23.2	9.066667	123.8	7.533333	224.7	7
26.58	9	127.1	7.5	227.7	7
29.92	8.966667	130.5	7.5	231	6.966667
33.2	8.9	133.8	7.466667	234.4	6.9
36.74	8.8	137.1	7.466667	237.7	6.9
40.17	8.766667	140.6	7.4	241	6.9
43.25	8.7	144.1	7.433333	244.5	6.9
46.67	8.633333	147.2	7.333333	248	7.5
50.14	8.6	150.6	7.366667	251.1	6.9
53.36	8.533333	154	7.3	254.5	6.933333
57.12	8.466667	157.3	7.266667	257.9	6.933333
60.06	8.4	161	7.233333	261.2	6.933333
63.5	8.366667	164	7.233333	264.9	6.933333
66.72	8.3	167.4	7.2	267.9	6.9
70.12	8.5	170.6	7.2	271.3	6.833333
73.45	8.2	174	7.2	274.7	6.8
76.8	8.166667	177.4	7.166667	277.9	6.8
80.45	8.1	180.7	7.166667	281.3	6.766667
83.5	8	184.4	7.133333	284.6	6.766667
86.81	8	187.4	7.133333	288.3	6.866667
90.2	7.933333	190.7	7.1	291.3	6.8
93.66	7.9	194.1	7.1	294.8	6.833333
96.87	7.833333	197.4	7.066667	298	6.833333
100.3	7.833333	200.8	7.066667	301.5	6.933333
103.8	7.766667	204.3	7.033333	304.7	6.866667

Time (sec)	% FST	Time (sec)	% FST	Time (sec)	% FST
308.2	6.866667	409.1	6.6	509.3	5.533333
311.6	6.9	412.1	6.533333	513	5.5
314.8	6.866667	415.5	6.5	516	5.466667
318.1	6.9	418.7	6.533333	519.4	5.466667
321.5	6.733333	422.1	6.533333	522.6	5.466667
324.8	6.7	425.5	6.533333	526	5.533333
328.6	6.7	428.7	6.533333	529.4	5.433333
331.6	6.7	432.5	6.433333	532.7	5.4
334.9	6.7	435.5	6.4	536.4	5.366667
338.3	6.666667	438.8	6.4	539.4	5.333333
341.7	6.666667	442.3	6.4	542.7	5.3
345	6.633333	445.6	6.3	546.1	5.333333
348.5	6.7	448.9	6.3	549.6	5.266667
351.9	6.666667	452.4	6.233333	552.7	5.266667
355	6.7	455.8	6.166667	556.3	5.266667
358.4	6.733333	458.9	6.166667	559.7	5.233333
361.8	6.666667	462.3	6.066667	562.9	5.266667
365.2	6.633333	465.7	6.033333	566.2	5.233333
368.8	6.566667	469	6.1	569.7	5.166667
371.8	6.566667	472.8	5.9	572.9	5.166667
375.2	6.566667	475.7	5.866667	576.7	5.166667
378.5	6.6	479.1	5.8	579.6	5.166667
381.8	6.566667	482.3	5.8	583	5.133333
385.2	6.566667	485.7	5.733333	586.2	5.133333
388.5	6.566667	489.1	5.733333	589.6	5.1
392.2	6.566667	492.4	5.666667	593	5.1
395.2	6.566667	496.1	5.633333	596.3	5.1
398.7	6.566667	499.1	5.6	600	5.066667
401.9	6.566667	502.6	5.566667	603	5.066667
405.4	6.566667	505.8	5.533333	606.5	5.066667

Kaolin concentration (% volume) = 14% and Spindle speed 400 RPM

Time (sec)	% FST	Time (sec)	% FST	Time (sec)	% FST
5.907	16.2	106.2	13.3	207	12.96667
9.266	13.36667	109.7	13.26667	210.2	12.8
12.44	13.36667	113.2	13.26667	213.6	12.76667
15.77	13.4	116.3	13.23333	217.1	12.76667
19.22	13.6	119.7	13.23333	220.2	12.76667
22.47	13.43333	123.1	13.2	223.6	12.73333
26.22	13.43333	126.4	13.16667	226.9	12.73333
29.16	13.46667	130.1	13.16667	230.3	12.73333
32.58	13.5	133.1	13.13333	234	12.7
35.95	13.53333	136.5	13.13333	237	12.7
39.2	13.5	139.9	13.1	240.4	12.7
42.59	13.53333	143.1	13.1	243.8	12.66667
46.11	13.56667	146.5	13.06667	247	12.66667
49.55	13.5	150	13.03333	250.4	12.66667
52.64	13.53333	153.5	13.03333	253.9	12.63333
56.06	13.5	156.5	13	257.4	12.6
59.5	13.5	160	12.96667	260.5	12.56667
62.75	13.5	163.4	12.96667	263.9	12.6
66.52	13.5	166.7	12.96667	267.2	12.56667
69.44	13.5	170.4	12.96667	270.6	12.6
72.87	13.5	173.3	12.93333	274.3	12.33333
76.11	13.46667	176.8	12.93333	277.2	12.53333
79.5	13.43333	180	12.93333	280.7	12.56667
82.83	13.43333	183.4	12.9	283.9	12.53333
86.12	13.43333	186.7	12.86667	287.3	12.56667
89.84	13.4	190	12.86667	290.6	12.53333
92.87	13.4	193.7	12.86667	294	12.53333
96.2	13.36667	196.8	12.83333	297.7	12.5
99.58	13.33333	200.1	12.83333	300.7	12.5
103	13.33333	203.5	12.83333	304	12.5

Time (sec)	% FST	Time (sec)	% FST	Time (sec)	% FST
307.4	12.5	407.9	12.26667	508.5	11.96667
310.9	12.5	411.3	12.26667	511.8	11.96667
314.1	12.5	414.8	12.3	515.2	11.96667
317.5	12.5	418	12.26667	518.7	11.96667
321	12.5	421.5	12.3	521.9	11.96667
324.1	12.46667	424.9	12.3	525.4	11.96667
327.5	12.5	428	12.26667	528.8	11.96667
330.9	12.46667	431.4	12.26667	532	11.96667
334.2	12.46667	434.8	12.23333	535.3	11.93333
338	12.43333	438.1	12.23333	538.6	11.93333
340.9	12.43333	441.8	12.23333	542	11.9
344.3	12.4	444.8	12.23333	545.8	11.86667
347.7	12.36667	448.2	12.2	548.8	11.9
351.1	12.4	451.6	12.16667	552.1	11.9
354.3	12.36667	455	12.16667	555.5	11.86667
357.7	12.4	458.2	12.16667	558.8	11.86667
361.3	12.36667	461.6	12.13333	562.1	11.86667
364.4	12.36667	465.2	12.13333	565.7	11.86667
367.8	12.4	468.3	12.13333	569.1	11.86667
371.2	12.36667	471.7	12.16667	572.2	11.86667
374.5	12.36667	475.1	12.13333	575.6	11.83333
378.2	12.36667	478.4	12.13333	579	11.83333
381.2	12.33333	482.1	12.06667	582.3	11.83333
384.6	12.33333	485.1	12.06667	586	11.83333
387.8	12.33333	488.5	12	589	11.83333
391.2	12.33333	491.7	11.96667	592.4	11.8
394.5	12.33333	495.1	11.96667	595.7	11.8
397.9	12.33333	498.5	11.96667	599	11.8
401.6	12.3	501.8	11.96667	602.4	11.8
404.6	12.3	505.5	11.96667	605.7	11.83333

Kaolin concentration (% volume) = 17% and Spindle speed 400 RPM

Time (sec)	% FST	Time (sec)	% FST	Time (sec)	% FST
7.14	31.1	107.4	36.66667	208	36.66667
10.5	31.26667	110.7	36.66667	211.3	36.66667
13.53	31.9	114.4	36.66667	214.6	36.66667
17	32.66667	117.4	36.66667	218.3	36.66667
20.22	33.16667	120.8	36.66667	221.3	36.66667
23.58	33.66667	124.1	36.66667	224.8	36.66667
27.45	34	127.6	36.66667	228	36.66667
30.39	34.33333	131.4	36.66667	231.4	36.66667
33.81	34.33333	134.3	36.66667	235.3	36.66667
36.98	34.66667	137.7	36.66667	238.2	36.66667
40.33	35	140.9	36.66667	241.6	36.66667
43.78	35	144.3	36.66667	244.8	36.33333
47.08	35.33333	147.7	36.66667	248.2	36.33333
50.78	35.33333	151	36.66667	251.6	36.33333
53.81	35.66667	154.7	36.66667	254.9	36.33333
57.14	35.66667	157.7	36.66667	258.6	36.33333
60.51	36	161	36.66667	261.6	36.33333
63.98	36	164.4	36.66667	265	36.33333
67.16	36	167.9	36.66667	268.3	36.33333
70.67	36	171	36.66667	271.8	36.33333
74.11	36.33333	174.6	36.66667	275	36.33333
77.2	36.33333	178	36.66667	278.5	36.33333
80.61	36.33333	181.2	36.66667	281.9	36.33333
84.05	36.33333	184.5	36.66667	285.1	36.33333
87.3	36.33333	188	36.66667	288.4	36.33333
91.06	36.66667	191.2	36.66667	291.9	36.33333
94	36.66667	195	36.66667	295.1	36.33333
97.42	36.66667	197.9	36.66667	298.9	36.33333
100.8	36.66667	201.3	36.66667	301.8	36.33333
104	36.66667	204.7	36.66667	305.2	36.33333

Time (sec)	% FST	Time (sec)	% FST	Time (sec)	% FST
308.6	36.33333	409.2	35.33333	509.6	35
311.9	36.33333	412.5	35.33333	513	35
315.2	36	415.8	35.33333	516.4	34.66667
318.5	36	419.1	35.33333	519.7	34.66667
322.2	36	422.5	35.33333	523	34.66667
325.2	36	426.1	35.33333	526.4	34.66667
328.7	36	429.2	35.33333	530	34.66667
331.9	36	432.6	35.33333	533.1	34.66667
335.4	36	436.1	35.33333	536.5	34.66667
339.2	36	439.2	35.33333	540	34.66667
342.1	36	443.1	35.33333	543.2	34.66667
345.5	36	446	35.33333	547	34.66667
348.7	36	449.4	35.33333	549.9	34.66667
352.1	36	452.6	35.33333	553.3	34.66667
355.5	36	456.2	35.33333	556.6	34.66667
358.8	35.66667	459.4	35.33333	560	34.66667
362.5	35.66667	462.7	35	563.3	34.33333
365.5	35.66667	466.4	35	566.6	34.33333
368.9	35.66667	469.4	35	570.3	34.33333
372.2	35.66667	472.8	35	573.3	34.33333
375.6	35.66667	476.1	35	576.7	34.33333
378.9	35.66667	479.6	35	580	34.33333
382.4	35.66667	482.8	35	583.5	34.33333
385.8	35.66667	486.3	35	586.7	34.33333
388.9	35.66667	489.7	35	590.2	34.33333
392.3	35.66667	492.9	35	593.6	34.33333
395.8	35.66667	496.2	35	596.8	34.33333
399	35.66667	499.7	35	600.1	34.33333
402.8	35.66667	502.9	35	603.6	34.33333
405.7	35.66667	506.7	35	606.8	34.33333

Kaolin concentration (% volume) = 19% and Spindle speed 400 RPM

Time (sec)	% FST	Time (sec)	% FST	Time (sec)	% FST
5.969	48.66667	106.2	59.66667	206.8	59.33333
9.234	51.33333	109.7	59.66667	210.7	59.33333
12.39	52.66667	113.1	59.66667	213.6	59.33333
15.73	53.66667	116.3	59.66667	217	59.33333
19.17	54.66667	119.6	59.66667	220.2	59.33333
22.41	55.33333	123.1	59.66667	223.5	59.33333
26.19	56	126.3	59.66667	227	59.33333
29.12	56.33333	130.1	59.66667	230.2	59.33333
32.55	56.66667	133	59.66667	234	59.33333
35.91	57	136.5	59.66667	237	59.33333
39.39	57.33333	139.8	59.66667	240.4	59.33333
42.55	57.66667	143.3	59.66667	243.7	59.33333
46.08	58	146.5	59.66667	247.2	59.33333
49.51	58	150	59.66667	250.4	59
52.59	58.33333	153.4	59.66667	253.9	59
56.01	58.33333	156.5	59.66667	257.3	59
59.45	58.66667	159.9	59.66667	260.4	59
62.7	58.66667	163.4	59.66667	263.8	59
66.47	59	166.6	59.66667	267.3	59
69.41	59	170.4	59.66667	270.5	59
72.83	59	173.3	59.66667	274.3	59
76.06	59.33333	176.7	59.66667	277.2	59
79.44	59.33333	180	59.66667	280.6	59
82.78	59.33333	183.4	59.66667	283.9	59
86.16	59.33333	186.7	59.66667	287.3	59
89.8	59.33333	190	59.66667	290.6	59
92.83	59.66667	193.7	59.66667	294	59
96.16	59.66667	196.7	59.66667	297.6	58.66667
99.53	59.66667	200.1	59.66667	300.6	58.66667
102.9	59.66667	203.4	59.33333	304	58.66667

Time (sec)	% FST	Time (sec)	% FST	Time (sec)	% FST
307.4	58.66667	408	58	508.5	57.33333
310.8	58.66667	411.2	57.66667	511.9	57.33333
314.6	58.66667	414.7	57.66667	515.2	57.33333
317.5	58.66667	418	58	518.6	57.33333
320.9	58.66667	421.3	58	521.8	57.33333
324.1	58.66667	424.8	58	525.3	57.33333
327.4	58.66667	428	57.66667	528.7	57
330.9	58.66667	431.3	57.66667	531.9	57
334.2	58.66667	434.8	57.66667	535.2	57
337.9	58.33333	438	57.66667	538.7	57
340.9	58.66667	441.8	57.66667	542	57
344.3	58.33333	444.8	57.66667	545.7	57
347.6	58.33333	448.2	57.66667	548.7	57
351.1	58.33333	451.5	57.66667	552.1	57
354.2	58.33333	455	57.66667	555.5	57
357.8	58.33333	458.2	57.66667	558.9	57.33333
361.2	58.33333	461.7	57.66667	562.1	57
364.3	58.33333	465.1	57.66667	565.6	57
367.7	58.33333	468.2	57.66667	569	57
371.2	58.33333	471.6	57.66667	572.1	57
374.4	58.33333	475.1	57.66667	575.5	57
378.2	58.33333	478.4	57.66667	579	57
381.1	58.33333	482.1	57.66667	582.2	57
384.5	58	485	57.66667	586	57
387.8	58	488.5	57.66667	588.9	57
391.2	58	491.8	57.33333	592.4	57
394.5	58	495.1	57.33333	595.7	57
397.9	58	498.4	57.33333	599	57
401.5	58	501.8	57.33333	602.3	57
404.5	58	505.4	57.33333	605.7	57

Kaolin concentration (% volume) = 22% and Spindle speed 75 RPM

Time (sec)	% FST	Time (sec)	% FST	Time (sec)	% FST
6.875	63	107.1	74.33333	207.8	76.33333
10	66	110.5	74	211.1	76.66667
13.39	66.66667	113.9	74.66667	214.6	76.33333
17.02	67.33333	117.2	74.33333	217.8	76.33333
20.16	68	120.9	74.66667	221.2	76.33333
23.37	68.33333	124	74.33333	224.8	76.66667
26.77	68.66667	127.3	74.66667	227.9	76.66667
30.12	69	130.7	74.66667	231.2	76.66667
33.45	69.33333	134	75	234.5	76.66667
36.91	69.66667	137.9	75	237.9	76.66667
40.36	70	140.8	75	241.2	77
43.5	70	144.2	75	244.6	77
46.95	70.66667	147.4	75	248.1	77
50.17	71	150.8	75.33333	251.3	77.33333
53.52	71.33333	154.2	75.33333	254.7	77
57.28	71.33333	157.4	75.33333	258.1	77
60.34	71.33333	161.2	75.33333	261.3	77
63.66	71.66667	164.3	75.66667	265.1	77
66.91	72	167.6	75.66667	268	77
70.28	72.33333	170.8	75.66667	271.5	77
73.61	72.33333	174.2	75.66667	274.7	77.33333
76.97	72.33333	177.6	75.66667	278.2	77.33333
80.66	73	180.9	76	281.6	77
83.77	73	184.5	76	284.9	77
87.12	73.33333	187.7	76	288.4	77.33333
90.58	73.33333	190.9	76	291.6	77.33333
93.81	73.66667	194.4	76.33333	294.9	77.33333
97.09	73.33333	197.7	76.33333	298.3	77.33333
100.5	74	201	76	301.7	77.33333
104	74	204.4	76.33333	305	77.66667

Time (sec)	% FST	Time (sec)	% FST	Time (sec)	% FST
308.5	77.66667	409.3	78	509.5	78
311.7	77.33333	412.2	78	513.2	78
315	77.33333	415.7	78	516.1	78
318.4	77.33333	419	77.66667	519.6	78
321.7	77.66667	422.3	77.66667	522.8	78
325.1	77.66667	425.7	78	526.3	78
328.7	77.66667	429	78	529.5	78
331.9	77.66667	432.6	78	532.9	78
335.1	77.66667	435.7	78	536.6	78
338.6	77.66667	439	78	539.7	78
341.9	77.66667	442.4	78	542.9	78
345.2	77.66667	445.7	78	546.4	78
348.5	77.66667	449.1	78	549.6	78
352	77.66667	452.5	78	553	78
355.3	77.66667	456	78	556.5	78
358.6	77.66667	459.1	78	559.9	78
362	77.66667	462.5	78.33333	563	78
365.3	77.66667	465.8	78	566.4	78
368.6	77.66667	469.3	78	569.7	78
371.9	77.66667	472.9	78	573.2	78
375.4	78	475.8	78	576.8	78
378.7	78	479.3	78	579.8	78
382	78	482.6	78	583.2	78
385.4	77.66667	486.1	78	586.6	78
388.8	77.66667	489.2	78	589.8	78
392.3	78.33333	492.7	78	593.2	77.66667
395.5	78	496.2	78	596.7	78
399	77.66667	499.5	78	600.2	78
402.2	78	502.8	78	603.4	78
405.5	77.66667	506.2	78	606.7	78

Appendix 6: Granusil Silica sand settling tests

For all tests reported in this section:

Sensor system	MV1
Temperature	20^0C
$CaCl_2.2H_20$:Kaolin (w/w)	0.001
Sand concentration (% volume)	20%

Kaolin concentration (% volume) = 10% and Spindle speed 200 RPM

Time (sec)	% FST	Time (sec)	% FST	Time (sec)	% FST
6.719	5.2	107	3.266667	207.7	2.833333
9.781	4.8	110.3	3.233333	210.9	2.833333
13.19	4.733333	113.7	3.233333	214.2	2.833333
16.86	4.7	117	3.2	217.7	2.833333
19.89	4.666667	120.7	3.166667	221	2.8
23.22	4.633333	123.8	3.166667	224.7	2.8
26.58	4.533333	127.1	3.166667	227.7	2.8
29.94	4.466667	130.5	3.133333	231	2.8
33.23	4.466667	133.8	3.133333	234.4	2.8
36.75	4.366667	137.1	3.1	237.9	2.766667
40.17	4.3	140.7	3.1	241	2.766667
43.28	4.2	144.1	3.066667	244.6	2.766667
46.69	4.133333	147.2	3.066667	248	2.733333
50.12	4.066667	150.6	3.066667	251.1	2.733333
53.5	4	154	3.033333	254.5	2.733333
57.16	3.9	157.3	3	257.9	2.733333
60.08	3.8	161	3	261.3	2.733333
63.5	3.766667	164	3	265	2.7
66.87	3.7	167.4	3	267.9	2.7
70.11	3.666667	170.6	3	271.3	2.666667
73.45	3.6	174	2.966667	274.7	2.7
76.81	3.533333	177.4	2.966667	277.9	2.7
80.47	3.5	180.7	2.966667	281.3	2.7
83.5	3.466667	184.4	2.933333	284.6	2.666667
86.83	3.433333	187.4	2.9	288.3	2.666667
90.2	3.4	190.7	2.9	291.3	2.666667
93.67	3.333333	194.1	2.866667	294.8	2.666667
96.91	3.333333	197.6	2.9	298.1	2.633333
100.4	3.3	200.8	2.866667	301.5	2.633333
103.8	3.266667	204.3	2.866667	304.7	2.6

Time (sec)	% FST	Time (sec)	% FST	Time (sec)	% FST
308.2	2.6	408.6	2.433333	509.3	2.333333
311.6	2.6	412.1	2.433333	512.5	2.3
314.8	2.6	415.5	2.433333	516	2.3
318.1	2.6	418.7	2.4	519.4	2.266667
321.6	2.6	422.1	2.433333	522.6	2.266667
324.9	2.566667	425.4	2.4	526.1	2.3
328.6	2.566667	428.7	2.4	529.4	2.266667
331.6	2.566667	432.5	2.4	532.6	2.266667
334.9	2.566667	435.5	2.4	536.4	2.266667
338.3	2.533333	438.8	2.4	539.4	2.266667
341.8	2.566667	442.2	2.366667	542.7	2.266667
345	2.566667	445.7	2.4	546.1	2.266667
348.5	2.533333	448.9	2.4	549.5	2.266667
351.9	2.533333	452.4	2.366667	552.7	2.233333
355	2.533333	455.8	2.366667	556.3	2.266667
358.4	2.533333	458.9	2.333333	559.7	2.233333
361.8	2.5	462.3	2.366667	562.9	2.233333
365.1	2.5	465.7	2.366667	566.2	2.233333
368.9	2.5	469	2.333333	569.7	2.233333
371.8	2.5	472.8	2.333333	572.9	2.233333
375.2	2.5	475.8	2.333333	576.7	2.233333
378.5	2.5	479.1	2.333333	579.6	2.233333
381.8	2.466667	482.4	2.333333	583	2.2
385.2	2.5	485.7	2.3	586.3	2.233333
388.5	2.466667	489.1	2.3	589.6	2.233333
392.2	2.466667	492.5	2.333333	593	2.233333
395.2	2.466667	496.1	2.333333	596.3	2.233333
398.7	2.466667	499.2	2.3	600	2.2
401.9	2.466667	502.6	2.3	603	2.2
405.4	2.466667	506.1	2.266667	606.5	2.2

Kaolin concentration (% volume) = 14% and Spindle speed 200 RPM

Time (sec)	% FST	Time (sec)	% FST	Time (sec)	% FST
6.813	10.66667	107.1	11.36667	207.7	11.63333
9.875	10.63333	110.6	11.43333	211	11.66667
13.41	10.7	113.8	11.43333	214.4	11.63333
16.83	10.76667	117.3	11.43333	217.7	11.6
19.94	10.8	120.7	11.43333	221.2	11.63333
23.33	10.86667	123.8	11.46667	224.6	11.66667
26.78	10.83333	127.2	11.46667	227.7	11.63333
30.03	10.83333	130.7	11.46667	231.1	11.6
33.8	10.86667	133.9	11.43333	234.6	11.56667
36.83	10.9	137.7	11.46667	237.8	11.63333
40.16	10.86667	140.6	11.46667	241.6	11.63333
43.39	10.86667	144.1	11.5	244.5	11.6
46.77	10.86667	147.3	11.53333	248	11.56667
50.12	10.86667	150.7	11.56667	251.3	11.6
53.47	10.9	154	11.53333	254.6	11.6
57.12	10.93333	157.4	11.56667	257.9	11.6
60.19	10.9	161	11.6	261.2	11.56667
63.49	10.96667	164.1	11.63333	264.9	11.56667
66.86	11.03333	167.5	11.63333	268	11.6
70.33	11.06667	170.7	11.63333	271.4	11.56667
73.58	11.06667	174.2	11.66667	274.7	11.6
77.02	11.13333	177.5	11.63333	278.1	11.53333
80.45	11.16667	180.9	11.63333	281.9	11.53333
83.61	11.23333	184.4	11.66667	284.8	11.53333
86.95	11.26667	187.5	11.6	288.3	11.5
90.39	11.3	190.9	11.6	291.4	11.5
93.69	11.3	194.3	11.63333	294.9	11.46667
97.41	11.36667	197.6	11.63333	298.2	11.43333
100.5	11.43333	201.3	11.63333	301.5	11.4
103.8	11.4	204.4	11.66667	305.2	11.33333

Time (sec)	% FST	Time (sec)	% FST	Time (sec)	% FST
308.3	11.3	409.1	10.4	509.4	9.566667
311.6	11.3	412.2	10.33333	513	9.6
315	11.23333	415.5	10.3	516.1	9.6
318.4	11.23333	418.9	10.3	519.4	9.5
321.6	11.13333	422.3	10.26667	522.8	9.5
325.1	11.1	425.6	10.26667	526.2	9.433333
328.5	11.1	428.9	10.16667	529.4	9.4
331.7	11.06667	432.5	10.16667	532.9	9.4
335	11	435.6	10.13333	536.4	9.366667
338.5	11	439	10.13333	539.5	9.366667
341.7	10.93333	442.4	10.1	542.9	9.3
345.5	10.93333	445.7	10.06667	546.3	9.333333
348.4	10.9	449.4	10.03333	549.6	9.3
351.9	10.83333	452.3	10.03333	553.3	9.233333
355.2	10.8	455.8	10.03333	556.2	9.233333
358.5	10.8	459.2	9.933333	559.7	9.233333
361.8	10.76667	462.5	9.933333	562.9	9.2
365.2	10.73333	465.7	9.933333	566.4	9.2
368.8	10.66667	469.1	9.9	569.6	9.133333
371.9	10.63333	472.7	9.833333	573	9.1
375.3	10.63333	475.8	9.866667	576.7	9.166667
378.6	10.63333	479.2	9.8	579.7	9.066667
381.9	10.6	482.6	9.766667	583.2	9.066667
385.3	10.56667	485.9	9.766667	586.6	9.033333
388.7	10.53333	489.7	9.733333	589.8	9.033333
392.2	10.56667	492.6	9.733333	593.6	8.966667
395.3	10.46667	496.1	9.666667	596.5	9
398.8	10.46667	499.3	9.666667	600	8.933333
402.1	10.43333	502.7	9.633333	603.2	8.933333
405.4	10.36667	506	9.6	606.6	8.9

Kaolin concentration (% volume) = 17% and Spindle speed 200 RPM

Time (sec)	% FST	Time (sec)	% FST	Time (sec)	% FST
5.985	20.36667	106.8	24.6	206.9	24.6
9.25	21.16667	109.7	24.63333	210.7	24.6
12.61	21.53333	113.2	24.63333	213.7	24.63333
15.97	21.83333	116.4	24.6	217.1	24.63333
19.19	22.1	119.8	24.66667	220.3	24.56667
22.55	22.3	123.1	24.73333	223.7	24.56667
26.2	22.46667	126.4	24.76667	227	24.56667
29.24	22.7	130.1	24.76667	230.4	24.66667
32.7	22.86667	133.3	24.76667	234	24.6
35.92	23.03333	136.5	24.83333	237.1	24.6
39.41	23.13333	139.9	24.86667	240.4	24.56667
42.62	23.23333	143.3	24.83333	243.8	24.56667
46.09	23.43333	146.6	24.86667	247.2	24.56667
49.52	23.53333	150	24.86667	250.5	24.5
52.69	23.63333	153.5	24.9	253.9	24.36667
56.03	23.66667	156.6	24.93333	257.4	24.33333
59.47	23.8	160	24.86667	260.5	24.33333
62.78	23.93333	163.3	24.9	263.9	24.3
66.49	24	166.7	24.9	267.3	24.23333
69.53	24	170.4	24.86667	270.6	24.23333
72.86	24.06667	173.5	24.86667	274.3	24.26667
76.24	24.16667	176.8	24.8	277.4	24.23333
79.69	24.26667	180.2	24.83333	280.7	24.16667
82.86	24.3	183.4	24.83333	284.1	24.1
86.24	24.36667	186.8	24.76667	287.5	24.1
89.83	24.43333	190.3	24.73333	290.7	24.1
92.92	24.43333	193.7	24.66667	294.2	24.1
96.31	24.46667	196.8	24.66667	297.7	24.03333
99.77	24.46667	200.2	24.7	300.7	24.03333
103	24.5	203.7	24.63333	304.2	24.06667

Time (sec)	% FST	Time (sec)	% FST	Time (sec)	% FST
307.6	24.1	408.1	23.33333	508.6	23
310.9	24.1	411.4	23.4	512	22.96667
314.6	24	414.8	23.4	515.4	22.93333
317.5	24.03333	418.5	23.36667	518.7	22.96667
321	24.06667	421.5	23.36667	522.4	22.9
324.2	24	424.9	23.36667	525.4	22.86667
327.6	23.86667	428.3	23.4	528.8	22.83333
330.9	23.7	431.5	23.36667	532	22.8
334.3	23.63333	434.8	23.33333	535.5	22.86667
338	23.63333	438.2	23.33333	538.7	22.83333
341	23.63333	441.8	23.4	542.1	22.76667
344.3	23.56667	444.9	23.36667	545.7	22.76667
347.7	23.53333	448.2	23.36667	548.9	22.76667
351.1	23.56667	451.6	23.3	552.1	22.73333
354.4	23.53333	454.9	23.33333	555.5	22.7
357.8	23.53333	458.3	23.33333	558.8	22.66667
361.3	23.46667	461.7	23.33333	562.2	22.63333
364.5	23.43333	465.2	23.3	565.7	22.66667
367.8	23.5	468.4	23.26667	569.1	22.63333
371.2	23.46667	471.8	23.3	572.2	22.56667
374.5	23.4	475.1	23.33333	575.7	22.53333
378.2	23.4	478.5	23.26667	579	22.56667
381.3	23.43333	482.1	23.16667	582.3	22.53333
384.6	23.43333	485.3	23.2	586	22.46667
388	23.36667	488.5	23.2	589.1	22.43333
391.4	23.36667	491.9	23.16667	592.4	22.46667
394.6	23.36667	495.3	23.06667	595.9	22.46667
398.1	23.4	498.5	23.06667	599.1	22.43333
401.6	23.4	502	23.03333	602.4	22.4
404.7	23.36667	505.5	23.06667	605.9	22.4

Kaolin concentration (% volume) = 19% and Spindle speed 200 RPM

Time (sec)	% FST	Time (sec)	% FST	Time (sec)	% FST
6.609	29.23333	107	33.13333	207.7	32.63333
9.734	30.73333	110.3	33.1	210.9	32.66667
13.14	31.1	113.7	33.06667	214.2	32.66667
16.84	31.43333	117	33.06667	217.7	32.63333
19.89	31.63333	120.7	33.13333	221	32.56667
23.22	31.8	123.9	33.13333	224.7	32.53333
26.58	31.96667	127.1	33.1	227.8	32.56667
30.05	32.16667	130.5	33.06667	231	32.53333
33.22	32.3	134	33.1	234.4	32.46667
36.75	32.36667	137.1	33.1	237.9	32.4
40.17	32.46667	140.5	33.1	241	32.4
43.27	32.6	144.1	33.03333	244.5	32.43333
46.69	32.7	147.2	33.03333	248	32.36667
50.02	32.73333	150.6	33.03333	251.1	32.26667
53.41	32.76667	154.1	33.06667	254.5	32.23333
57.14	32.83333	157.3	33	258	32.3
60.06	32.86667	161	33	261.2	32.23333
63.5	32.9	164	32.96667	265	32.13333
66.72	32.93333	167.4	33	267.9	32.1
70.12	32.93333	170.6	33	271.3	32.1
73.47	32.96667	174	32.93333	274.5	32.06667
76.81	33.03333	177.4	32.86667	277.9	32.03333
80.48	33	180.7	32.9	281.3	32
83.5	33	184.4	32.9	284.6	31.96667
86.83	33	187.4	32.9	288.3	32
90.19	33.06667	190.7	32.8	291.3	31.93333
93.66	33.13333	194.1	32.76667	294.8	31.86667
96.89	33.1	197.5	32.8	298	31.83333
100.4	33.03333	201.3	32.73333	301.5	31.8
103.8	33.1	204.3	32.73333	304.7	31.83333

Time (sec)	% FST	Time (sec)	% FST	Time (sec)	% FST
308.2	31.76667	408.6	30.76667	509.3	29.63333
311.6	31.7	412.1	30.73333	513	29.66667
314.8	31.66667	415.5	30.66667	516	29.63333
318.1	31.7	418.7	30.6	519.4	29.6
321.6	31.66667	422.1	30.6	522.6	29.53333
324.8	31.63333	425.4	30.6	525.9	29.5
328.6	31.56667	428.7	30.56667	529.4	29.53333
331.7	31.53333	432.5	30.46667	532.7	29.53333
334.9	31.56667	435.5	30.43333	536.4	29.43333
338.3	31.53333	438.8	30.43333	539.4	29.43333
341.8	31.43333	442.2	30.4	542.7	29.43333
344.9	31.26667	445.7	30.33333	546.1	29.46667
348.5	31.5	448.9	30.23333	549.5	29.43333
351.9	31.43333	452.4	30.23333	552.7	29.36667
355	31.33333	455.8	30.23333	556.3	29.33333
358.4	31.3	458.9	30.16667	559.7	29.36667
361.8	31.3	462.3	30.1	562.8	29.33333
365.1	31.3	465.7	30.06667	566.2	29.3
368.9	31.2	469.1	30.03333	569.7	29.23333
371.8	31.16667	472.8	30.03333	572.9	29.2
375.2	31.16667	475.7	29.93333	576.7	29.26667
378.5	31.16667	479.1	29.9	579.6	29.23333
381.8	31.13333	482.4	29.9	583	29.16667
385.2	31.06667	485.7	29.9	586.4	29.1
388.6	30.96667	489.1	29.86667	589.7	29.1
392.2	30.96667	492.5	29.8	593	29.13333
395.2	30.96667	496.1	29.73333	596.3	29.1
398.7	30.9	499.1	29.76667	600	29.03333
402.2	30.83333	502.6	29.76667	603	29
405.4	30.76667	505.9	29.66667	606.5	29.03333

Kaolin concentration (% volume) = 22% and Spindle speed 75 RPM

Time (sec)	% FST	Time (sec)	% FST	Time (sec)	% FST
6.735	47.33333	107.1	56.66667	207.7	58.33333
9.719	50.33333	110.3	57	210.9	58.66667
13.19	51.33333	113.6	56.66667	214.2	58.66667
16.86	51.66667	117.1	56.66667	217.6	58.33333
19.8	51.66667	120.3	57	221	58.33333
23.19	52	123.9	57.33333	224.6	58.66667
26.59	52.66667	127.1	57.33333	227.7	59
29.95	53	130.6	57	231	58.66667
33.19	53	133.8	57	234.3	58.66667
36.78	53.33333	137.1	57.33333	237.7	58.66667
40.2	53.66667	140.5	57.33333	241.1	59
43.28	54	144.1	57.33333	244.4	59
46.69	54	147.2	57.66667	248	59
50.14	54	150.6	58	251.2	58.66667
53.5	54.66667	153.9	57.66667	254.5	59
56.64	54.66667	157.3	57.66667	257.8	59.33333
60.17	54.66667	160.7	57.66667	261.1	59
63.49	54.66667	164.1	58	265	59
66.75	55.33333	167.4	58	268	59
70.09	55.33333	170.8	57.66667	271.3	59.33333
73.44	55.66667	174	58	274.5	59
76.8	55.66667	177.3	58.33333	278	59
80.49	55.66667	180.7	58.33333	281.2	59
83.61	56	184.4	58	284.7	59.33333
86.81	56	187.5	58	288.3	59.33333
90.19	56	190.7	58.33333	291.3	59
93.67	56	194.2	58.66667	294.8	59
96.89	56.66667	197.5	58.33333	298	59.33333
100.3	56.66667	200.8	58.33333	301.4	59.33333
103.8	56.33333	204.2	58.33333	304.7	59.33333

Time (sec)	% FST	Time (sec)	% FST	Time (sec)	% FST
308	59	408.6	59.66667	509.3	59.66667
311.6	59	412.1	59.33333	513	59.33333
314.8	59.33333	415.5	59.33333	515.9	59.66667
318.1	59.33333	418.8	59.66667	519.4	59.66667
321.6	59.33333	422.2	59.66667	522.7	59.66667
324.8	59	425.5	59.33333	525.9	59.33333
328.5	59	428.8	59.33333	529.4	59.33333
331.6	59.66667	432.5	59.66667	532.7	59.66667
334.9	59.33333	435.5	59.66667	536.4	59.66667
338.3	59	438.8	59.33333	539.5	59.66667
341.7	59.33333	442.2	59.33333	542.7	59.33333
345	59.66667	445.6	59.66667	546.2	59.66667
348.4	59.33333	448.9	59.66667	549.5	59.66667
351.9	59	452.3	59.66667	552.8	59.66667
355.2	59.33333	455.8	59.33333	556.3	59.33333
358.5	59.33333	459	59.66667	559.7	59.33333
361.8	59.66667	462.3	59.66667	563	59.66667
365.2	59.33333	465.7	59.33333	566.3	59.66667
368.9	59.33333	469	59.33333	569.6	59.66667
371.8	59.33333	472.7	59.33333	573	59.33333
375.2	59.66667	475.7	59.33333	576.7	59.66667
378.6	59.66667	479.1	59.66667	579.6	59.66667
381.8	59.33333	482.5	59.33333	583	59.66667
385.3	59	485.7	59.66667	586.4	59.33333
388.5	59.33333	489.2	59.66667	589.8	59.66667
392.2	59.66667	492.4	59.66667	593	59.66667
395.3	59.66667	496.1	59.66667	596.5	59.66667
398.6	59.33333	499.2	59.33333	600	59.33333
402	59.33333	502.5	59.66667	603.1	59.66667
405.3	59.66667	505.8	59.66667	606.5	60

Appendix 7: Lane Mountain sand-kaolin-water mixtures' rheological tests

For all tests reported in this section:

Sensor system	MV1
Temperature	20^0C
$CaCl_2.2H_20$:Kaolin (w/w)	0.001

Combination: Sand 0% and Kaolin 14%

Sand concentration (% volume)	0
Kaolin concentration (% volume)	15
Mixture density (kg/m^3)	1254
Bingham yield stress (Pa)	10.6
Bingham plastic viscosity (mPa.s)	7.7

RPM	Torque (N.m)
196.3	0.00222
229.5	0.00231
262.6	0.00241
295.7	0.0025
328.9	0.00259
362	0.00267
362	0.00267
328.9	0.00258
295.7	0.00249
262.6	0.0024
229.5	0.00231
196.3	0.00222

Combination: Sand 5% and Kaolin 14%

Sand concentration (% volume)	5
Kaolin concentration (% volume)	15
Mixture density (kg/m^3)	1308
Bingham yield stress (Pa)	11.6
Bingham plastic viscosity (mPa.s)	8.2

RPM	Torque (N.m)
196.3	0.00241
229.5	0.00251
262.6	0.00261
295.7	0.0027
328.9	0.0028
362	0.00288
362	0.00288
328.9	0.00278
295.7	0.00268
262.6	0.00259
229.5	0.00249
196.3	0.00239

Combination: Sand 10% and Kaolin 14%

Sand concentration (% volume)	10.5
Kaolin concentration (% volume)	15
Mixture density (kg/m^3)	1385
Bingham yield stress (Pa)	12.3
Bingham plastic viscosity (mPa.s)	7.9

RPM	Torque (N.m)
196.3	0.00253
229.5	0.00264
262.6	0.00272
295.7	0.0028
328.9	0.00288
362	0.00296
362	0.00295
328.9	0.00286
295.7	0.00276
262.6	0.00266
229.5	0.00255
196.3	0.00244

Combination: Sand 15% and Kaolin 14%

Sand concentration (% volume)	15.5
Kaolin concentration (% volume)	15
Mixture density (kg/m^3)	1456
Bingham yield stress (Pa)	12.7
Bingham plastic viscosity (mPa.s)	9.8

RPM	Torque (N.m)
196.3	0.00269
229.5	0.00281
262.6	0.00293
295.7	0.00305
328.9	0.00318
362	0.00328
362	0.00326
328.9	0.00313
295.7	0.00301
262.6	0.0029
229.5	0.00281
196.3	0.0027

Combination: Sand 20% and Kaolin 14%

Sand concentration (% volume)	19.3
Kaolin concentration (% volume)	15
Mixture density (kg/m^3)	1525
Bingham yield stress (Pa)	14.8
Bingham plastic viscosity (mPa.s)	9.3

RPM	Torque (N.m)
196.3	0.00304
229.5	0.00318
262.6	0.00331
295.7	0.0034
328.9	0.00346
362	0.00357
362	0.00354
328.9	0.0034
295.7	0.00328
262.6	0.00315
229.5	0.00306
196.3	0.00295

Combination: Sand 0% and Kaolin 17%

Sand concentration (% volume)	0
Kaolin concentration (% volume)	16.9
Mixture density (kg/m^3)	1287
Bingham yield stress (Pa)	24.6
Bingham plastic viscosity (mPa.s)	11.7

RPM	Torque (N.m)
196.3	0.00471
229.5	0.00487
262.6	0.00501
295.7	0.00514
328.9	0.00527
362	0.0054
362	0.0054
328.9	0.00527
295.7	0.00514
262.6	0.00501
229.5	0.00486
196.3	0.0047

Combination: Sand 5% and Kaolin 17%

Sand concentration (% volume)	5.1
Kaolin concentration (% volume)	16.9
Mixture density (kg/m^3)	1357
Bingham yield stress (Pa)	25.0
Bingham plastic viscosity (mPa.s)	13.7

RPM	Torque (N.m)
196.3	0.00491
229.5	0.00508
262.6	0.00523
295.7	0.00539
328.9	0.00556
362	0.00572
362	0.00571
328.9	0.00557
295.7	0.00541
262.6	0.00525
229.5	0.00508
196.3	0.00491

Combination: Sand 10% and Kaolin 17%

Sand concentration (% volume)	10.7
Kaolin concentration (% volume)	16.9
Mixture density (kg/m^3)	1433
Bingham yield stress (Pa)	26.5
Bingham plastic viscosity (mPa.s)	16.6

RPM	Torque (N.m)
196.3	0.0053
229.5	0.00552
262.6	0.00573
295.7	0.00593
328.9	0.00612
362	0.0063
362	0.00631
328.9	0.00615
295.7	0.00597
262.6	0.00577
229.5	0.00557
196.3	0.00537

Combination: Sand 15% and Kaolin 17%

Sand concentration (% volume)	15.1
Kaolin concentration (% volume)	16.9
Mixture density (kg/m^3)	1488
Bingham yield stress (Pa)	28.7
Bingham plastic viscosity (mPa.s)	18.8

RPM	Torque (N.m)
196.3	0.00582
229.5	0.00608
262.6	0.00634
295.7	0.00655
328.9	0.00676
362	0.00695
362	0.00695
328.9	0.00675
295.7	0.00654
262.6	0.00632
229.5	0.00609
196.3	0.00587

Combination: Sand 20% and Kaolin 17%

Sand concentration (% volume)	21
Kaolin concentration (% volume)	16.9
Mixture density (kg/m^3)	1567
Bingham yield stress (Pa)	32.2
Bingham plastic viscosity (mPa.s)	22.7

RPM	Torque (N.m)
196.3	0.00667
229.5	0.00701
262.6	0.00731
295.7	0.00756
328.9	0.00779
362	0.00802
362	0.00798
328.9	0.0077
295.7	0.00741
262.6	0.00715
229.5	0.0069
196.3	0.00665

Combination: Sand 0% and Kaolin 19%

Sand concentration (% volume)	0
Kaolin concentration (% volume)	19
Mixture density (kg/m^3)	1322
Bingham yield stress (Pa)	42.1
Bingham plastic viscosity (mPa.s)	17.5

RPM	Torque (N.m)
196.3	0.00786
229.5	0.0081
262.6	0.00832
295.7	0.00852
328.9	0.00872
362	0.00891
362	0.00891
328.9	0.00873
295.7	0.00854
262.6	0.00834
229.5	0.00813
196.3	0.00789

Combination: Sand 5% and Kaolin 19%

Sand concentration (% volume)	5.5
Kaolin concentration (% volume)	19
Mixture density (kg/m^3)	1396
Bingham yield stress (Pa)	42.7
Bingham plastic viscosity (mPa.s)	19.7

RPM	Torque (N.m)
196.3	0.0081
229.5	0.00841
262.6	0.00866
295.7	0.0089
328.9	0.00913
362	0.00933
362	0.00922
328.9	0.00903
295.7	0.00883
262.6	0.00862
229.5	0.00838
196.3	0.00812

Combination: Sand 10% and Kaolin 19%

Sand concentration (% volume)	10.9
Kaolin concentration (% volume)	19
Mixture density (kg/m^3)	1468
Bingham yield stress (Pa)	47.3
Bingham plastic viscosity (mPa.s)	25.7

RPM	Torque (N.m)
196.3	0.00908
229.5	0.00947
262.6	0.00983
295.7	0.0102
328.9	0.0105
362	0.0107
362	0.0108
328.9	0.0105
295.7	0.0103
262.6	0.01
229.5	0.00972
196.3	0.00941

Combination: Sand 15% and Kaolin 19%

Sand concentration (% volume)	14.9
Kaolin concentration (% volume)	19
Mixture density (kg/m^3)	1522
Bingham yield stress (Pa)	51.8
Bingham plastic viscosity (mPa.s)	30.6

RPM	Torque (N.m)
196.3	0.0101
229.5	0.0106
262.6	0.0111
295.7	0.0114
328.9	0.0118
362	0.0121
362	0.0121
328.9	0.0118
295.7	0.0115
262.6	0.0112
229.5	0.0108
196.3	0.0105

Combination: Sand 20% and Kaolin 19%

Sand concentration (% volume)	20.6
Kaolin concentration (% volume)	19
Mixture density (kg/m^3)	1598
Bingham yield stress (Pa)	70.6
Bingham plastic viscosity (mPa.s)	41.4

RPM	Torque (N.m)
196.3	0.0139
229.5	0.0146
262.6	0.0152
295.7	0.0157
328.9	0.0161
362	0.0165
362	0.0164
328.9	0.016
295.7	0.0155
262.6	0.0151
229.5	0.0146
196.3	0.0141

Combination: Sand 0% and Kaolin 22%

Sand concentration (% volume)	0
Kaolin concentration (% volume)	21.9
Mixture density (kg/m^3)	1371
Bingham yield stress (Pa)	72.6
Bingham plastic viscosity (mPa.s)	25.9

RPM	Torque (N.m)
232.1	0.0136
257.9	0.0139
284.1	0.0142
310	0.0144
336	0.0146
362	0.0148
362	0.0148
336	0.0146
310	0.0144
284.1	0.0141
257.9	0.0139
232.1	0.0136

Combination: Sand 5% and Kaolin 22%

Sand concentration (% volume)	5.5
Kaolin concentration (% volume)	21.9
Mixture density (kg/m^3)	1438
Bingham yield stress (Pa)	81.1
Bingham plastic viscosity (mPa.s)	31.3

RPM	Torque (N.m)
232.1	0.0153
257.9	0.0156
284.1	0.016
310	0.0163
336	0.0165
362	0.0168
362	0.0169
336	0.0167
310	0.0164
284.1	0.0161
257.9	0.0159
232.1	0.0155

Combination: Sand 10% and Kaolin 22%

Sand concentration (% volume)	10.5
Kaolin concentration (% volume)	21.9
Mixture density (kg/m^3)	1504
Bingham yield stress (Pa)	95.0
Bingham plastic viscosity (mPa.s)	39.6

RPM	Torque (N.m)
232.1	0.0181
257.9	0.0186
284.1	0.019
310	0.0194
336	0.0198
362	0.0201
362	0.0201
336	0.0199
310	0.0195
284.1	0.0192
257.9	0.0188
232.1	0.0185

Combination: Sand 15% and Kaolin 22%

Sand concentration (% volume)	15.8
Kaolin concentration (% volume)	21.9
Mixture density (kg/m^3)	1574
Bingham yield stress (Pa)	104.6
Bingham plastic viscosity (mPa.s)	53.9

RPM	Torque (N.m)
208.8	0.0203
229.2	0.0208
249.3	0.0212
269.4	0.0216
289.8	0.0221
310	0.0225
310	0.0225
289.8	0.0222
269.4	0.0219
249.3	0.0216
229.2	0.0212
208.8	0.0208

Combination: Sand 20% and Kaolin 22%

Sand concentration (% volume)	21.4
Kaolin concentration (% volume)	21.9
Mixture density (kg/m^3)	1646
Bingham yield stress (Pa)	106.8
Bingham plastic viscosity (mPa.s)	125.4

RPM	Torque (N.m)
94.38	0.0205
105.5	0.0213
116.6	0.022
127.7	0.0225
138.9	0.0229
150	0.0235
150	0.0236
138.9	0.0233
127.7	0.0229
116.6	0.0225
105.5	0.022
94.61	0.0216

Appendix 8: Granusil Silica sand-kaolin-water mixtures' rheological tests

For all tests reported in this section:

Sensor system	MV1
Temperature	20^0C
$CaCl_2.2H_20$:Kaolin (w/w)	0.001

Combination: Sand 0% and Kaolin 14%

Sand concentration (% volume)	0
Kaolin concentration (% volume)	13.9
Mixture density (kg/m^3)	1236
Bingham yield stress (Pa)	9.0
Bingham plastic viscosity (mPa.s)	7.5

RPM	Torque (N.m)
64	0.00155
96.89	0.00167
130.2	0.00179
163.3	0.0019
196.3	0.00198
229.5	0.00207
262.6	0.00214
295.7	0.00222
328.9	0.00229
362	0.00236
362	0.00236
328.9	0.00228
295.7	0.00221
262.6	0.00213
229.5	0.00205
196.3	0.00197
163.3	0.00188
130.2	0.00178
97.69	0.00168
64	0.00155

Combination: Sand 5% and Kaolin 14%

Sand concentration (% volume)	4.9
Kaolin concentration (% volume)	13.9
Mixture density (kg/m^3)	1305
Bingham yield stress (Pa)	8.7
Bingham plastic viscosity (mPa.s)	9.4

RPM	Torque (N.m)
179.9	0.00199
165.1	0.00194
150	0.00188
135	0.00183
120	0.00177
120	0.00177
135	0.00182
150	0.00187
165.1	0.00191
179.9	0.00195

Combination: Sand 10% and Kaolin 14%

Sand concentration (% volume)	9.7
Kaolin concentration (% volume)	13.9
Mixture density (kg/m^3)	1372
Bingham yield stress (Pa)	9.3
Bingham plastic viscosity (mPa.s)	10.5

RPM	Torque (N.m)
179.9	0.00218
165.1	0.00212
150	0.00205
135	0.00199
120	0.00192
120	0.00191
135	0.00196
150	0.00201
165.1	0.00205
179.9	0.0021

Combination: Sand 15% and Kaolin 14%

Sand concentration (% volume)	16.4
Kaolin concentration (% volume)	13.9
Mixture density (kg/m^3)	1474
Bingham yield stress (Pa)	10.8
Bingham plastic viscosity (mPa.s)	8.6

RPM	Torque (N.m)
179.9	0.00234
165.1	0.00228
150	0.00223
135	0.00216
120	0.00209
120	0.00207
135	0.00211
150	0.00214
165.1	0.00217
179.9	0.00219

Combination: Sand 20% and Kaolin 14%

Sand concentration (% volume)	20
Kaolin concentration (% volume)	13.9
Mixture density (kg/m^3)	1525
Bingham yield stress (Pa)	11.1
Bingham plastic viscosity (mPa.s)	14.6

RPM	Torque (N.m)
179.9	0.00273
165.1	0.00263
150	0.00256
135	0.0025
120	0.00242
120	0.00239
135	0.0024
150	0.00239

Combination: Sand 0% and Kaolin 17%

Sand concentration (% volume)	0
Kaolin concentration (% volume)	17
Mixture density (kg/m^3)	1288
Bingham yield stress (Pa)	21.0
Bingham plastic viscosity (mPa.s)	13.5

RPM	Torque (N.m)
64	0.00356
96.91	0.00379
130.2	0.004
163.3	0.00418
196.3	0.00435
229.5	0.0045
262.6	0.00464
295.7	0.00477
328.9	0.0049
362	0.00501
362	0.00501
328.9	0.00488
295.7	0.00475
262.6	0.00462
229.5	0.00447
196.3	0.00432
163.3	0.00416
130.2	0.00398
97.69	0.00379
64	0.00353

Combination: Sand 5% and Kaolin 17%

Sand concentration (% volume)	5
Kaolin concentration (% volume)	17
Mixture density (kg/m^3)	1355
Bingham yield stress (Pa)	22.0
Bingham plastic viscosity (mPa.s)	15.8

RPM	Torque (N.m)
179.9	0.00454
165.1	0.00445
150	0.00435
135	0.00426
120	0.00416
120	0.00415
135	0.00422
150	0.0043
165.1	0.00437
179.9	0.00444

Combination: Sand 10% and Kaolin 17%

Sand concentration (% volume)	10.4
Kaolin concentration (% volume)	17
Mixture density (kg/m^3)	1431
Bingham yield stress (Pa)	23.8
Bingham plastic viscosity (mPa.s)	15.4

RPM	Torque (N.m)
179.9	0.00484
165.1	0.00474
150	0.00464
135	0.00454
120	0.00444
120	0.00442
135	0.0045
150	0.00456
165.1	0.00462
179.9	0.00468

Combination: Sand 15% and Kaolin 17%

Sand concentration (% volume)	16
Kaolin concentration (% volume)	17
Mixture density (kg/m^3)	1503
Bingham yield stress (Pa)	28.9
Bingham plastic viscosity (mPa.s)	16.9

RPM	Torque (N.m)
179.9	0.00578
165.1	0.00565
150	0.00553
135	0.00542
120	0.0053
120	0.00529
135	0.00536
150	0.00544
165.1	0.00551
179.9	0.00552

Combination: Sand 20% and Kaolin 17%

Sand concentration (% volume)	21.7
Kaolin concentration (% volume)	17
Mixture density (kg/m^3)	1582
Bingham yield stress (Pa)	38.1
Bingham plastic viscosity (mPa.s)	16.4

RPM	Torque (N.m)
179.9	0.0071
165.1	0.00704
150	0.00693
135	0.00678
120	0.00668
120	0.00674
135	0.00692
150	0.00696
165.1	0.00702
179.9	0.00701

Combination: Sand 0% and Kaolin 19%

Sand concentration (% volume)	0
Kaolin concentration (% volume)	19
Mixture density (kg/m^3)	1322
Bingham yield stress (Pa)	35.3
Bingham plastic viscosity (mPa.s)	18.3

RPM	Torque (N.m)
64	0.0058
96.89	0.00616
130.2	0.00646
163.3	0.00672
196.3	0.00695
229.5	0.00716
262.6	0.00736
295.7	0.00754
328.9	0.00772
362	0.00789
362	0.00788
328.9	0.00771
295.7	0.00753
262.6	0.00734
229.5	0.00714
196.3	0.00693
163.3	0.00669
130.2	0.00642
97.69	0.00611
64	0.00573

Combination: Sand 5% and Kaolin 19%

Sand concentration (% volume)	4.5
Kaolin concentration (% volume)	19
Mixture density (kg/m^3)	1385
Bingham yield stress (Pa)	35.7
Bingham plastic viscosity (mPa.s)	22.2

RPM	Torque (N.m)
179.9	0.00711
165.1	0.00699
150	0.00688
135	0.00675
120	0.00661
120	0.0066
135	0.00672
150	0.00684
165.1	0.00694
179.9	0.00705

Combination: Sand 10% and Kaolin 19%

Sand concentration (% volume)	9.6
Kaolin concentration (% volume)	19
Mixture density (kg/m^3)	1453
Bingham yield stress (Pa)	38.5
Bingham plastic viscosity (mPa.s)	22.5

RPM	Torque (N.m)
179.9	0.00766
165.1	0.00752
150	0.00738
135	0.00723
120	0.00707
120	0.00704
135	0.00715
150	0.00725
165.1	0.00733
179.9	0.00741

Combination: Sand 15% and Kaolin 19%

Sand concentration (% volume)	14.9
Kaolin concentration (% volume)	19
Mixture density (kg/m^3)	1521
Bingham yield stress (Pa)	39.4
Bingham plastic viscosity (mPa.s)	23.6

RPM	Torque (N.m)
179.9	0.00792
165.1	0.00777
150	0.00759
135	0.00741
120	0.00725
120	0.00723
135	0.00733
150	0.00745
165.1	0.0075
179.9	0.00755

Combination: Sand 20% and Kaolin 19%

Sand concentration (% volume)	20.4
Kaolin concentration (% volume)	19
Mixture density (kg/m^3)	1594
Bingham yield stress (Pa)	56.1
Bingham plastic viscosity (mPa.s)	30.1

RPM	Torque (N.m)
179.9	0.0108
165.1	0.0106
150	0.0105
135	0.0103
120	0.0101
120	0.0102
135	0.0104
150	0.0106
165.1	0.0107
179.9	0.0108

Combination: Sand 0% and Kaolin 22%

Sand concentration (% volume)	0
Kaolin concentration (% volume)	22.1
Mixture density (kg/m^3)	1375
Bingham yield stress (Pa)	69.3
Bingham plastic viscosity (mPa.s)	30.3

RPM	Torque (N.m)
128	0.0123
153.9	0.0127
179.9	0.013
206	0.0133
232.1	0.0136
257.9	0.0138
284.1	0.0141
310	0.0143
336	0.0146
362	0.0148
362	0.0148
336	0.0146
310	0.0143
284.1	0.0141
257.9	0.0138
232.1	0.0135
206	0.0132
179.9	0.0129
153.9	0.0126
128	0.0122

Combination: Sand 5% and Kaolin 22%

Sand concentration (% volume)	5.3
Kaolin concentration (% volume)	22.1
Mixture density (kg/m^3)	1444
Bingham yield stress (Pa)	70.3
Bingham plastic viscosity (mPa.s)	41.3

RPM	Torque (N.m)
179.9	0.0139
165.1	0.0136
150	0.0134
135	0.0132
120	0.0129
120	0.0129
135	0.0131
150	0.0133
165.1	0.0135
179.9	0.0137

Combination: Sand 10% and Kaolin 22%

Sand concentration (% volume)	10.5
Kaolin concentration (% volume)	22.1
Mixture density (kg/m^3)	1509
Bingham yield stress (Pa)	73.5
Bingham plastic viscosity (mPa.s)	44.2

RPM	Torque (N.m)
179.9	0.0145
165.1	0.0143
150	0.0141
135	0.0138
120	0.0135
120	0.0135
135	0.0138
150	0.014
165.1	0.0142
179.9	0.0144

Combination: Sand 15% and Kaolin 22%

Sand concentration (% volume)	16.1
Kaolin concentration (% volume)	22.1
Mixture density (kg/m^3)	1579
Bingham yield stress (Pa)	93.8
Bingham plastic viscosity (mPa.s)	56.4

RPM	Torque (N.m)
179.9	0.0187
165.1	0.0184
150	0.0181
135	0.0177
120	0.0173
120	0.0172
135	0.0175
150	0.0177
165.1	0.018
179.9	0.0182

Combination: Sand 20% and Kaolin 22%

Sand concentration (% volume)	20.5
Kaolin concentration (% volume)	22.1
Mixture density (kg/m^3)	1637
Bingham yield stress (Pa)	87.4
Bingham plastic viscosity (mPa.s)	135.6

RPM	Torque (N.m)
70	0.0172
62.3	0.0169
54.9	0.0166
47.5	0.0162
40	0.0158
40	0.0157
47.5	0.0161
54.9	0.0165
62.3	0.0168
70	0.0172

Appendix 9: Vane viscometer tests

For all tests reported in this section:

Sensor system (Vane)	FL10
Room Temperature	23^0C
$CaCl_2.2H_20$:Kaolin (w/w)	0.001

Combination: Sand 0% and Kaolin 17%

Sand concentration (% volume)	0
Kaolin concentration (% volume)	16.9
Mixture density (kg/m^3)	1287

	Highest torque (N.m)	Vane yield stress (Pa)	Average Vane yield stress (Pa)
Reading 1	0.0018	9.766326	9
Reading 2	0.00154	8.355635	
Reading 3	0.001615	8.762565	

Combination: Sand 15% and Kaolin 17%

Sand concentration (% volume)	16.2
Kaolin concentration (% volume)	16.9
Mixture density (kg/m^3)	1508

	Highest torque (N.m)	Vane yield stress (Pa)	Average Vane yield stress (Pa)
Reading 1	0.00239	12.96751	12.7
Reading 2	0.00232	12.58771	
Reading 3	0.0023	12.47919	

Combination: Sand 20% and Kaolin 17%

Sand concentration (% volume)	21.8
Kaolin concentration (% volume)	16.9
Mixture density (kg/m^3)	1585

	Highest torque (N.m)	Vane yield stress (Pa)	Average Vane yield stress (Pa)
Reading 1	0.00305	16.5485	15.9
Reading 2	0.002905	15.76177	
Reading 3	0.00284	15.40909	

Combination: Sand 0% and Kaolin 19%

Sand concentration (% volume)	0
Kaolin concentration (% volume)	18.7
Mixture density (kg/m^3)	1317

	Highest torque (N.m)	Vane yield stress (Pa)	Average Vane yield stress (Pa)
Reading 1	0.00304	16.49424	15.4
Reading 2	0.00288	15.62612	
Reading 3	0.002575	13.97127	

Combination: Sand 15% and Kaolin 19%

Sand concentration (% volume)	15.2
Kaolin concentration (% volume)	18.7
Mixture density (kg/m^3)	1520

	Highest torque (N.m)	Vane yield stress (Pa)	Average Vane yield stress (Pa)
Reading 1	0.00403	21.86572	21
Reading 2	0.00392	21.26889	
Reading 3	0.00367	19.91245	

Combination: Sand 20% and Kaolin 19%

Sand concentration (% volume)	21
Kaolin concentration (% volume)	18.7
Mixture density (kg/m^3)	1604

	Highest torque (N.m)	Vane yield stress (Pa)	Average Vane yield stress (Pa)
Reading 1	0.00499	27.07443	26.1
Reading 2	0.00484	26.26057	
Reading 3	0.00462	25.0669	

Appendix 10: Mixture concentration and density determination procedure

Consider a fines-water mixture, to which coarse particles are added to produce a coarse-fines-water mixture. A sample of fines-water mixture is collected in beaker 'b1', while a sample of coarse-fines-water mixture is taken in beaker 'b2'.

The target is to find the following:

- Fines volume concentration (C_f) in fines-water mixture
- Fines-water mixture density (ρ_{cf})
- Coarse volume concentration (C_C) in coarse-fines-water mixture
- Coarse-fines-water mixture density (ρ_{mix})

Direct weight measurement by scale

Weight of beaker b1	M_{b1}
Weight of beaker b1 and fines-water mixture	$M_{b1+f1+w1}$
After overnight drying of fines-water mixture in beaker b1, Weight of beaker b1 and fines	M_{b1+f1}
Weight of beaker b2	M_{b2}
Weight of beaker b2 and coarse-fines-water mixture	$M_{b2+f2+w2+C}$
After overnight drying of coarse-fines-water mixture in beaker b2, Weight of beaker b2, fines and coarse	$M_{b2+f2+C}$

Note that the weight ratio of fines: water in fines-water mixture is same with that of coarse-kaolin-water mixture, because the later mixture was actually produced by adding coarse particles to fines-water mixture.

Calculation procedure

Fines weight concentration in fines-water mixture, C_f (wt.)	$\left(\frac{M_{b1+f1}-M_{b1}}{M_{b1+f1+w1}-M_{b1}}\right)\times 100\%$
Fines volume concentration in fines-water mixture, C_f	$\left(\frac{\frac{C_f(wt.)}{\rho_f}}{\frac{C_f(wt.)}{\rho_f}+\frac{100-C_f(wt.)}{\rho_w}}\right)\times 100\%$
Fines-water mixture density, ρ_{cf}	$C_f\times\rho_f + (1- C_f)\times\rho_w$
Weight of water in fines-water mixture, M_{w1}	$M_{b1+f1+w1} - M_{b1+f1}$
Weight of fines in fines-water mixture, M_{f1}	$M_{b1+f1+w1} - M_{w1} - M_{b1}$
Weight of water in coarse-fines-water mixture, M_{w2}	$M_{b2+f2+w2+C} - M_{b2+f2+C}$
Weight of fines in coarse-fines-water mixture, M_{f2}	$M_{w2}\times\frac{M_{f1}}{M_{w1}}$
Weight of coarse in coarse-fines-water mixture, M_C	$M_{b2+f2+w2+C} - M_{b2} - M_{w2} - M_{f2}$
Coarse volume concentration in coarse-fines-water mixture, C_C	$\left(\frac{\frac{M_C}{\rho_C}}{\frac{M_C}{\rho_C}+\frac{M_{f2}}{\rho_f}+\frac{M_{w2}}{\rho_w}}\right)\times 100\%$
Fines volume concentration in coarse-fines-water mixture, $C_{f,mix}$	$\left(\frac{\frac{M_{f2}}{\rho_f}}{\frac{M_C}{\rho_C}+\frac{M_{f2}}{\rho_f}+\frac{M_{w2}}{\rho_w}}\right)\times 100\%$
Coarse-fines-water mixture density, ρ_{mix}	$C_C\times\rho_C + C_{f,mix}\times\rho_f + (1- C_C- C_{f,mix})\times\rho_w$